Collision Energy Dependence of Hydrodynamic Flow in Relativistic Heavy-Ion Collisions

Chun Shen and Ulrich Heinz

The Ohio State University

Quark Matter, Aug 14, 2012

Ref: C. Shen and U. Heinz, PRC **85** (2012) 054902

Little Bang

Relativistic Heavy-Ion Collisions

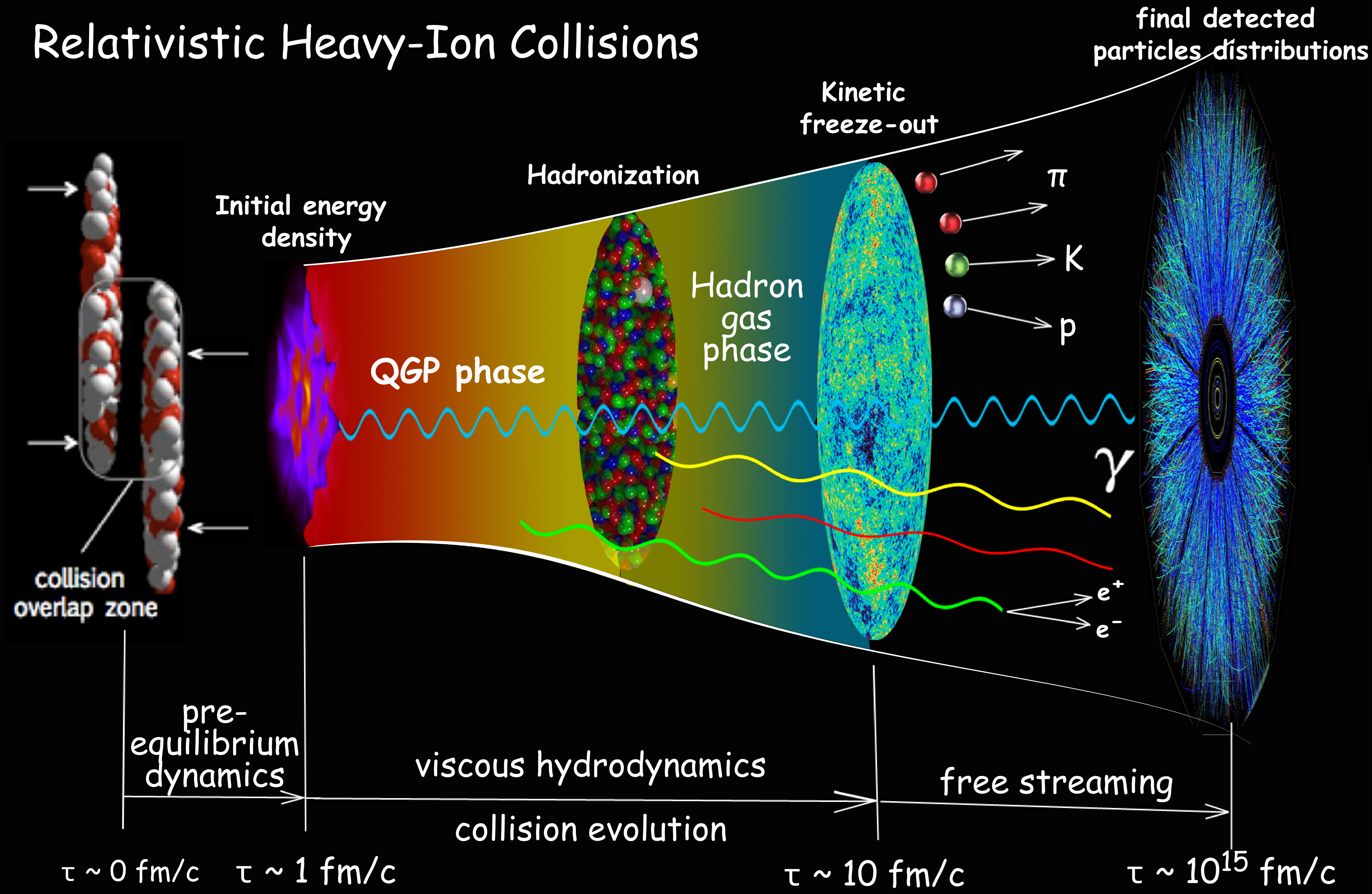

collision overlap zone

Initial energy density

QGP phase

Hadronization

Hadron gas phase

Kinetic freeze-out

final detected particles distributions

π

K

p

γ

e^+

e^-

pre-equilibrium dynamics

viscous hydrodynamics

free streaming

collision evolution

$\tau \sim 0$ fm/c

$\tau \sim 1$ fm/c

$\tau \sim 10$ fm/c

$\tau \sim 10^{15}$ fm/c

Motivation

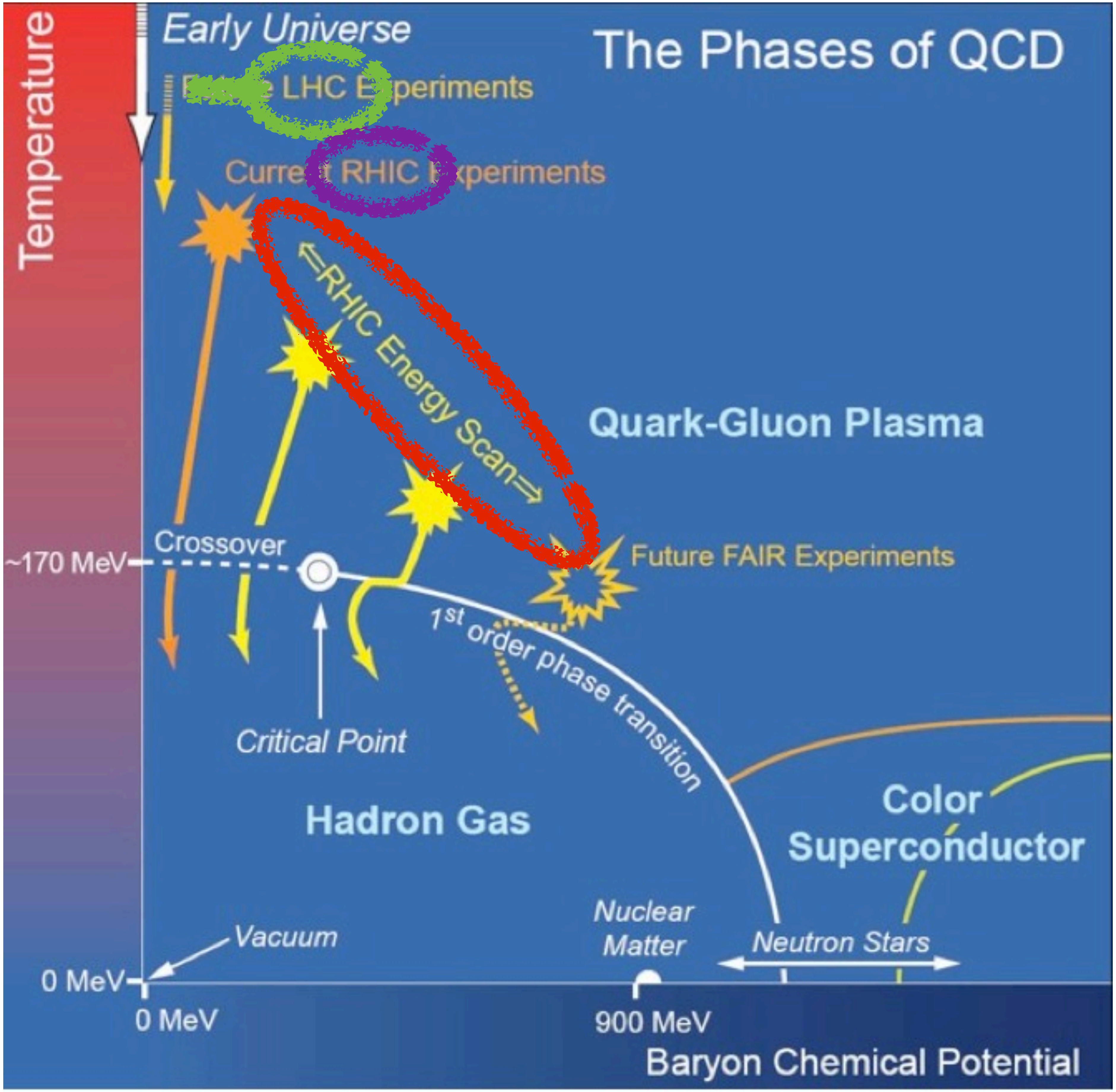
The Phases of QCD
Temperature
Early Universe
[illegible] LHC Experiments
Current RHIC Experiments
⇐RHIC Energy Scan⇒
Quark-Gluon Plasma
Future FAIR Experiments
Crossover
~170 MeV
1st order phase transition
Critical Point
Hadron Gas
Color Superconductor
Nuclear Matter
Neutron Stars
Vacuum
0 MeV
0 MeV
900 MeV
Baryon Chemical Potential

Hydro evolution

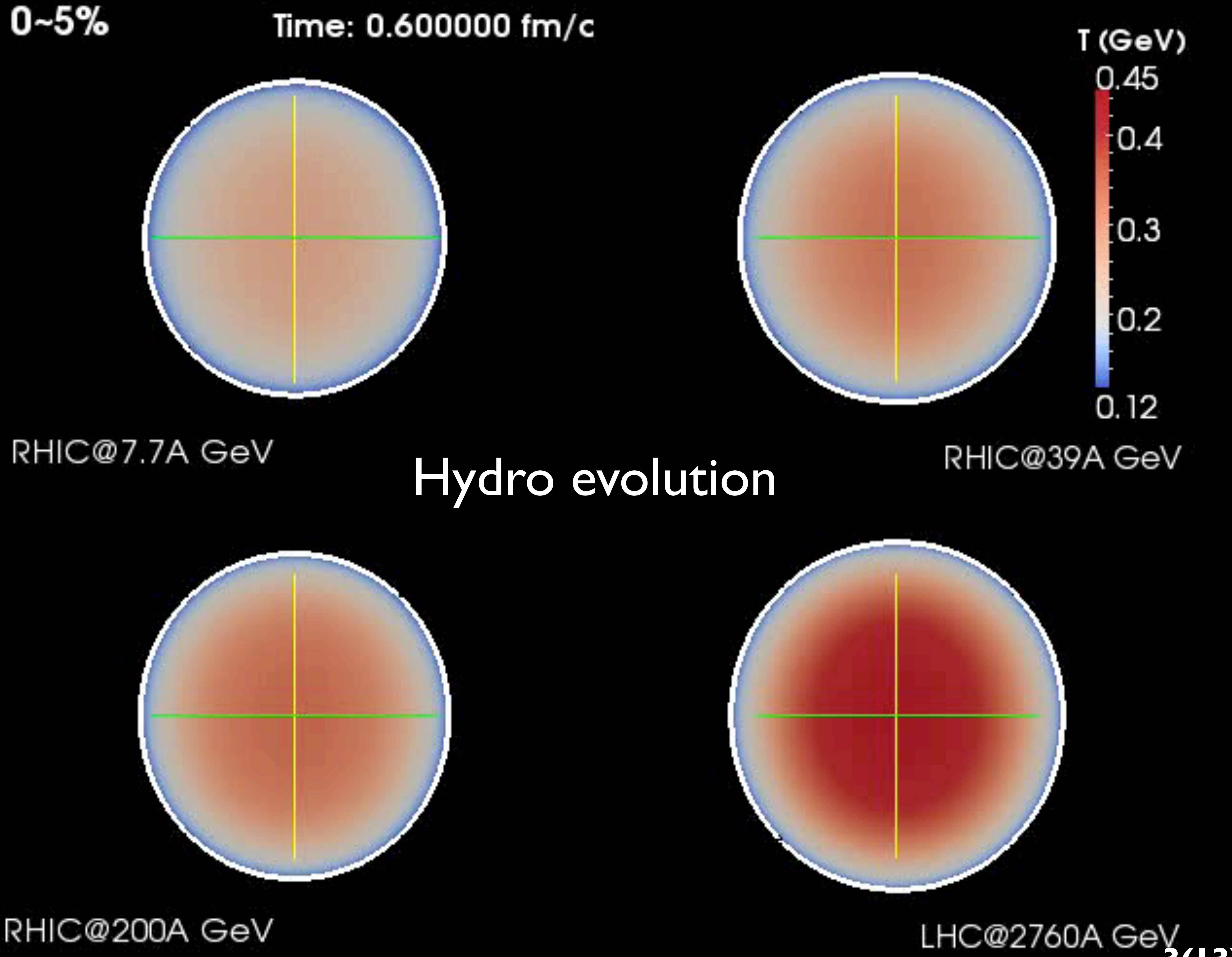

In Collaboration with visualization framework by MADAI collaboration, funded by the NSF under grant# NSF-PHY-09-41373

Global Observables

Collision energy (A GeV)	T_0 (MeV)	life time (fm/c)	produced particles per rapidity unit
AuAu@ 7.7	269.2	9.3	212.3
AuAu@ 11.5	287.5	10.0	266.7
AuAu@ 17.7	304.8	10.5	325.3
AuAu@ 19.6	308.7	10.6	339.2
AuAu@ 27	320.1	10.9	382.9
AuAu@ 39	332.2	11.2	432.7
AuAu@ 63	341.1	11.4	472.0
AuAu@ 200	378.6	12.2	661.9
PbPb@ 2760	485.2	14.2	1575.7

80% ↗

50% ↗

600% ↗

$1\text{MeV} \sim 10^{10}K \quad 1\text{fm/c} \sim 3 \times 10^{-24}s$

Centrality dependence of final charged multiplicity

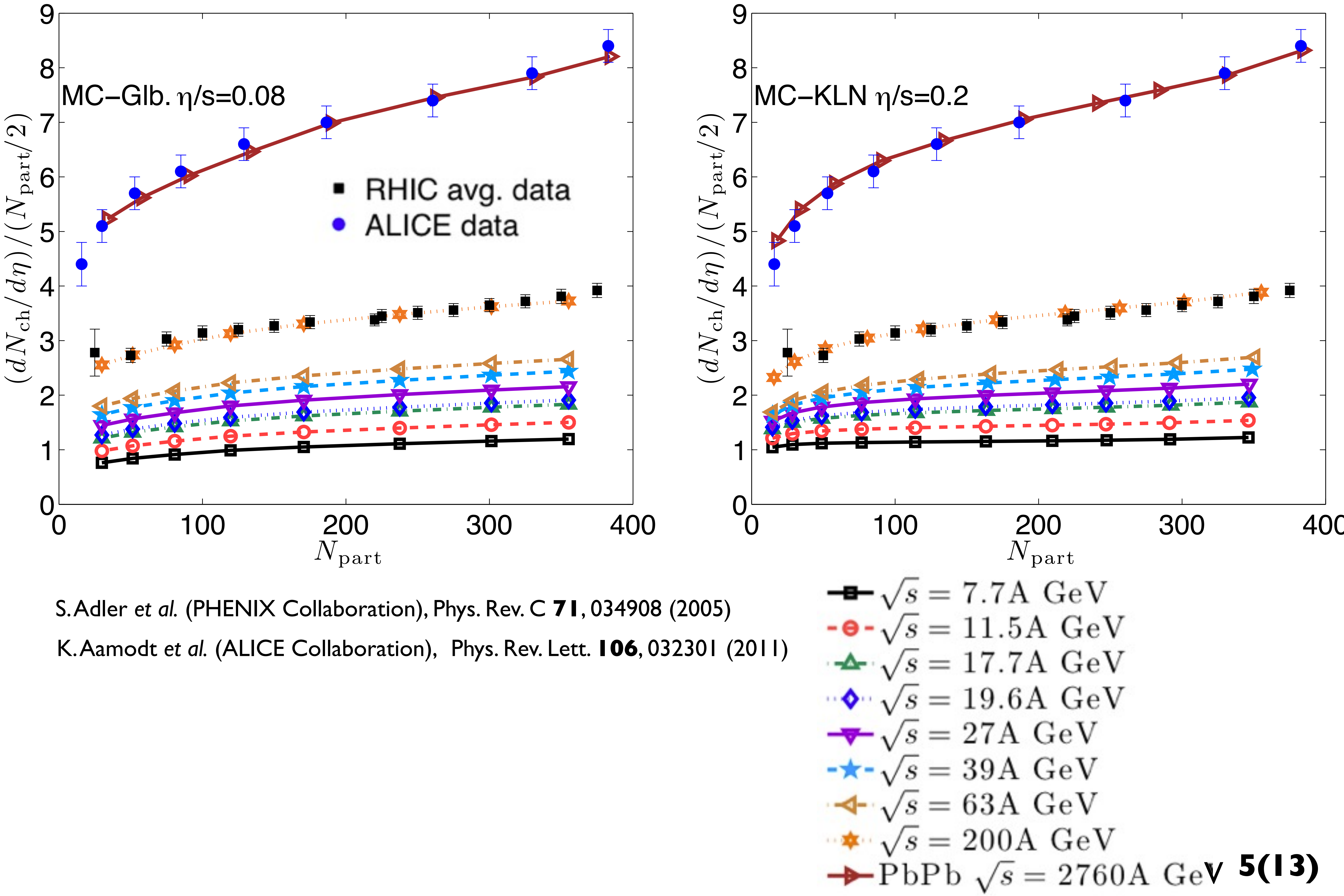

S. Adler *et al.* (PHENIX Collaboration), Phys. Rev. C **71**, 034908 (2005)

K. Aamodt *et al.* (ALICE Collaboration), Phys. Rev. Lett. **106**, 032301 (2011)

Centrality dependence of final charged multiplicity
Shape comparison

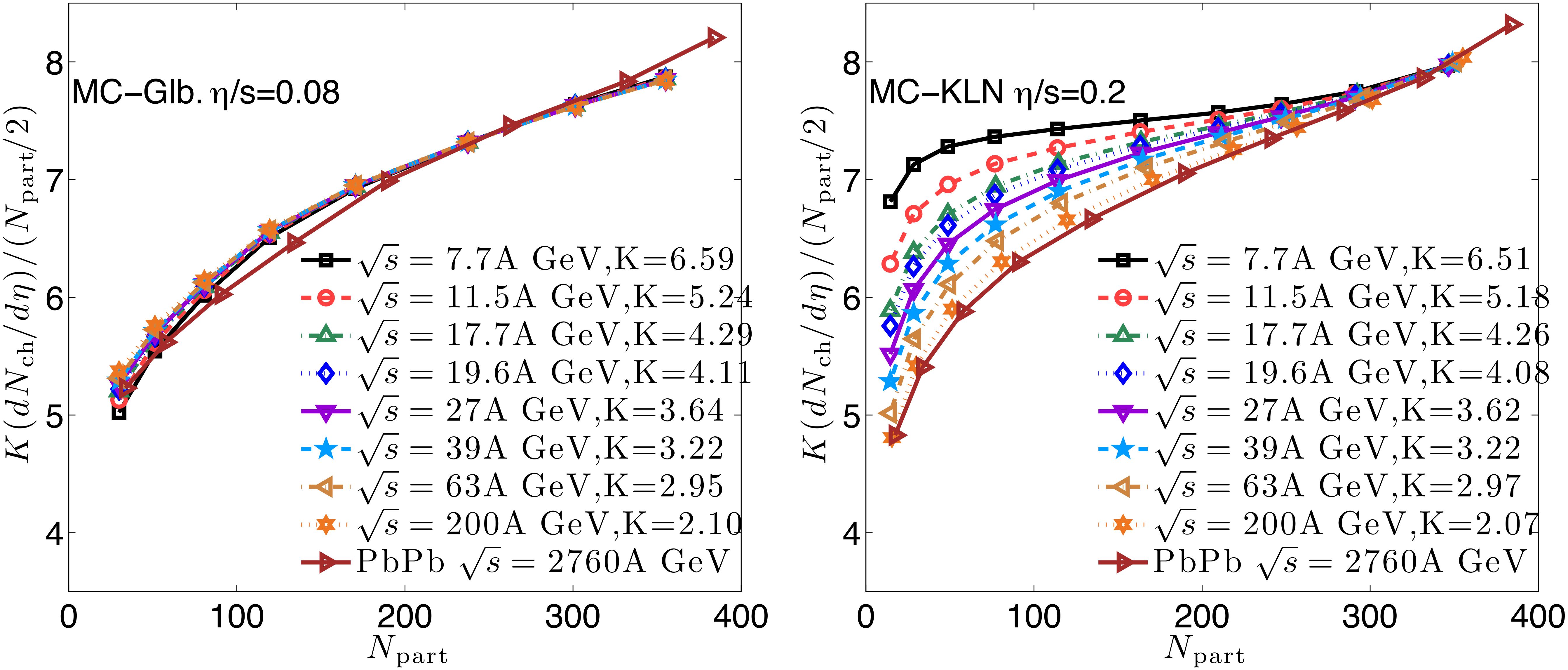

Centrality dependence of final charged multiplicity
Shape comparison

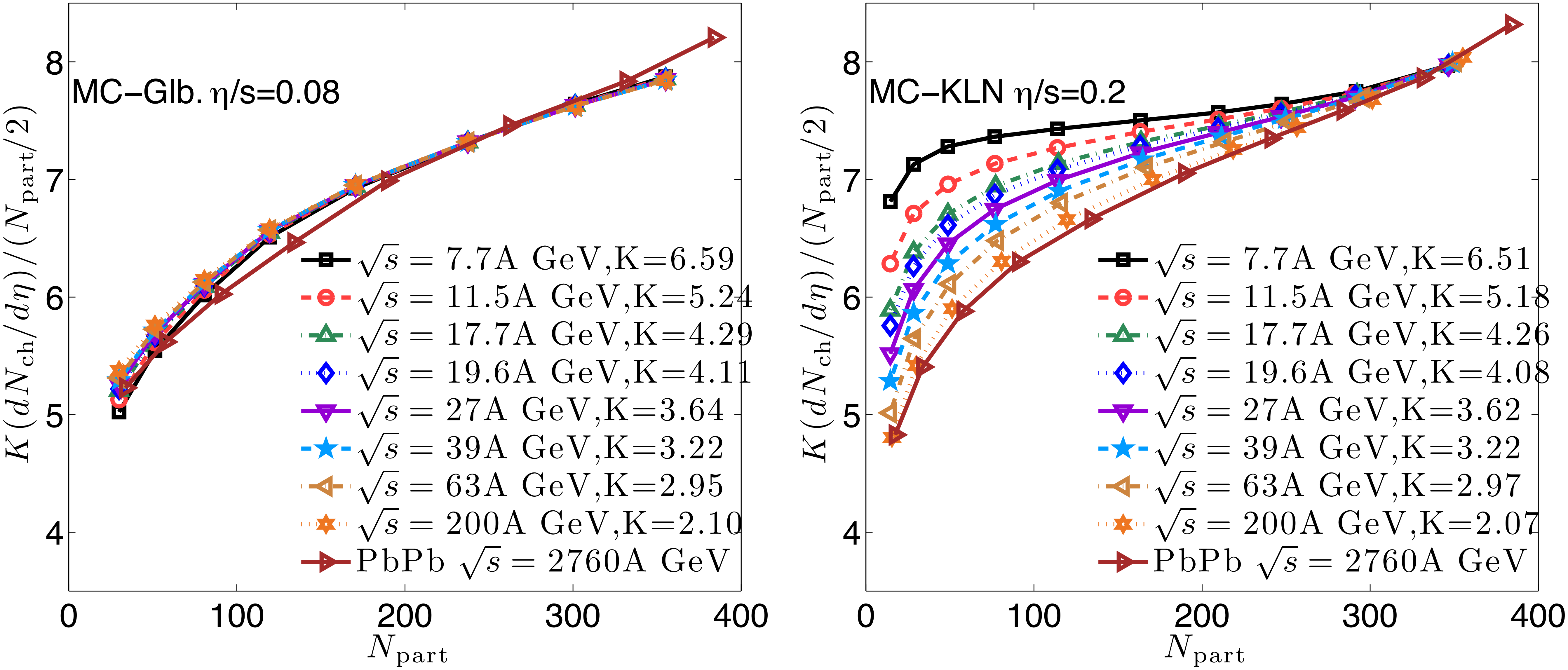

MC-Glb. shows good scaling behavior (fixed hard/soft ratio α)

MC-KLN: the slope of the curves get flatter as we go to the lower collision energy (not a viscous effect!)

radial flow and particle p_T-spectra

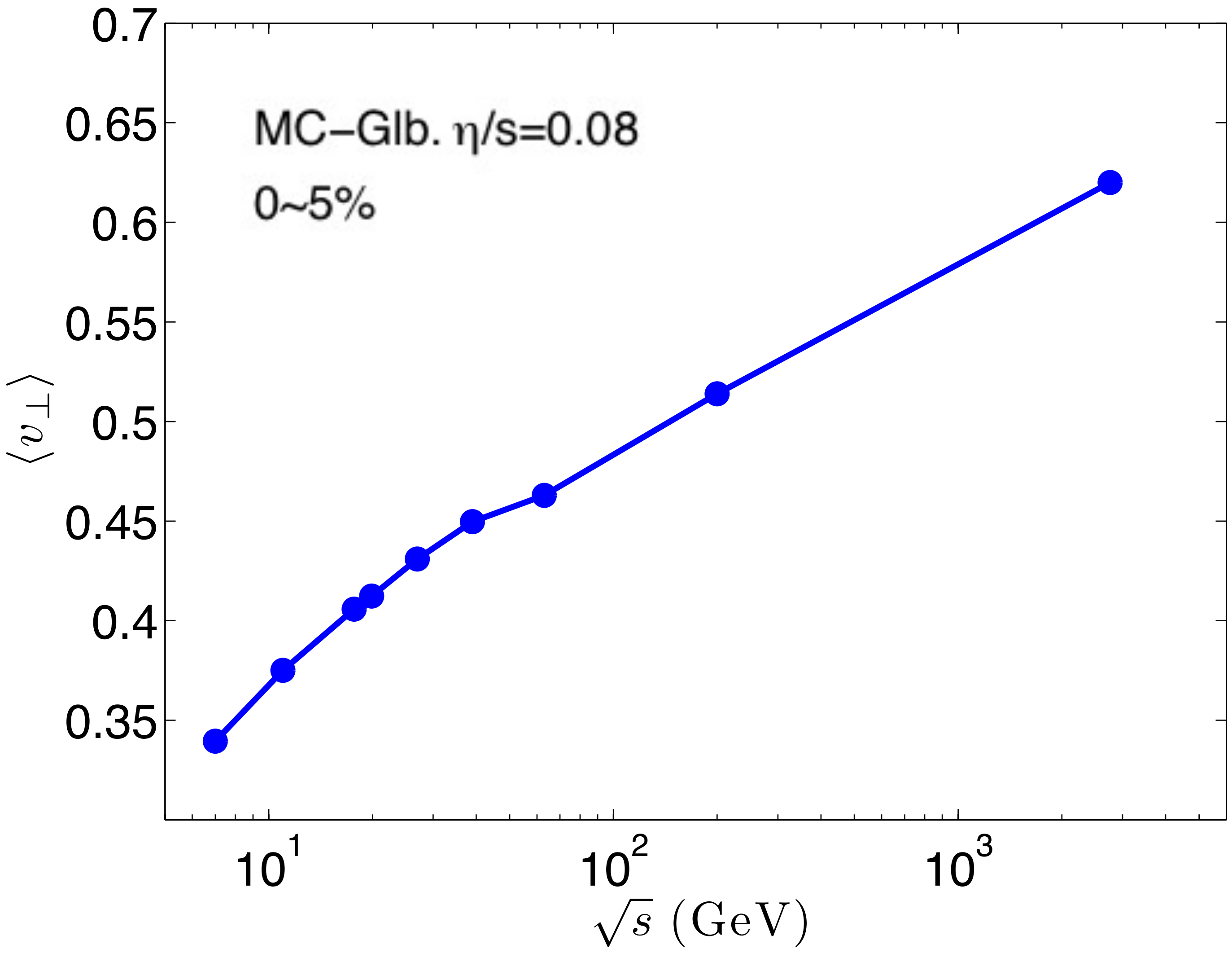

Along with $\sqrt{s}$ ↗

average radial flow $\langle v_\perp \rangle$ increases by 80%

radial flow and particle p_T-spectra

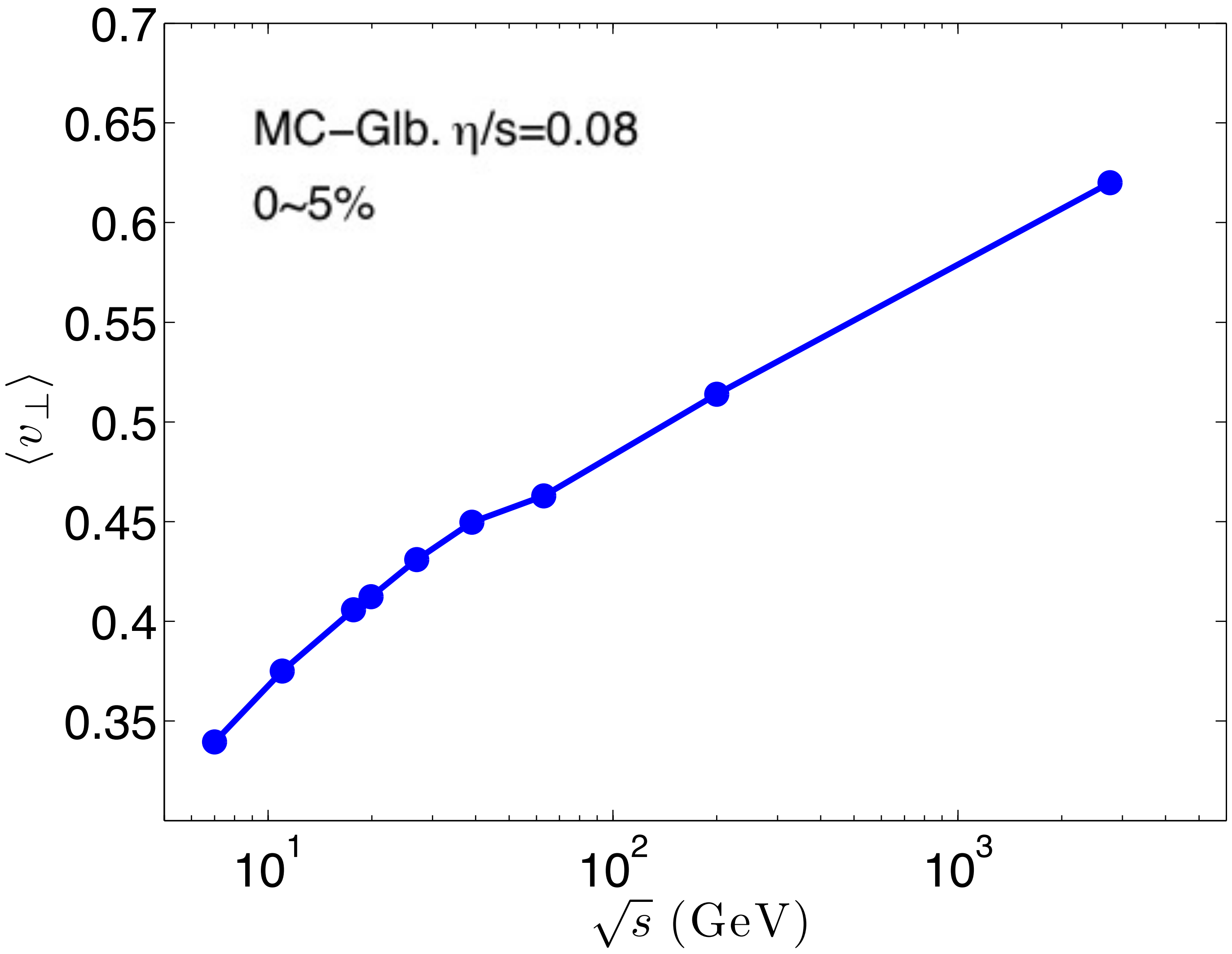

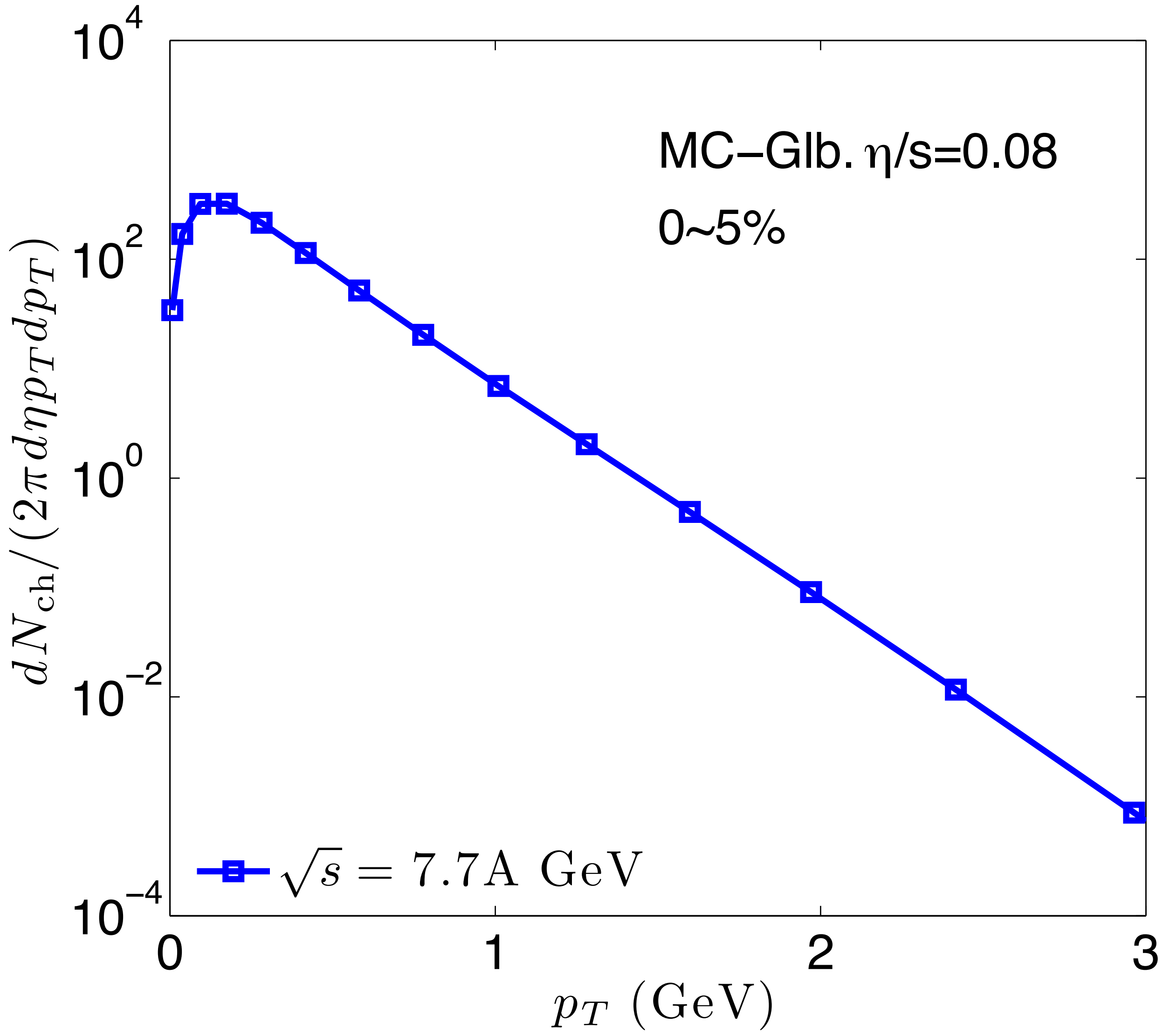

Along with $\sqrt{s}$

average radial flow $\langle v_\perp \rangle$ increases by 80%

the slope of particle p_T-spectra gets flatter

radial flow and particle p_T-spectra

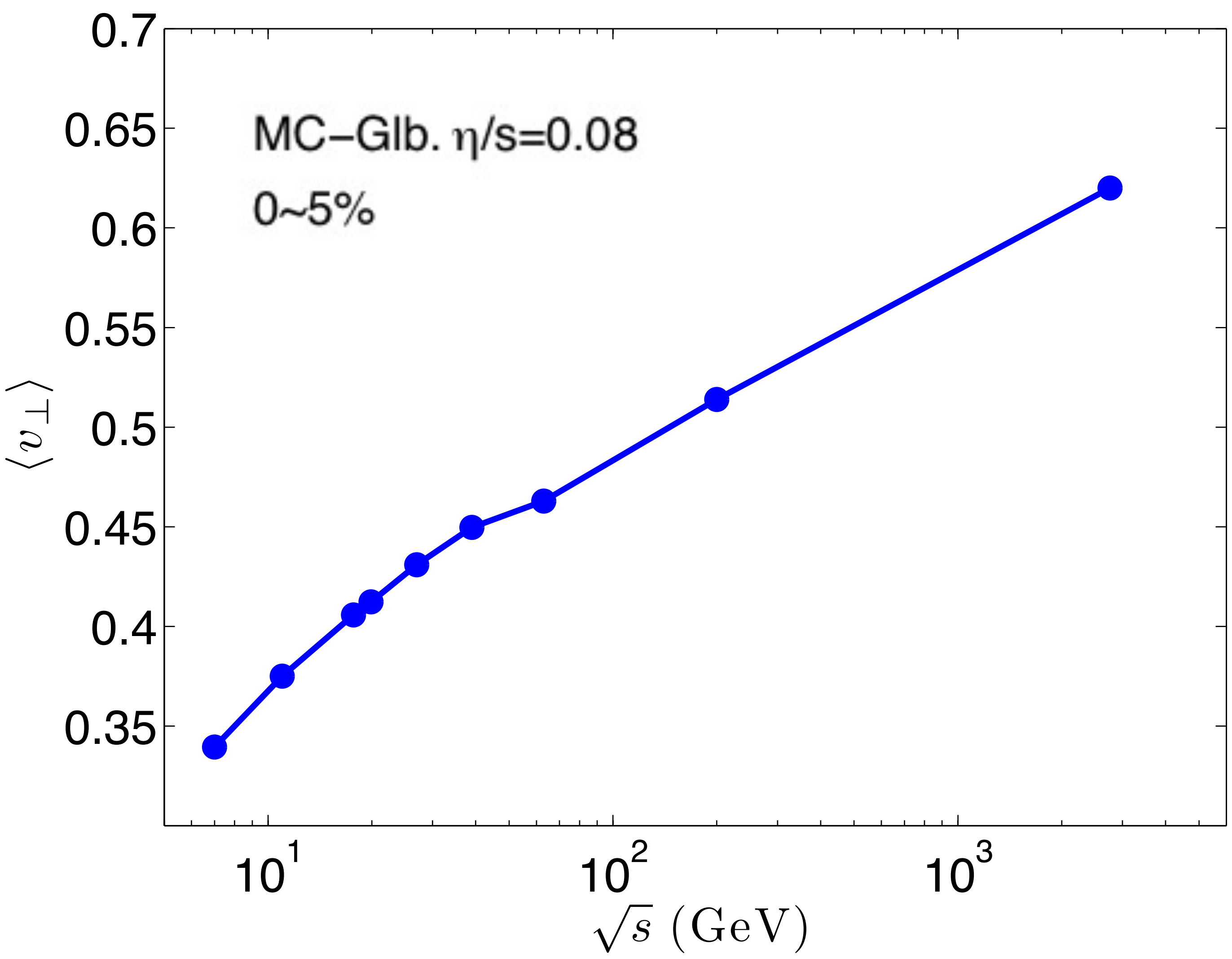

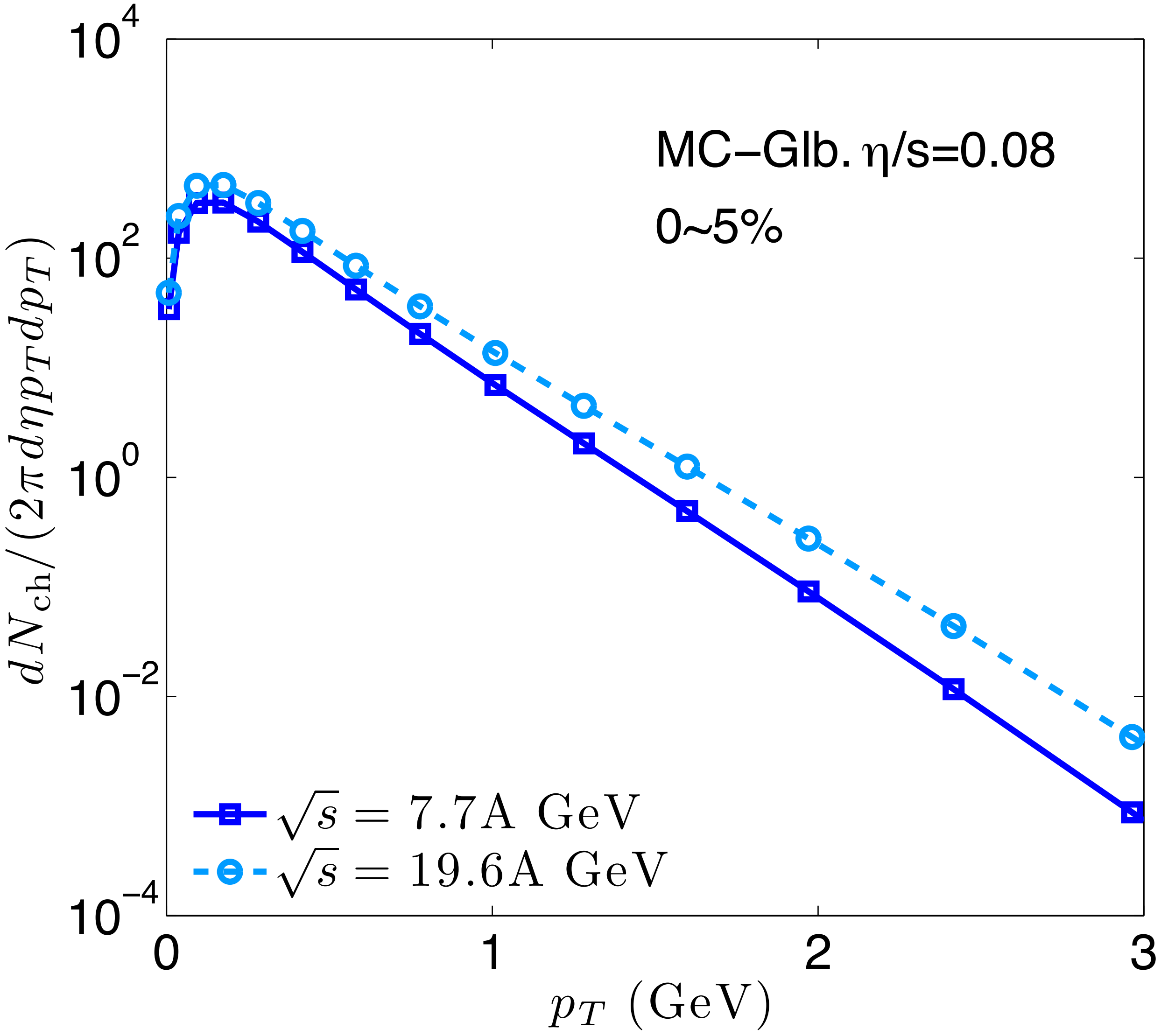

Along with $\sqrt{s}$

average radial flow $\langle v_\perp \rangle$ increases by 80%

the slope of particle p_T-spectra gets flatter

radial flow and particle p_T-spectra

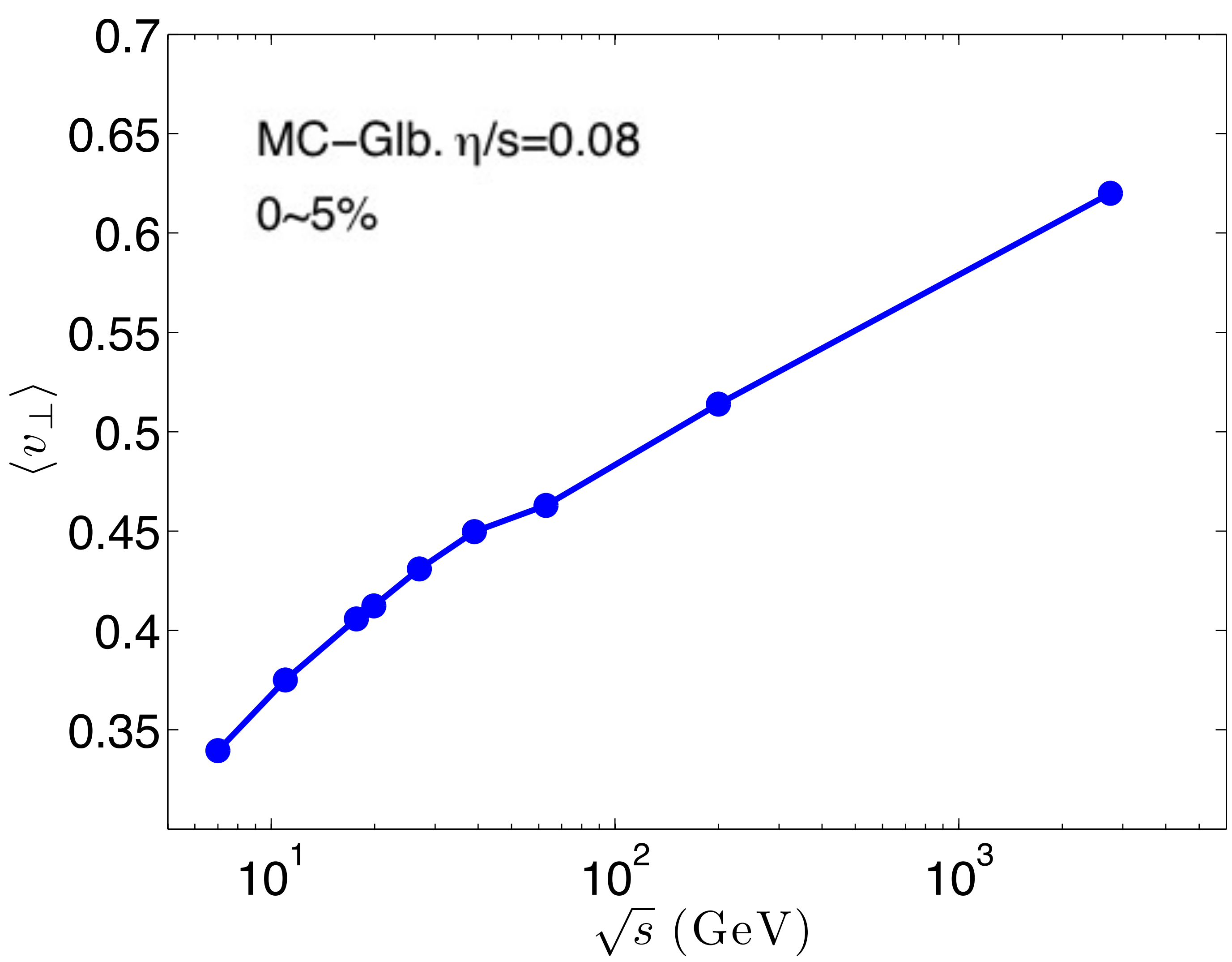

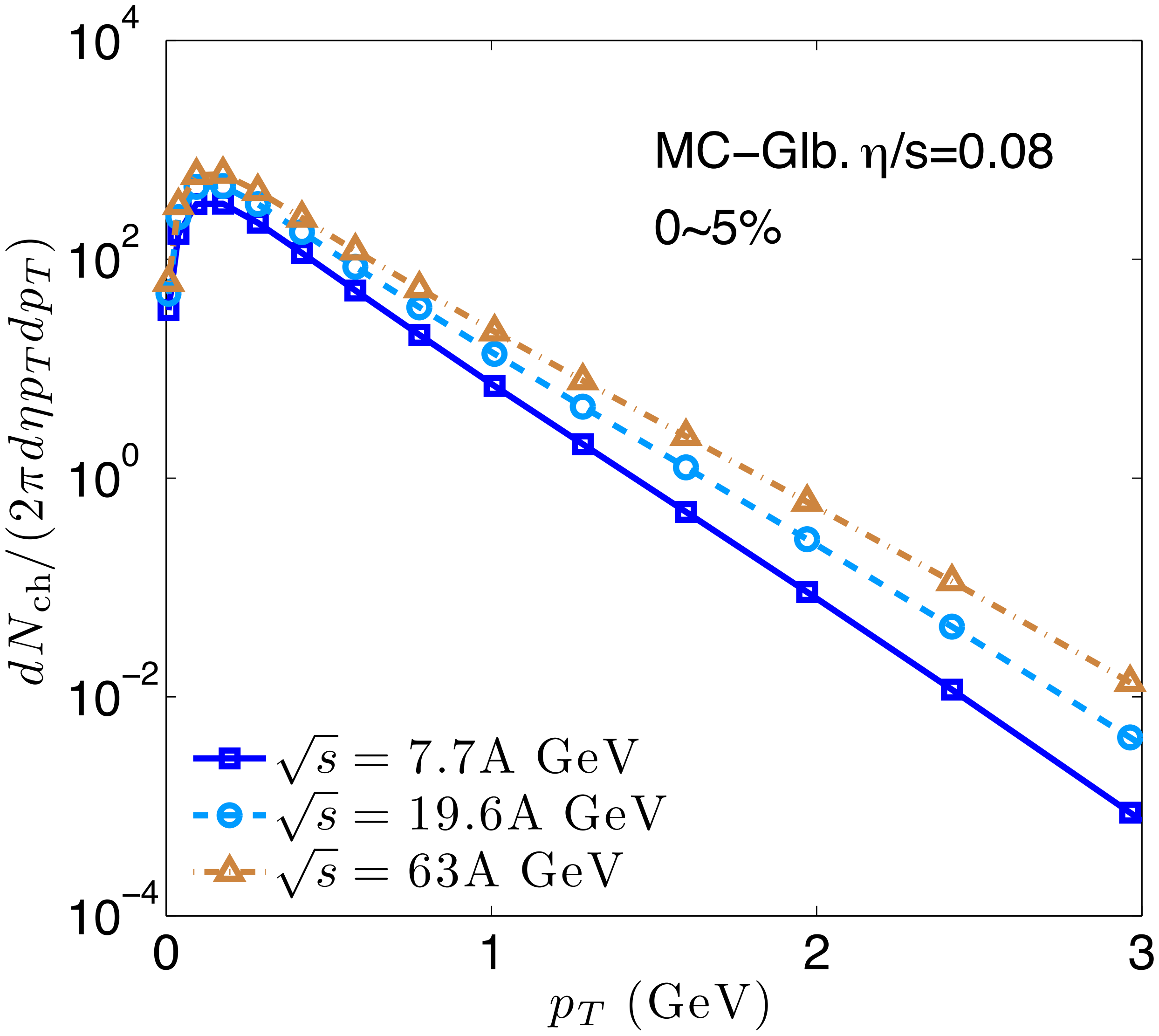

Along with $\sqrt{s}$

average radial flow $\langle v_\perp \rangle$ increases by 80%

the slope of particle p_T-spectra gets flatter

radial flow and particle p_T-spectra

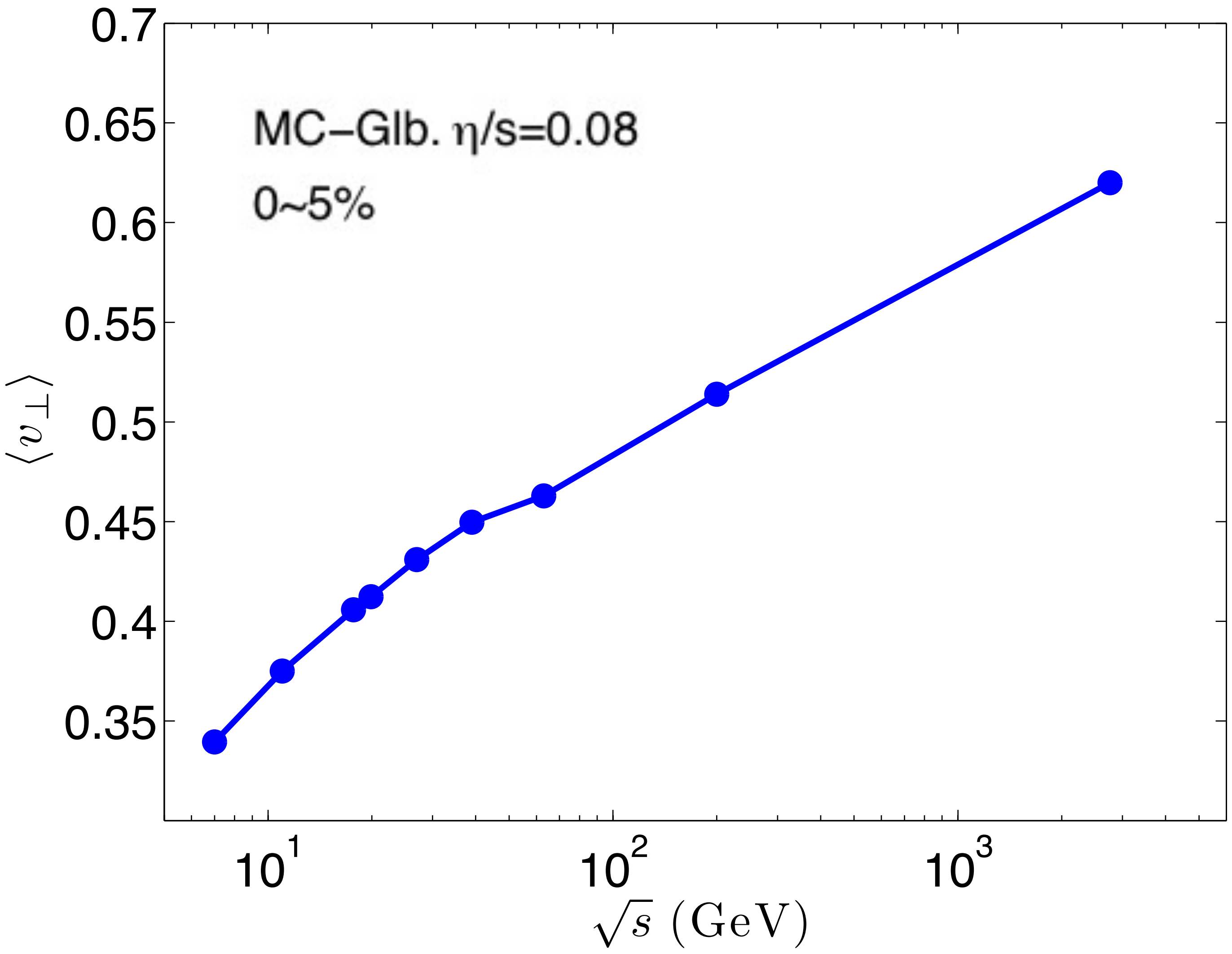

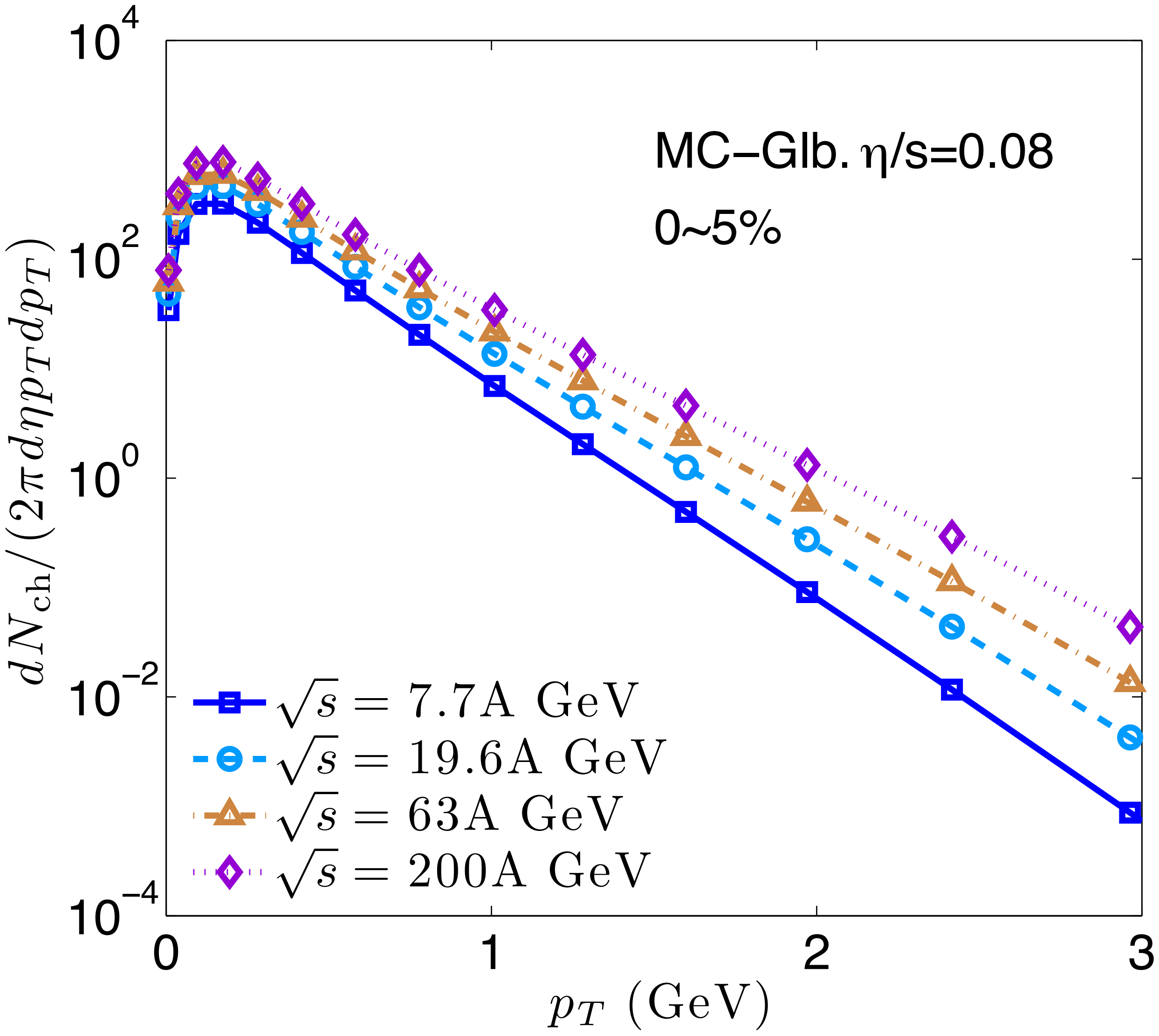

Along with $\sqrt{s}$

average radial flow $\langle v_\perp \rangle$ increases by 80%

the slope of particle p_T-spectra gets flatter

radial flow and particle p_T-spectra

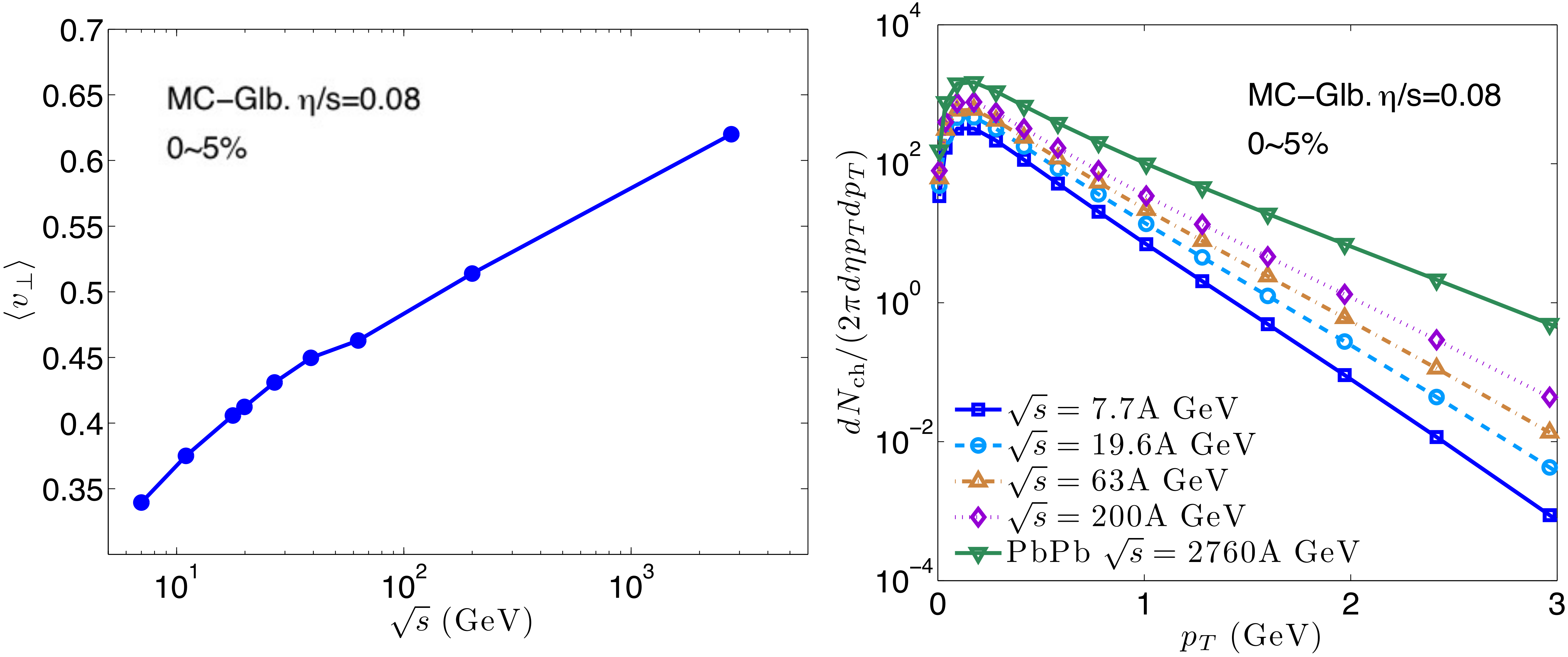

Along with $\sqrt{s}$

average radial flow $\langle v_\perp \rangle$ increases by 80%

the slope of particle p_T-spectra gets flatter

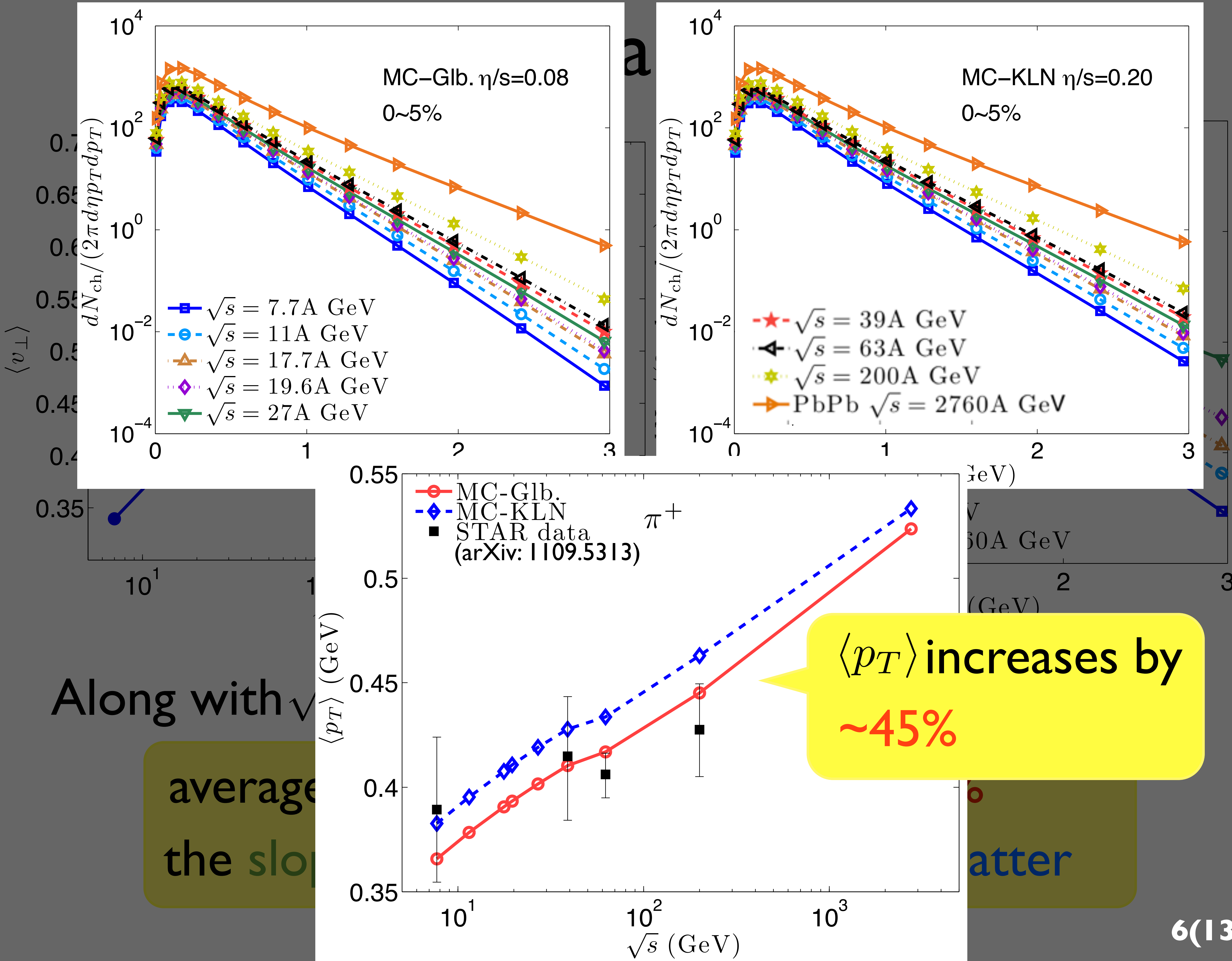

$\langle p_T \rangle$ increases by ~45%

Along with $\sqrt{}$

average

the slo

atter

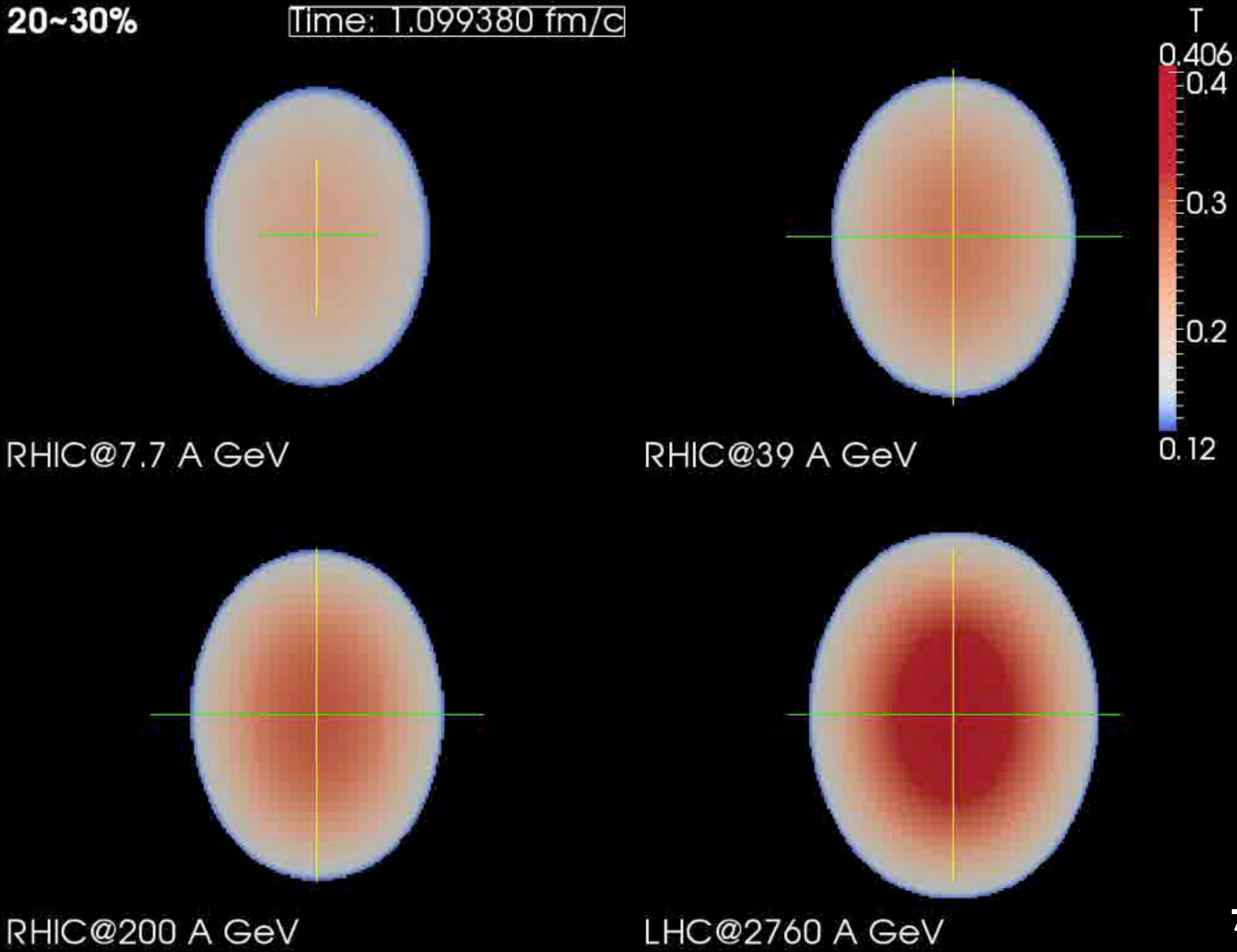
20~30%
Time: 1.099380 fm/c
T
0.406
0.4
0.3
0.2
0.12
RHIC@7.7 A GeV
RHIC@39 A GeV
RHIC@200 A GeV
LHC@2760 A GeV

Elliptic flow

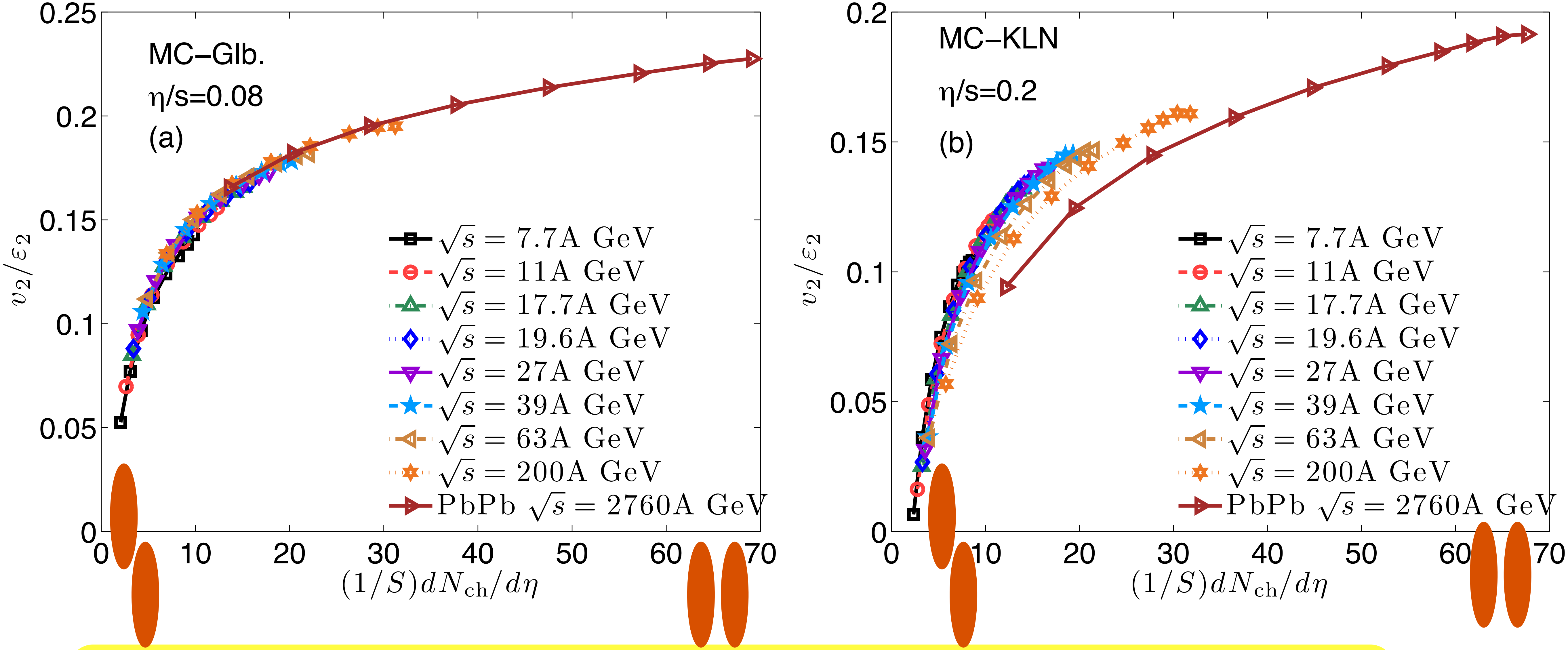

Good $\sqrt{s}$ scaling behavior for MC-Glauber model

Scaling breaks in MC-KLN model due to different centrality dependence of overlapping area

Elliptic flow

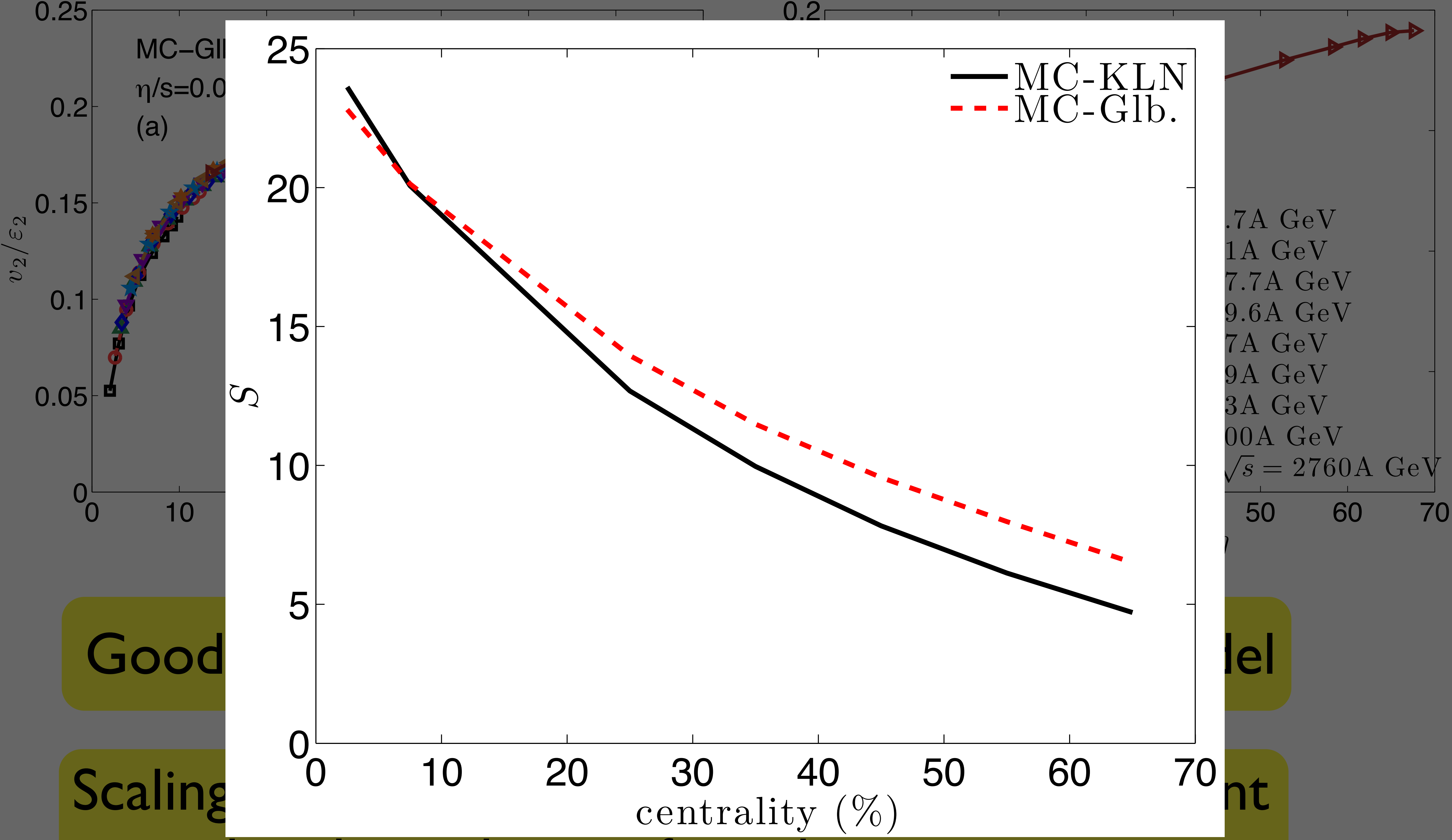

Good del

Scaling nt
centrality dependence of overlapping area

Elliptic flow

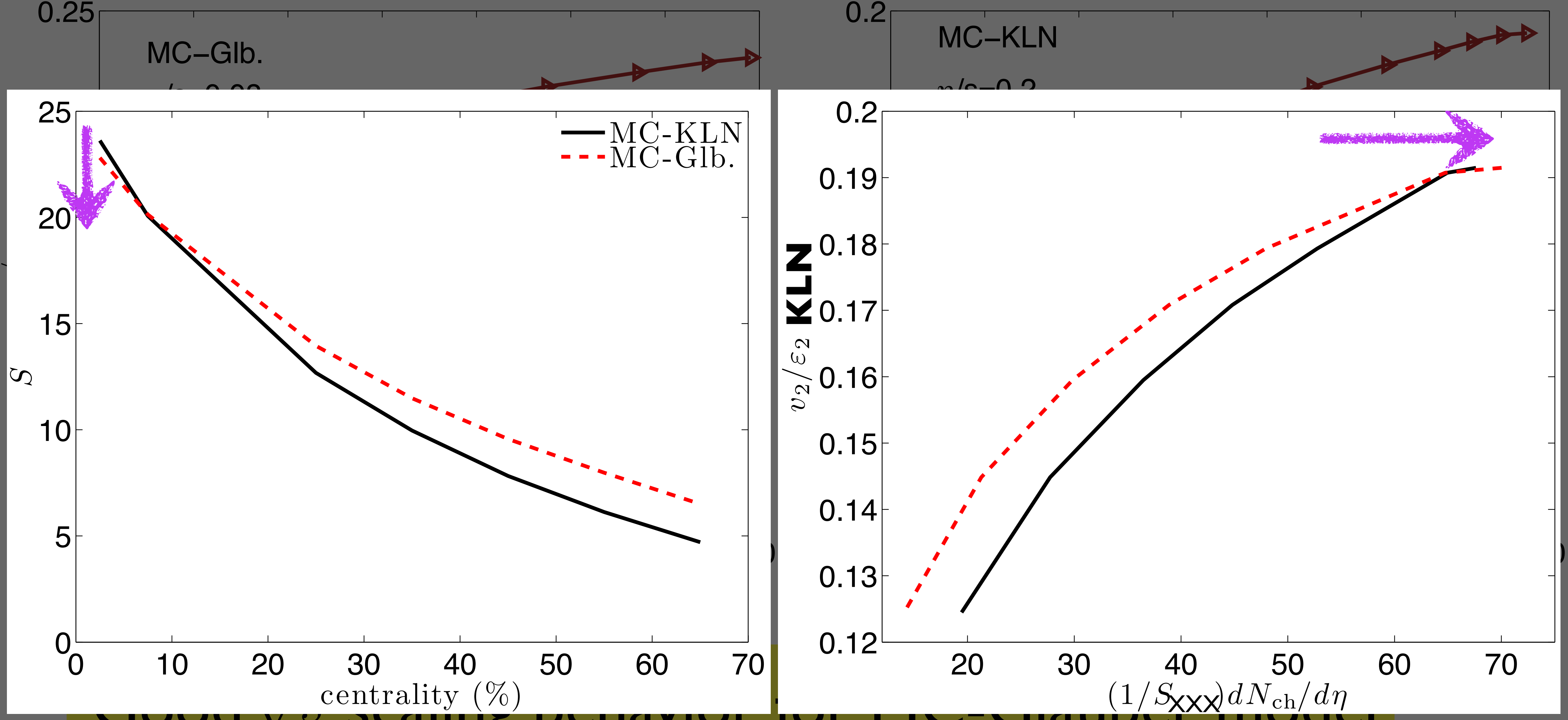

Good $\sqrt{S}$ scaling behavior for MC-Glauber model

Scaling breaks in MC-KLN model due to different centrality dependence of overlapping area

Elliptic flow

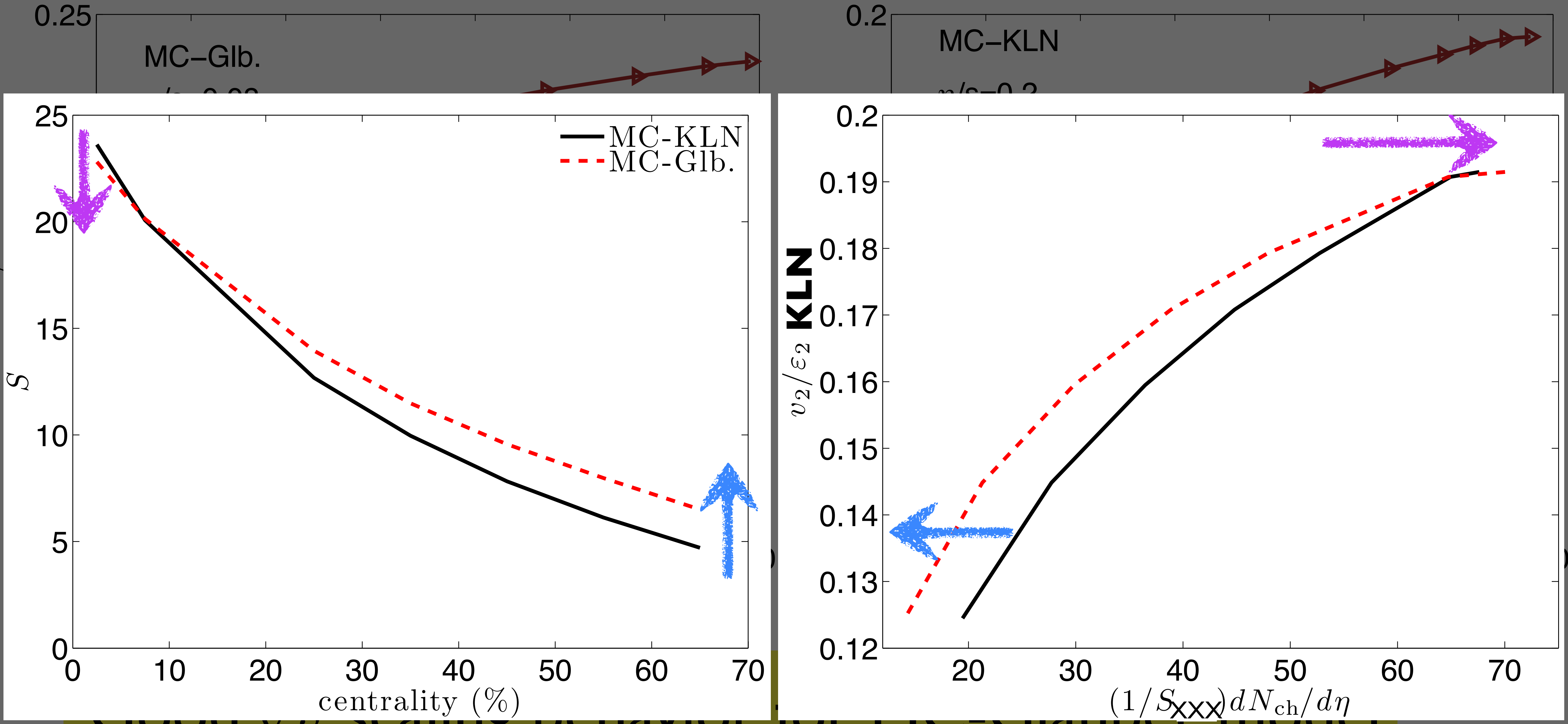

Good $\sqrt{s}$ scaling behavior for MC-Glauber model

Scaling breaks in MC-KLN model due to different centrality dependence of overlapping area

otic flow

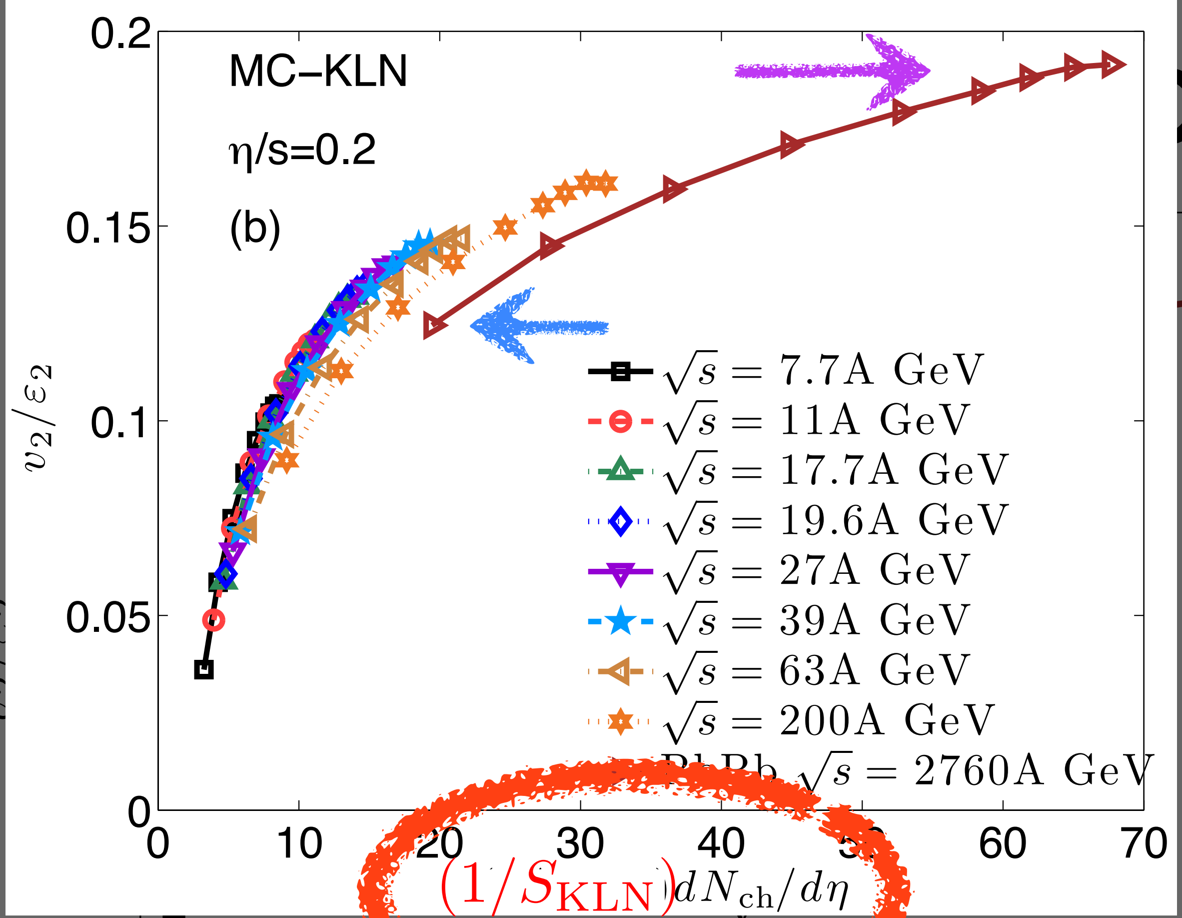

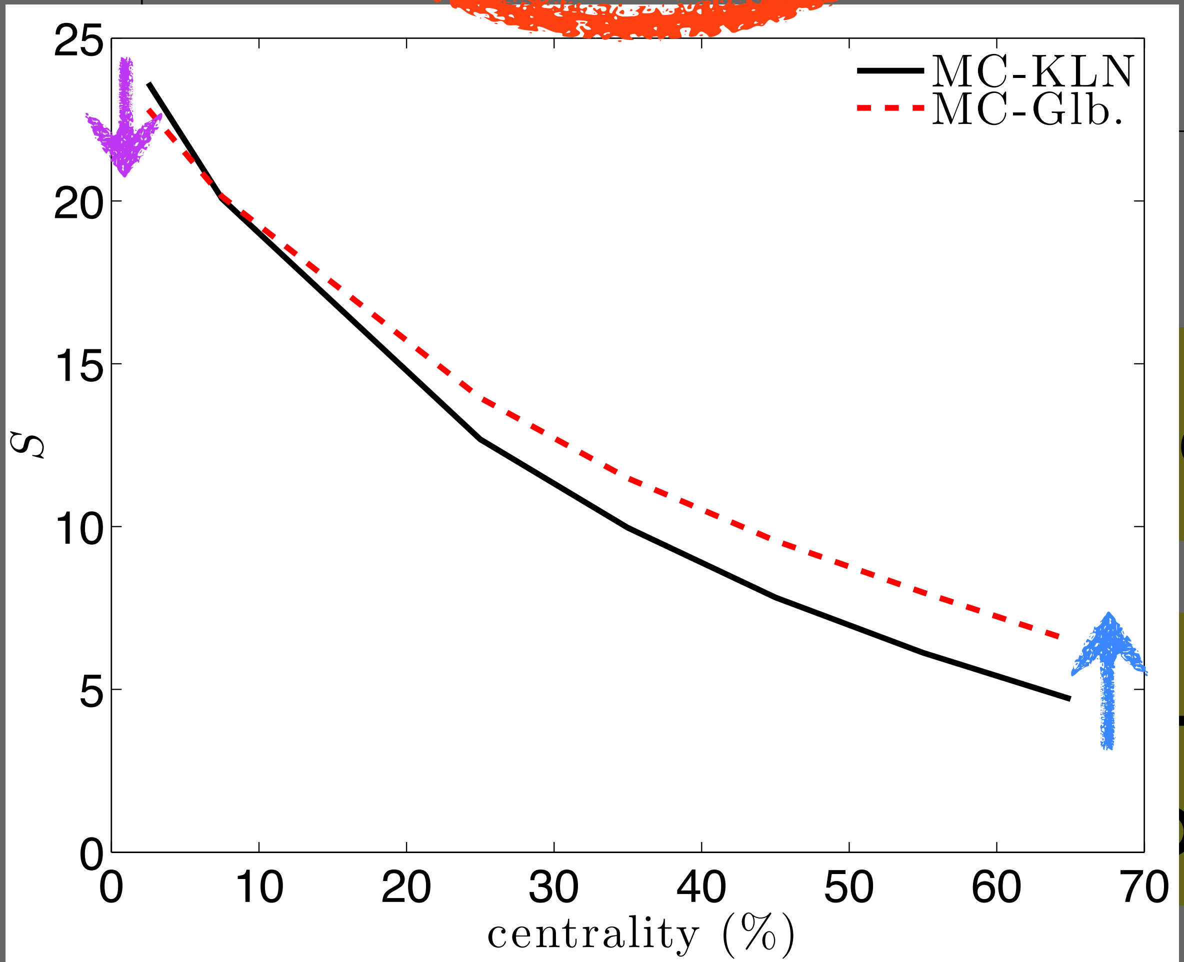

o

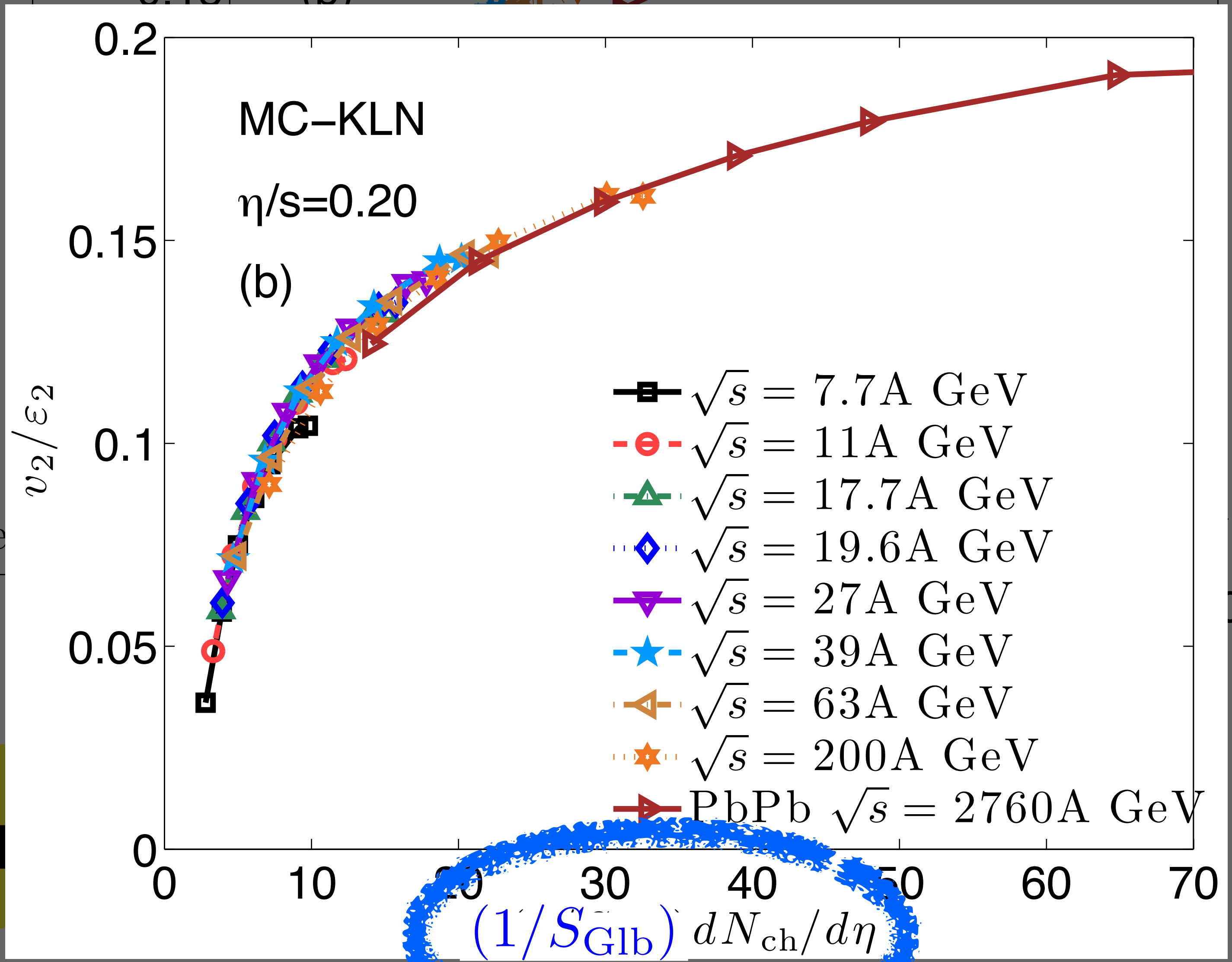

LN model due to different
f overlapping area

Differential $v_2(p_T)$

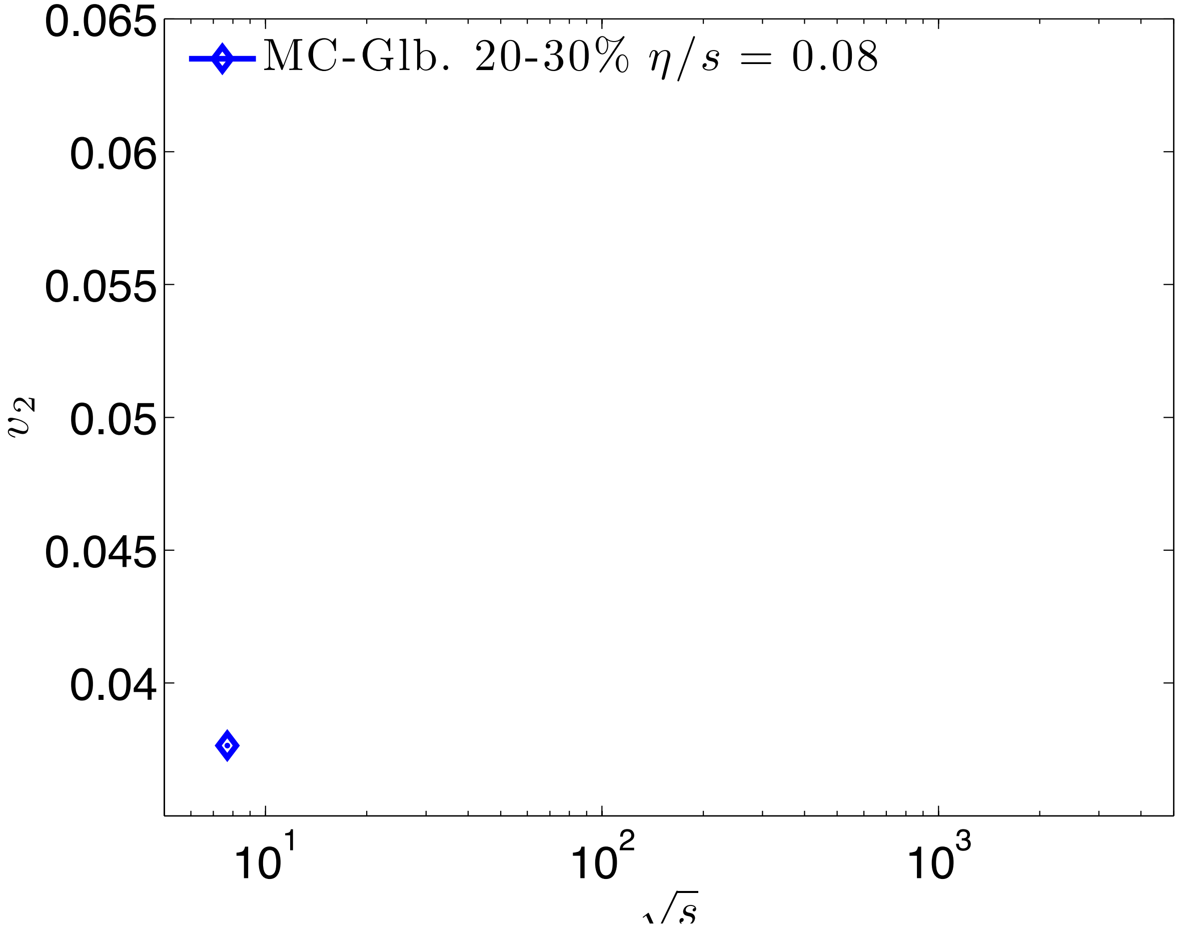

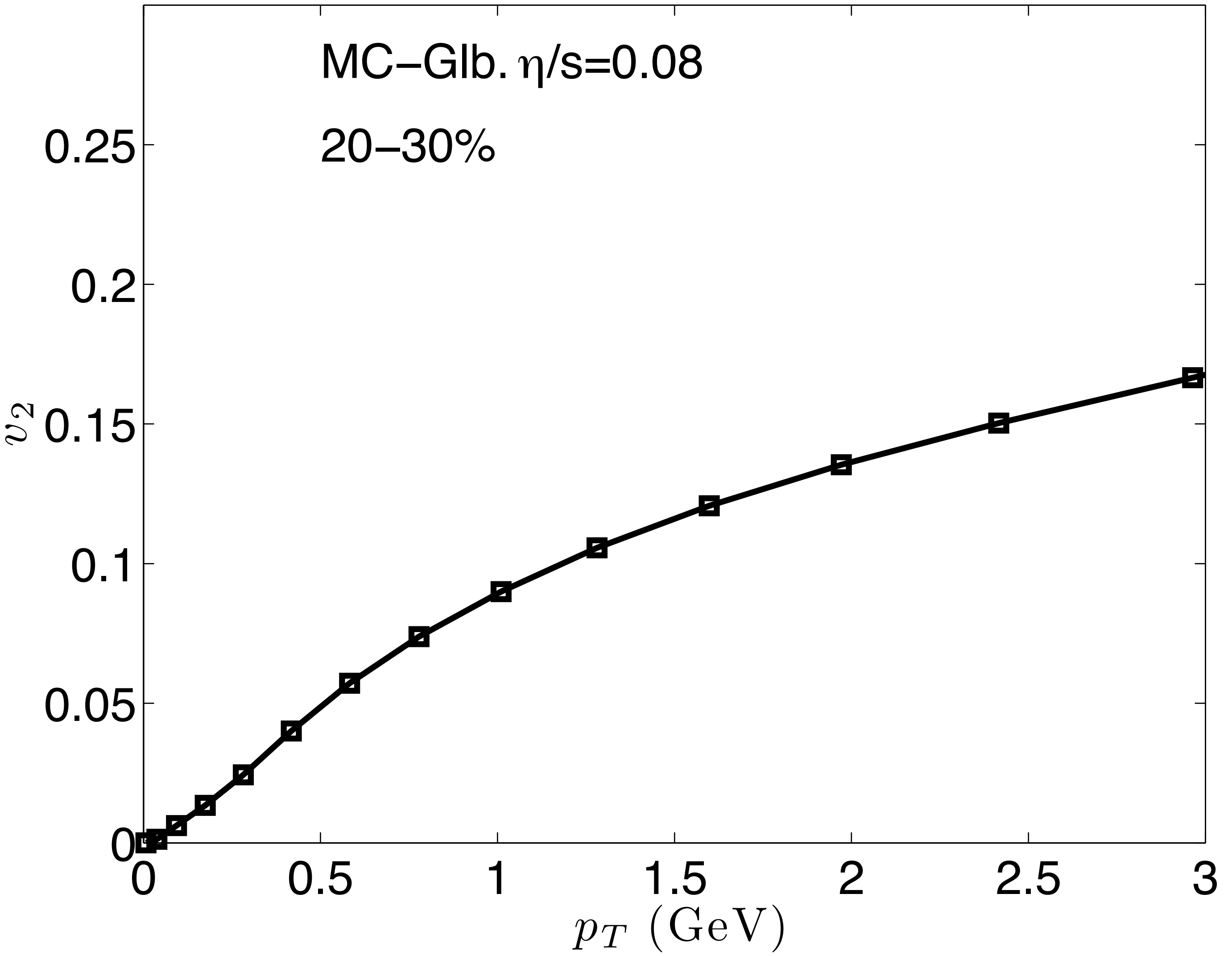

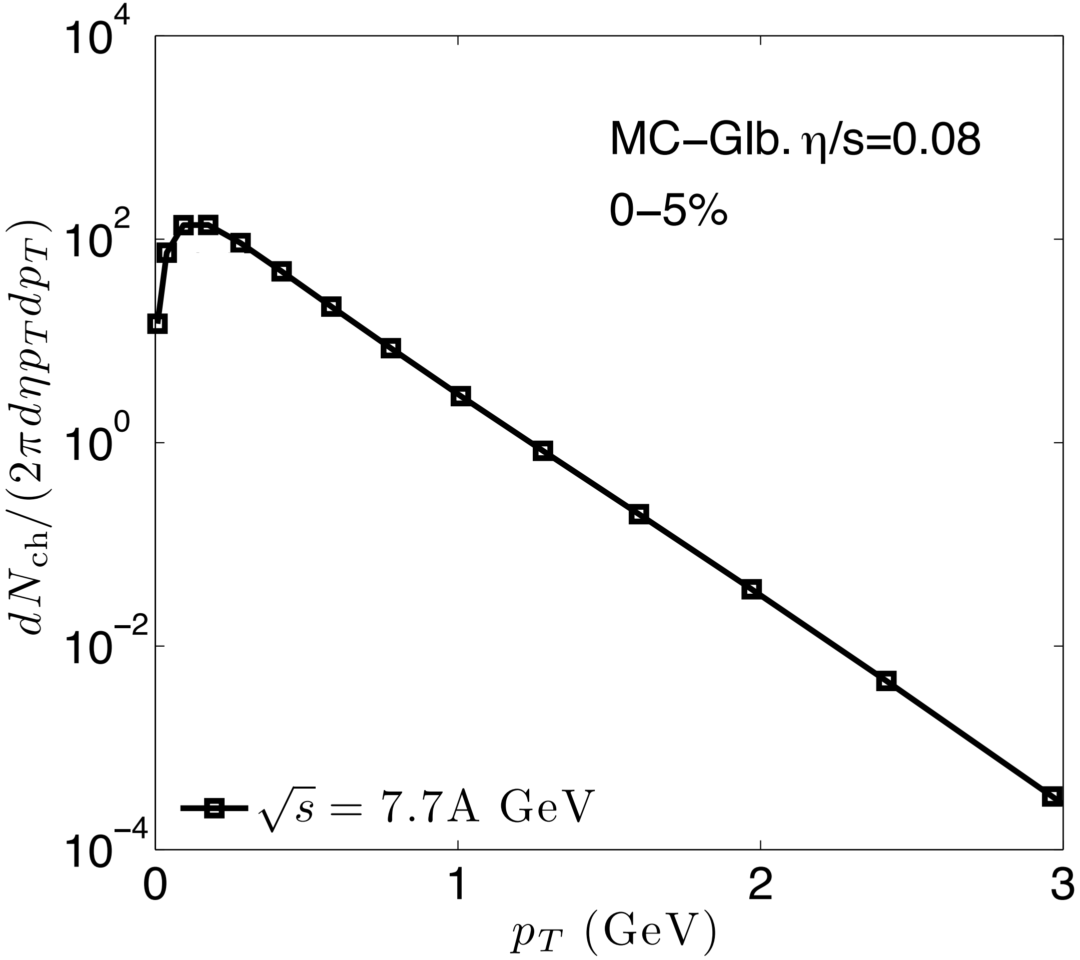

Differential $v_2(p_T)$

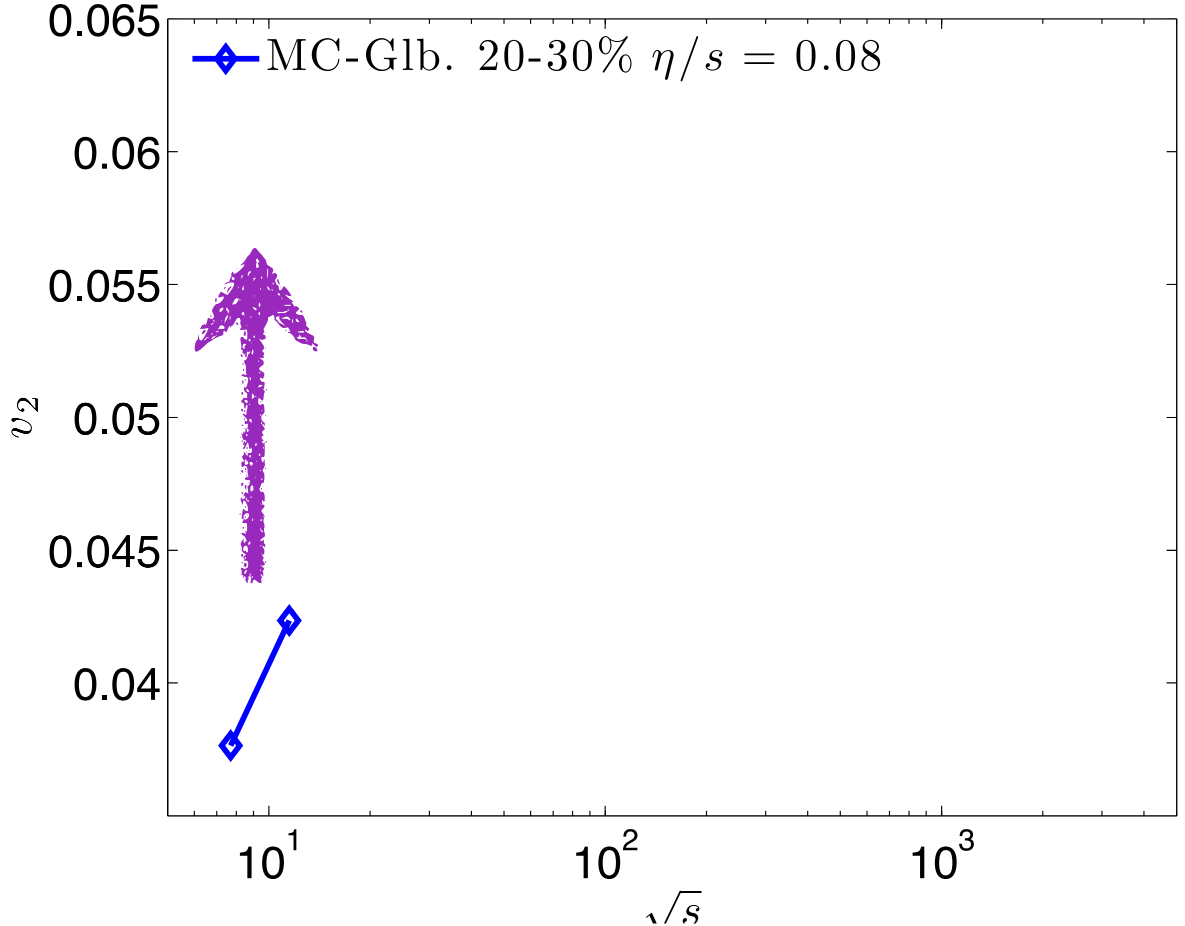

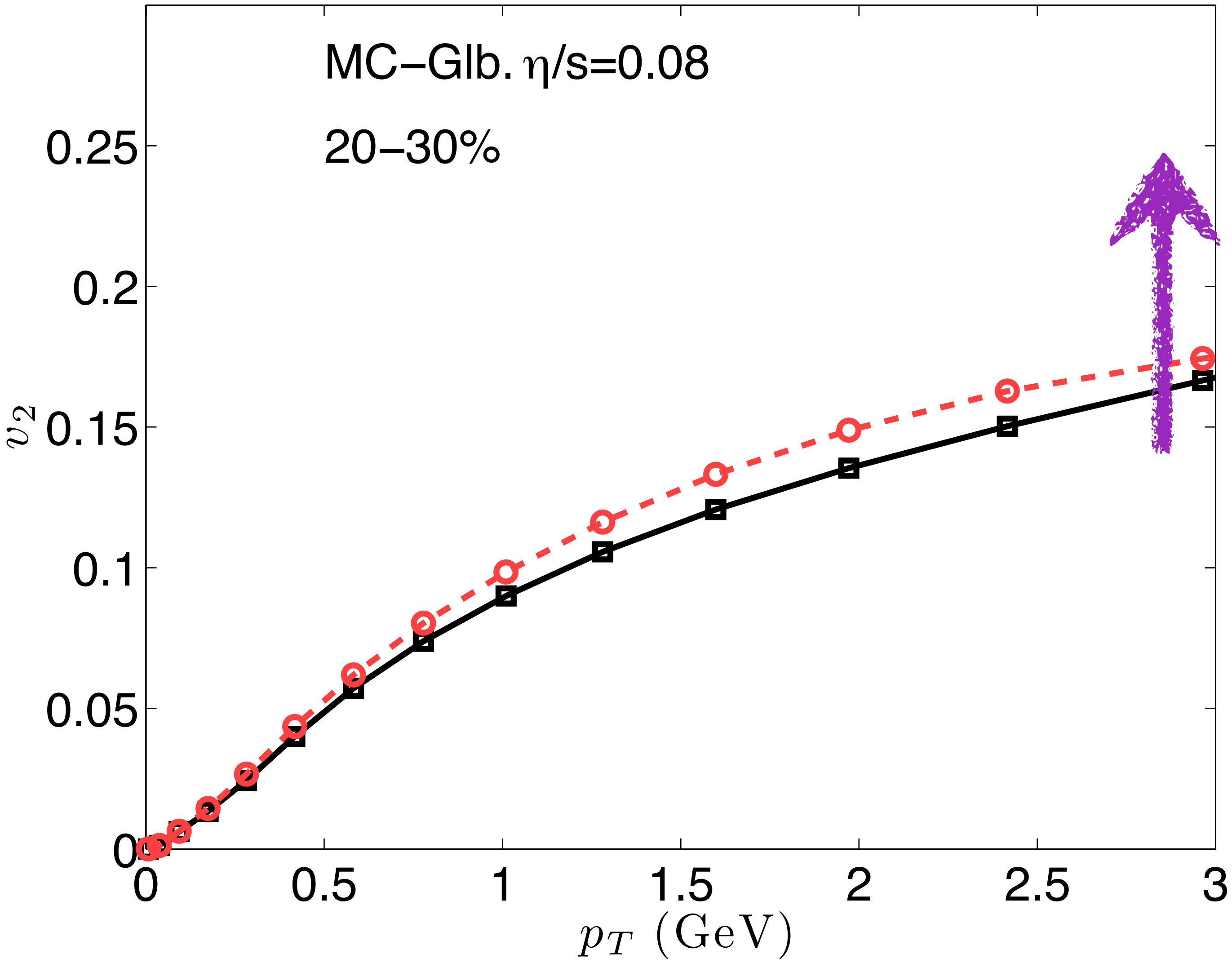

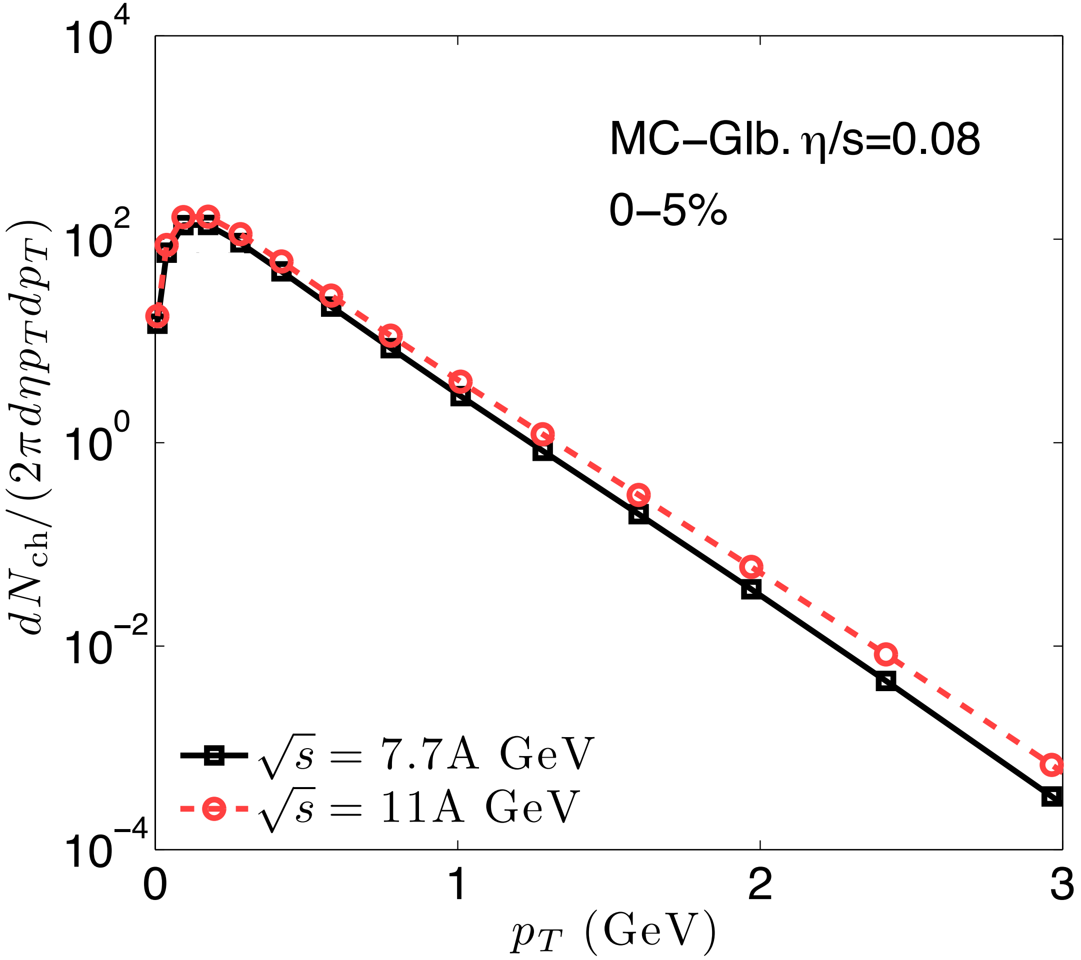

Differential $v_2(p_T)$

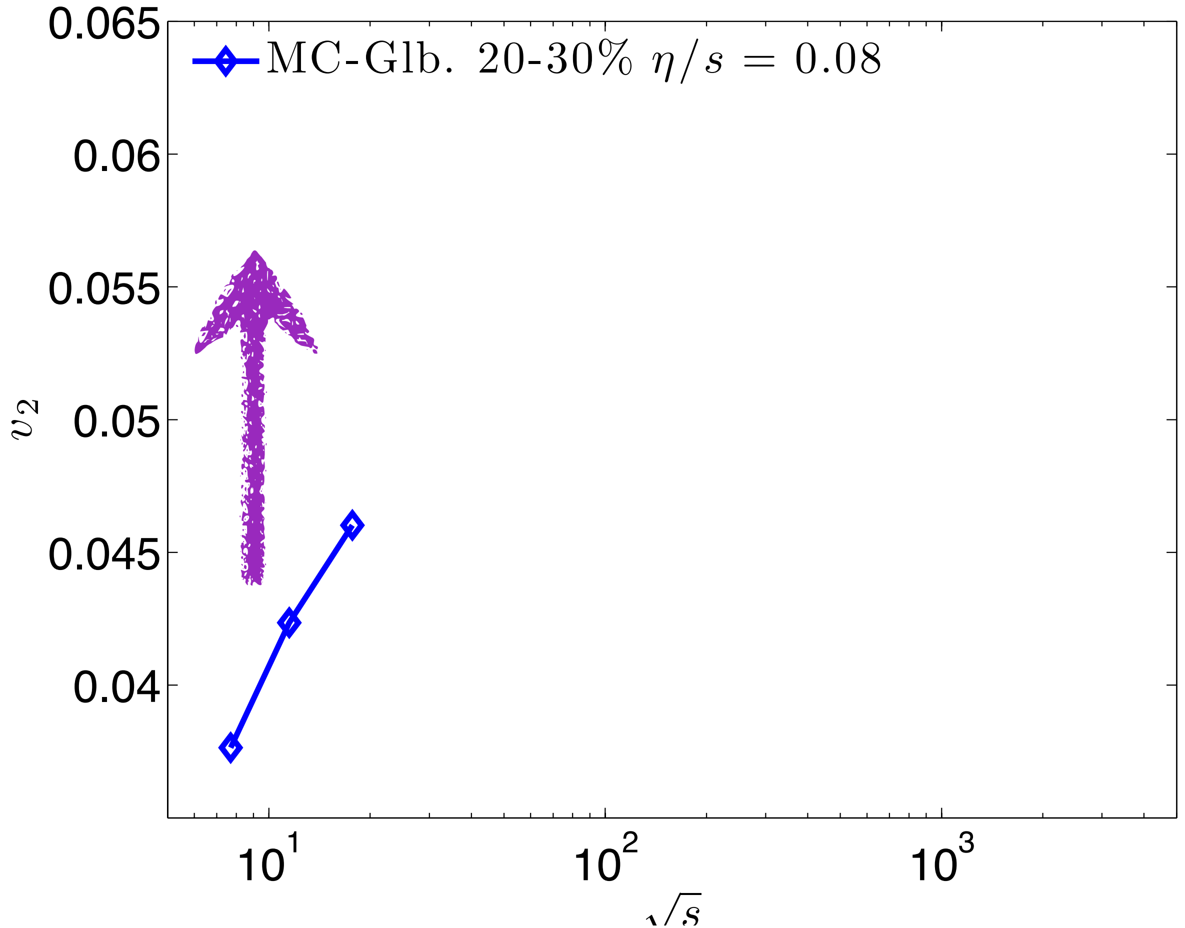

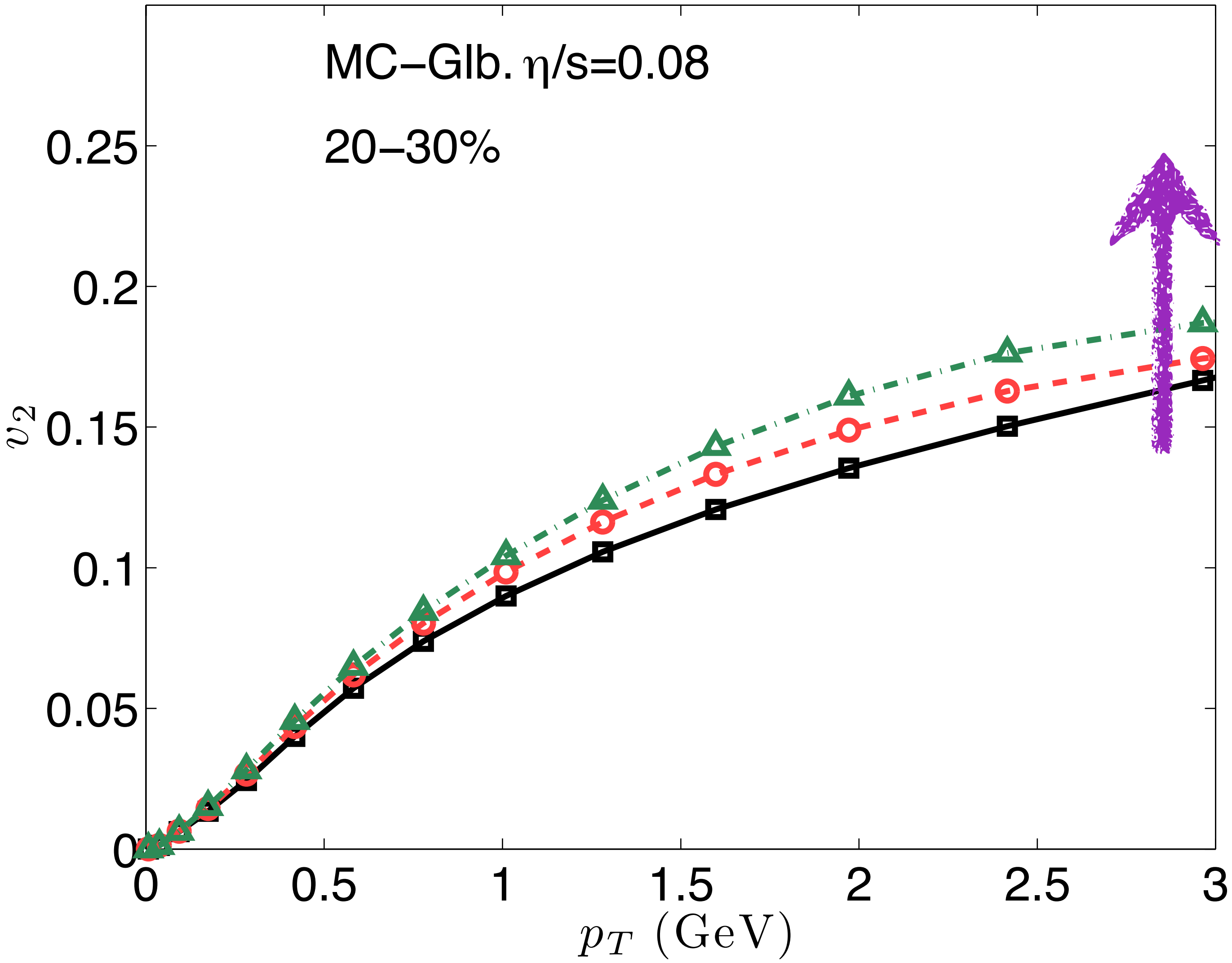

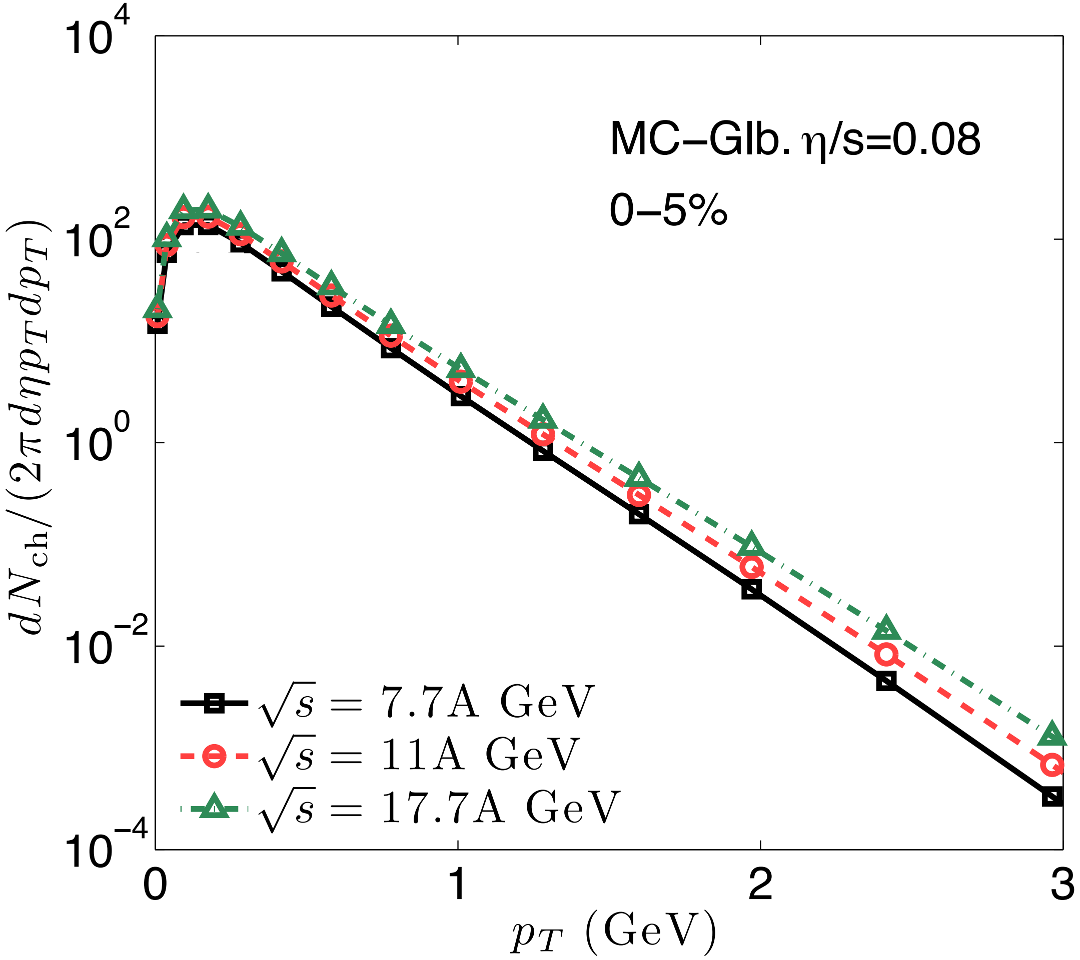

Differential $v_2(p_T)$

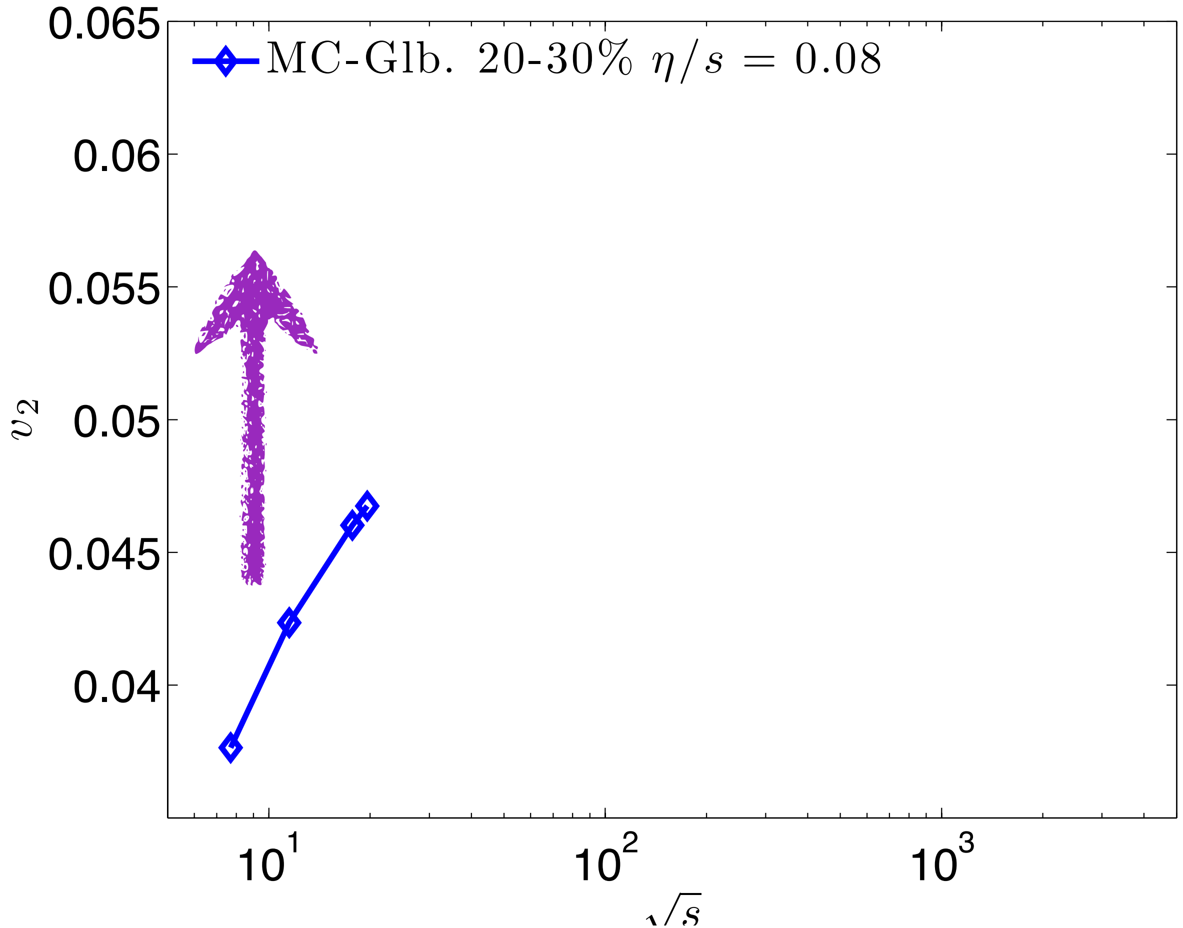

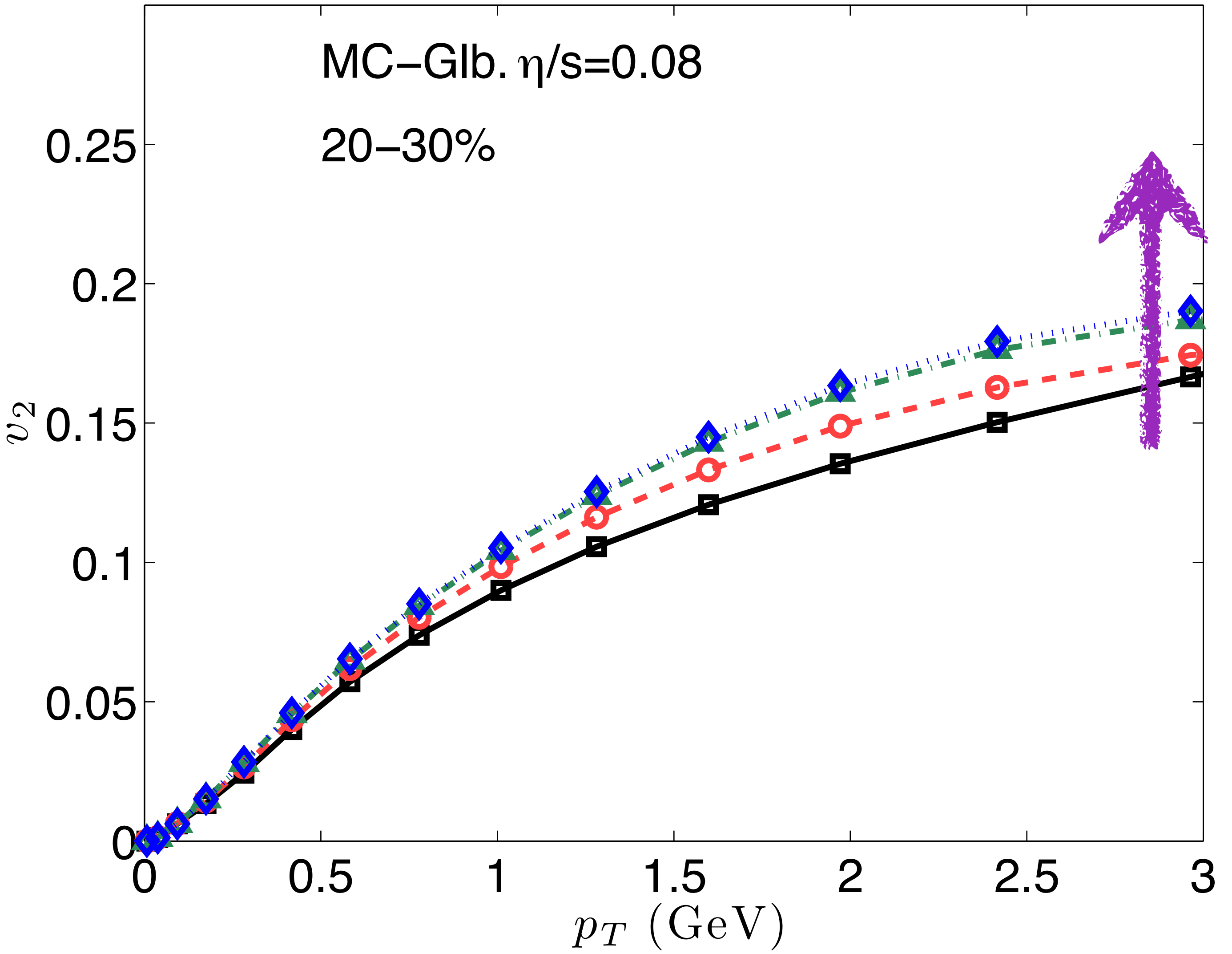

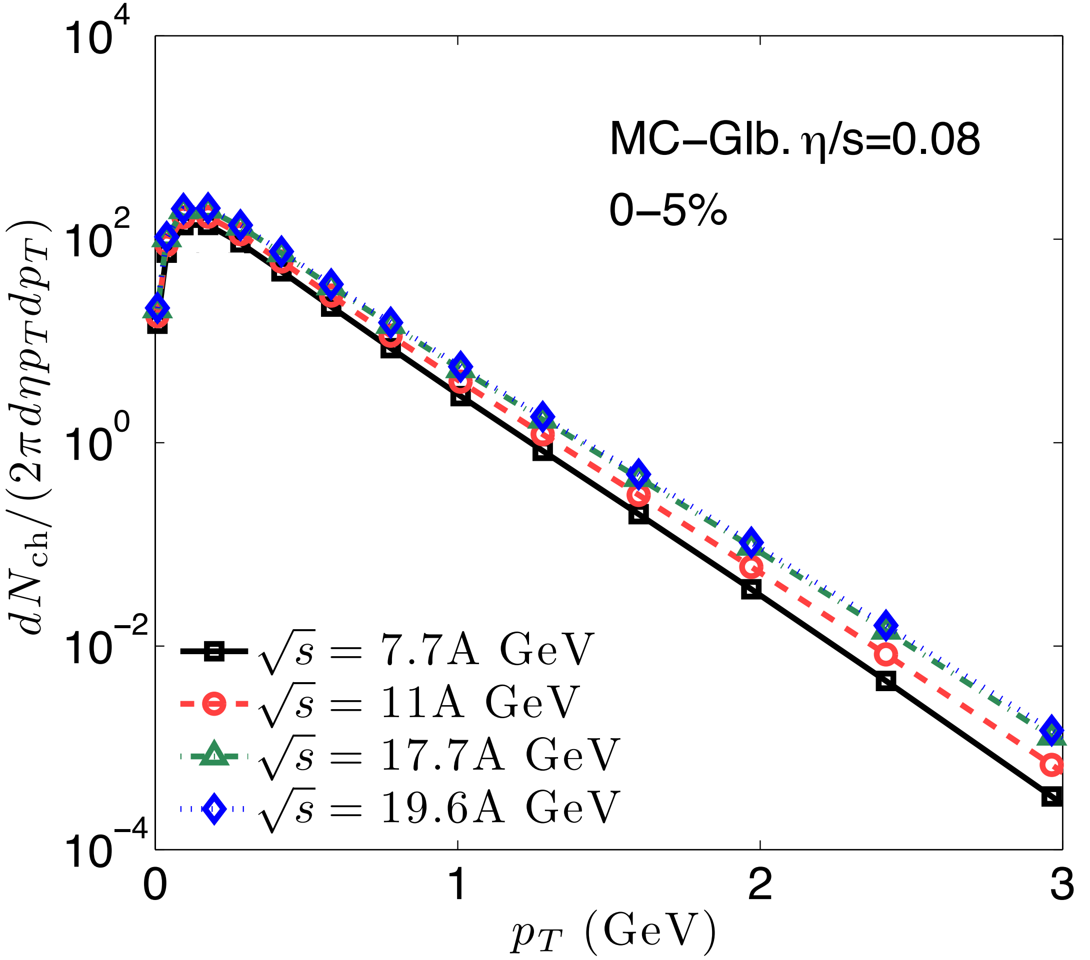

Differential $v_2(p_T)$

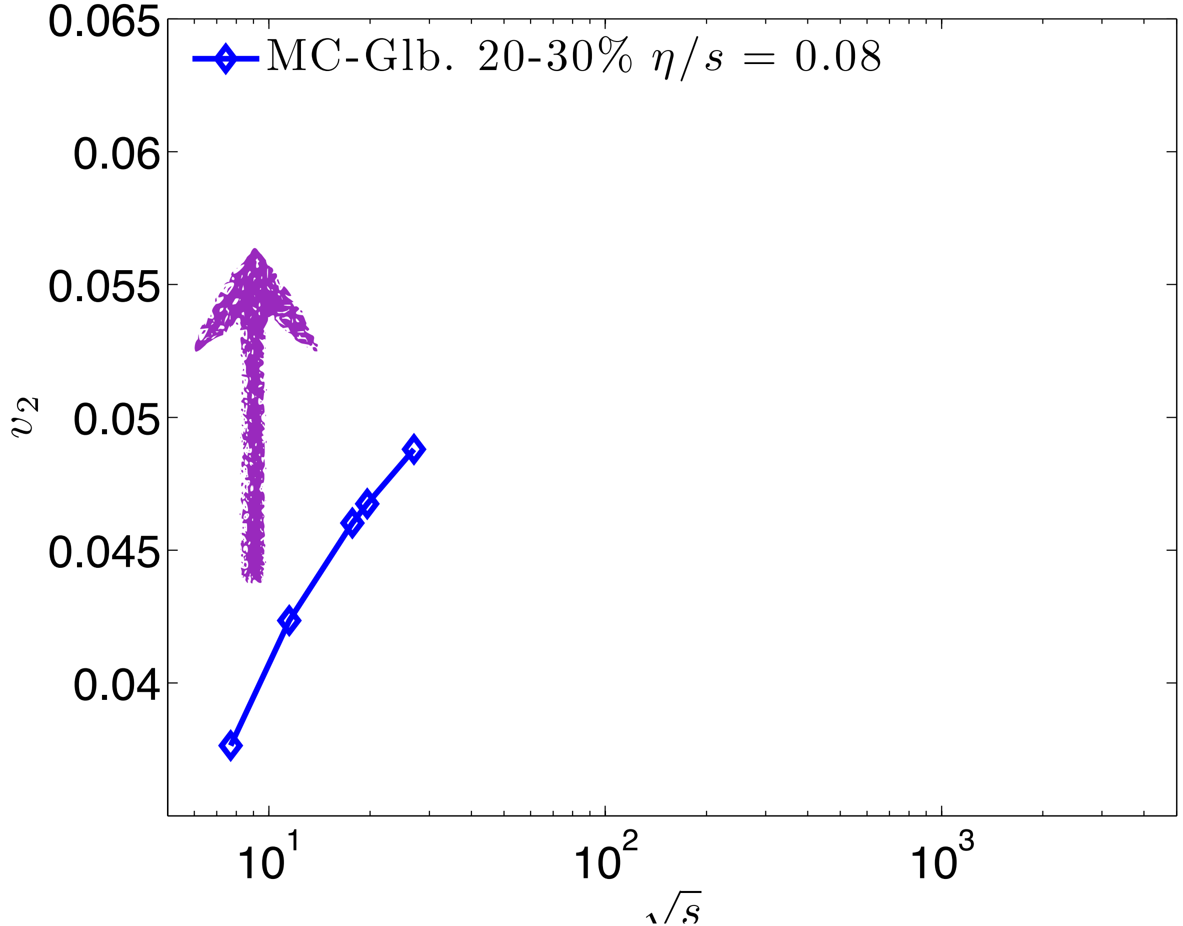

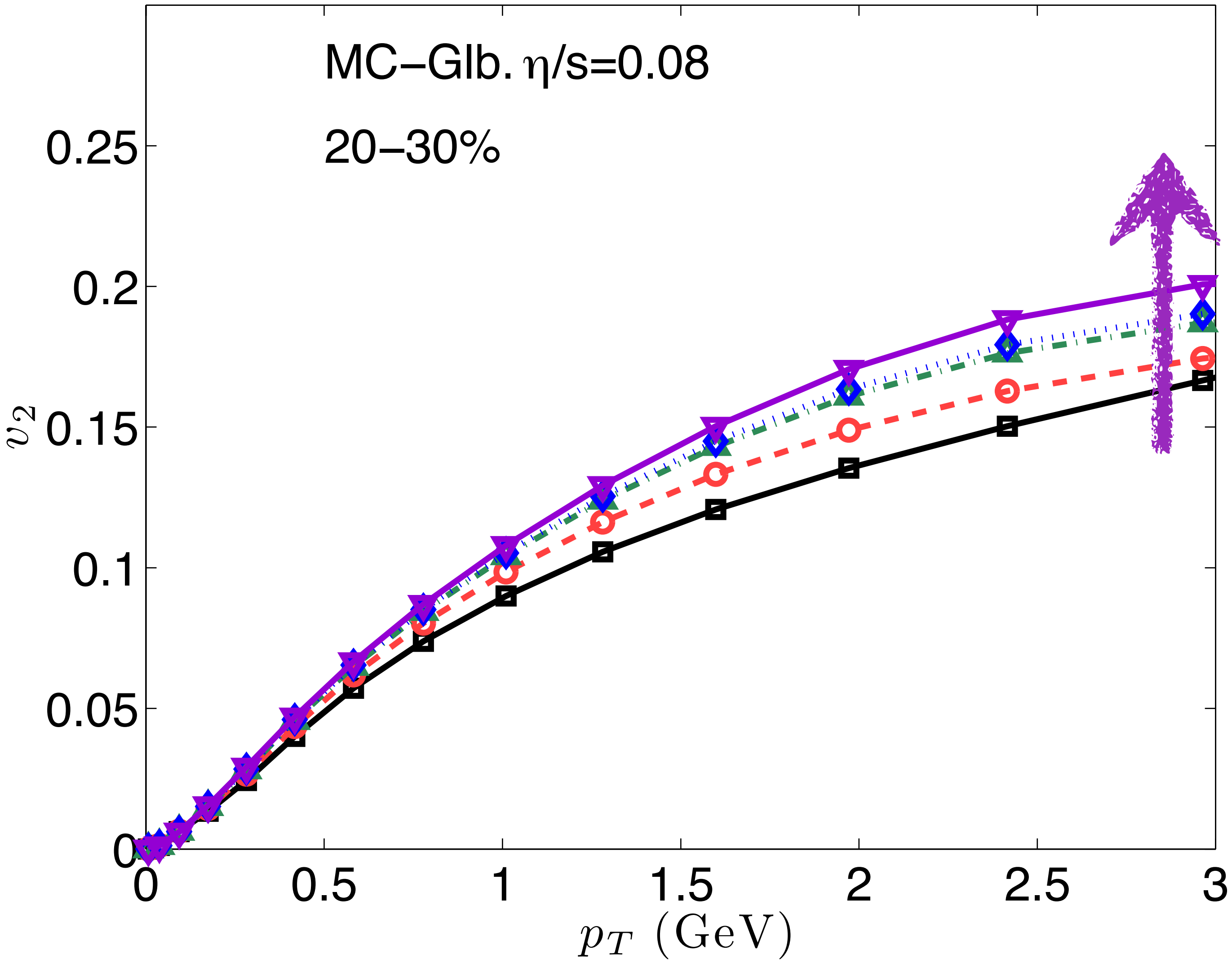

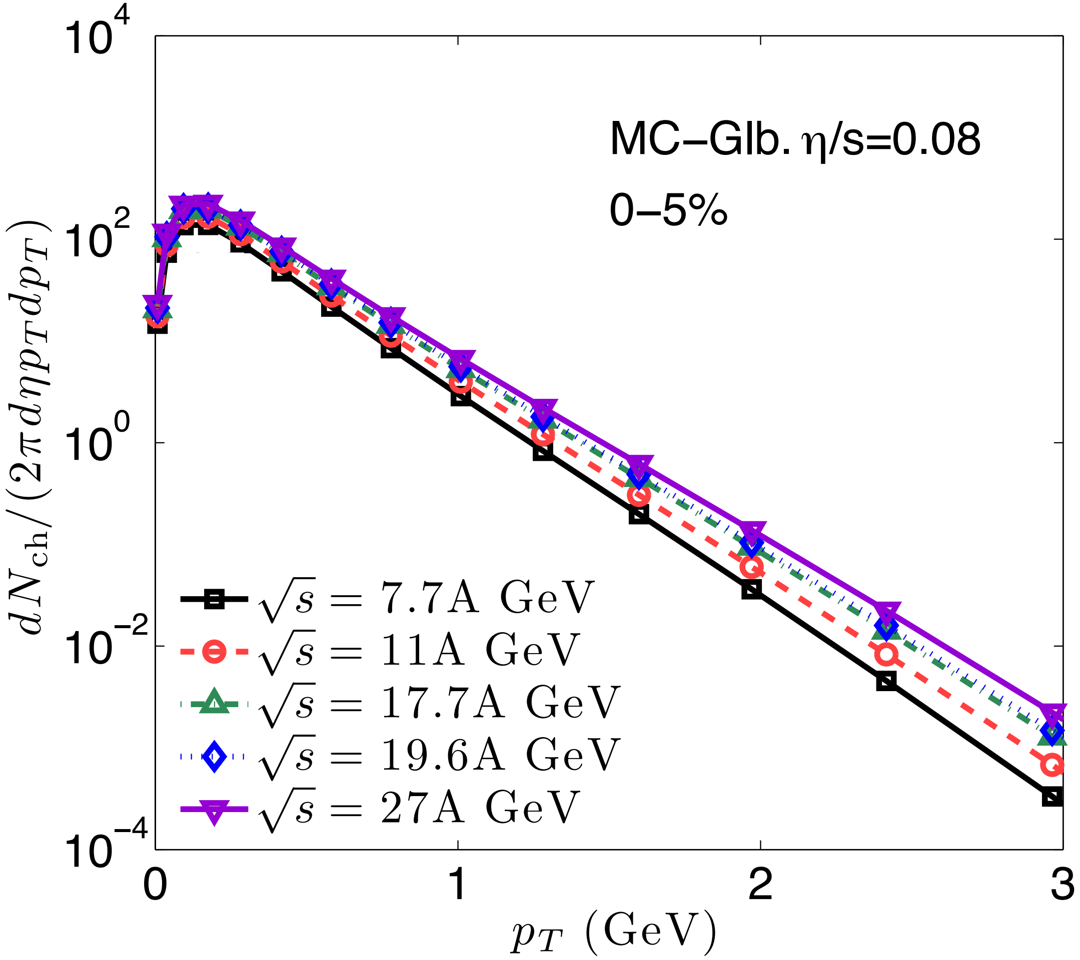

Differential $v_2(p_T)$

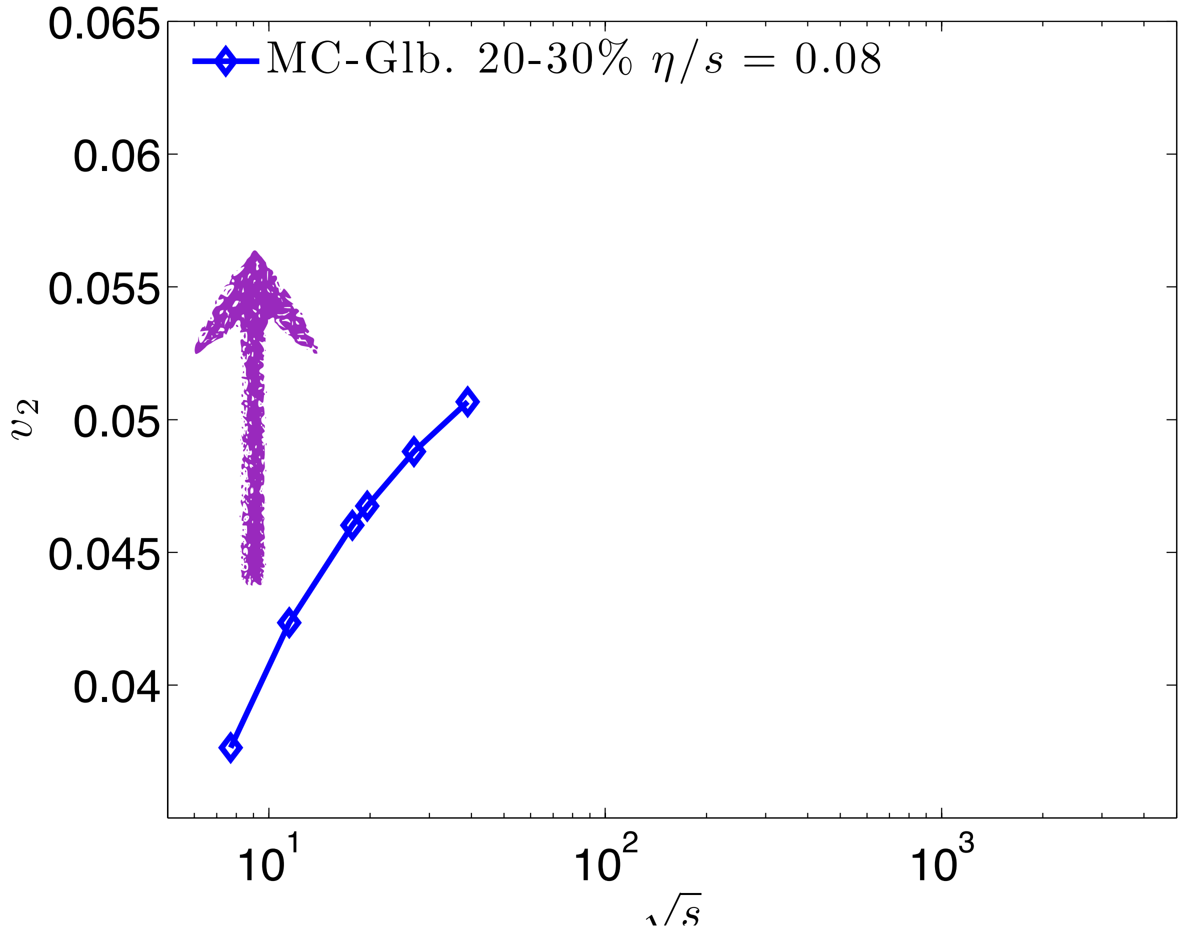

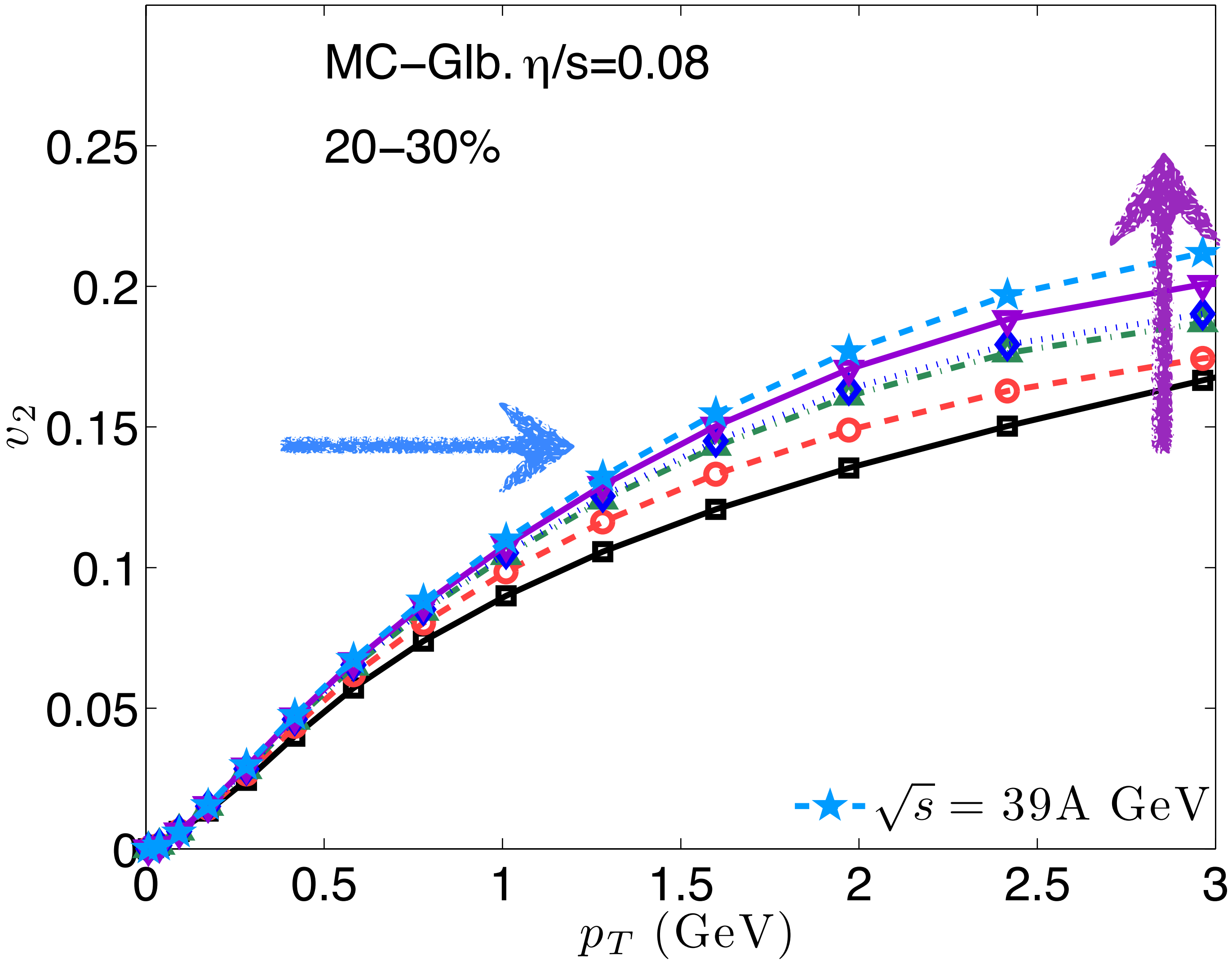

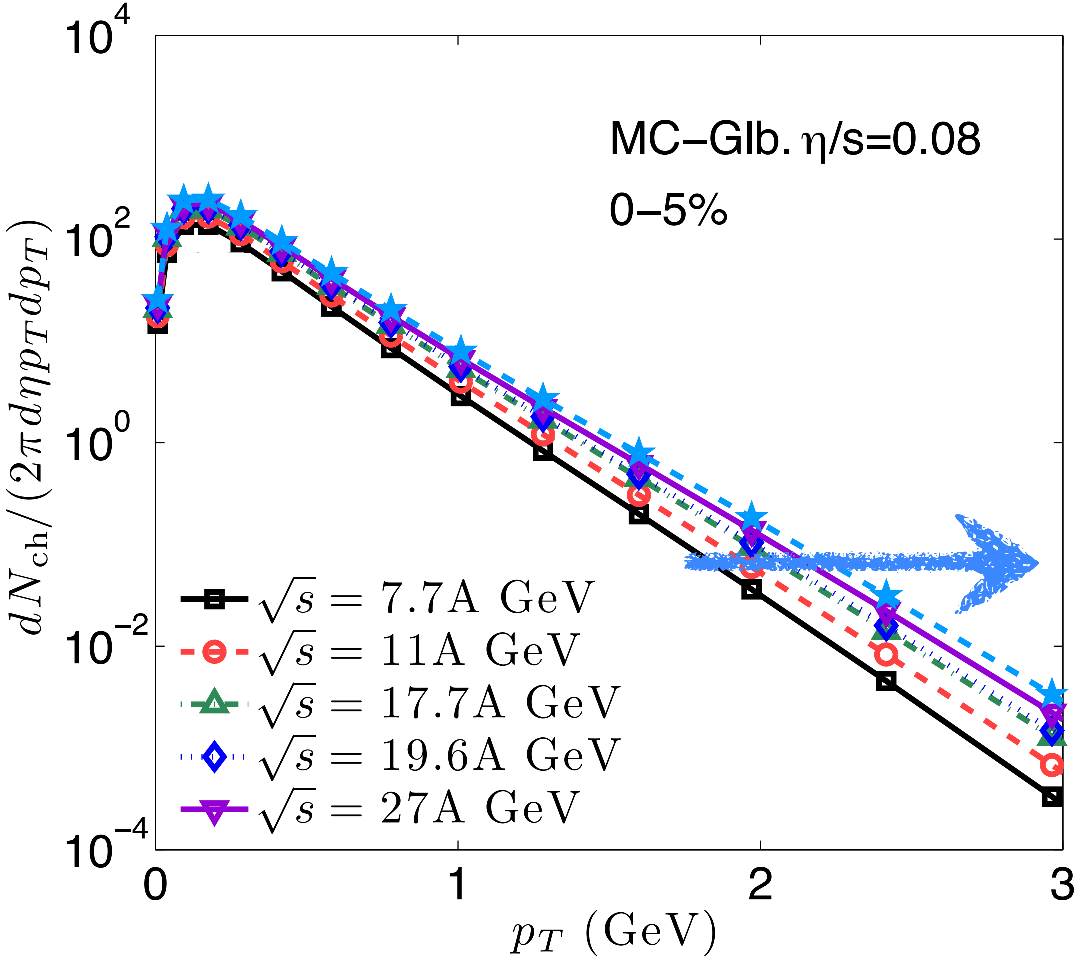

Differential v_2(p_T)

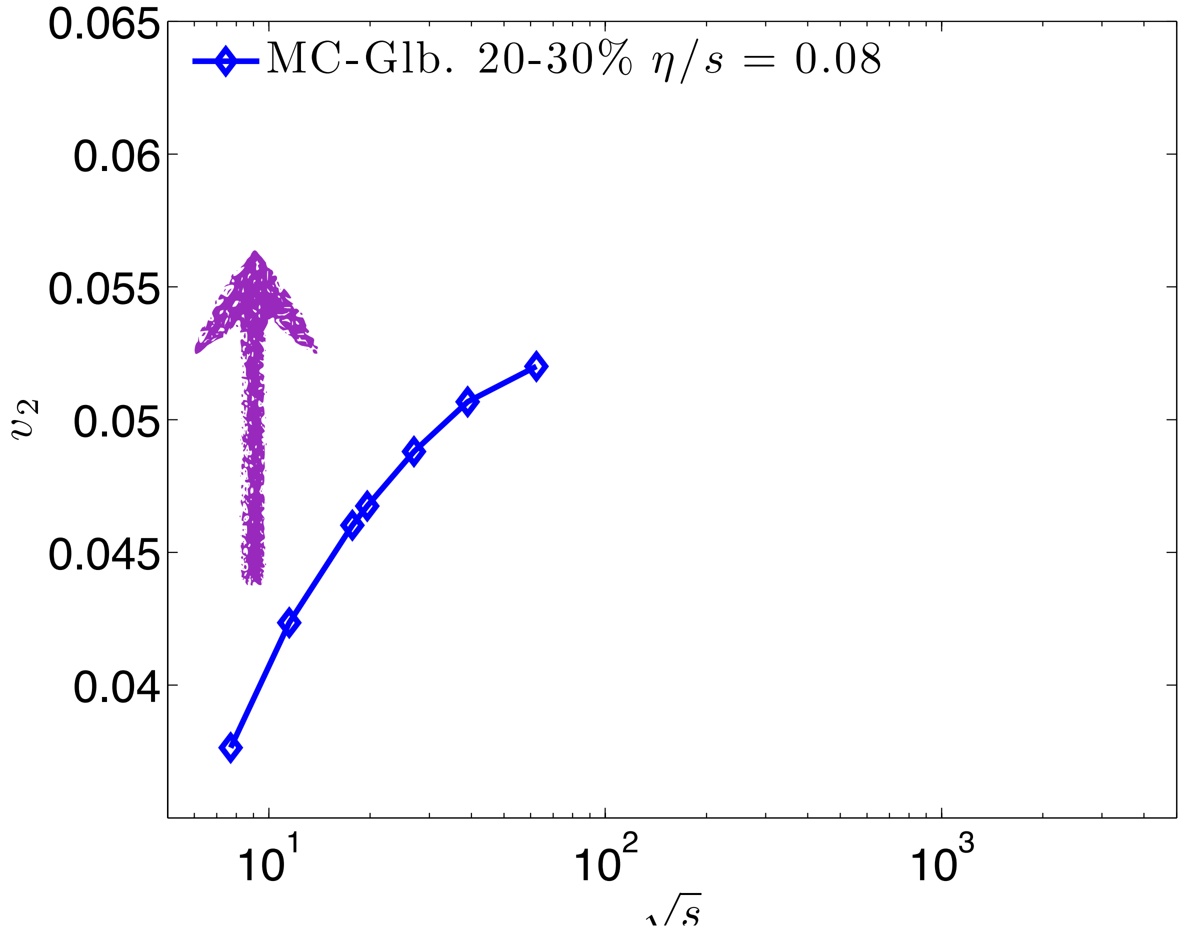

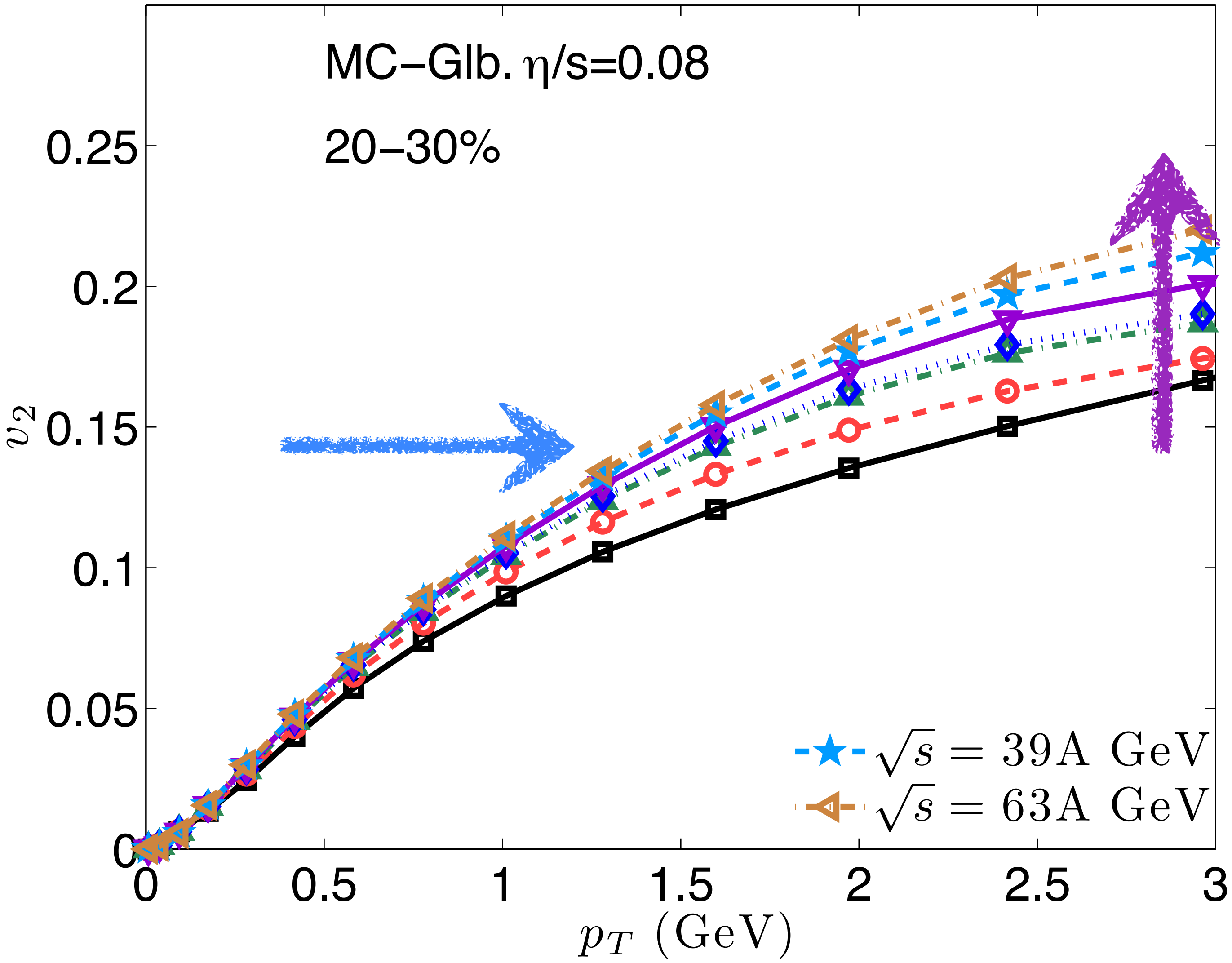

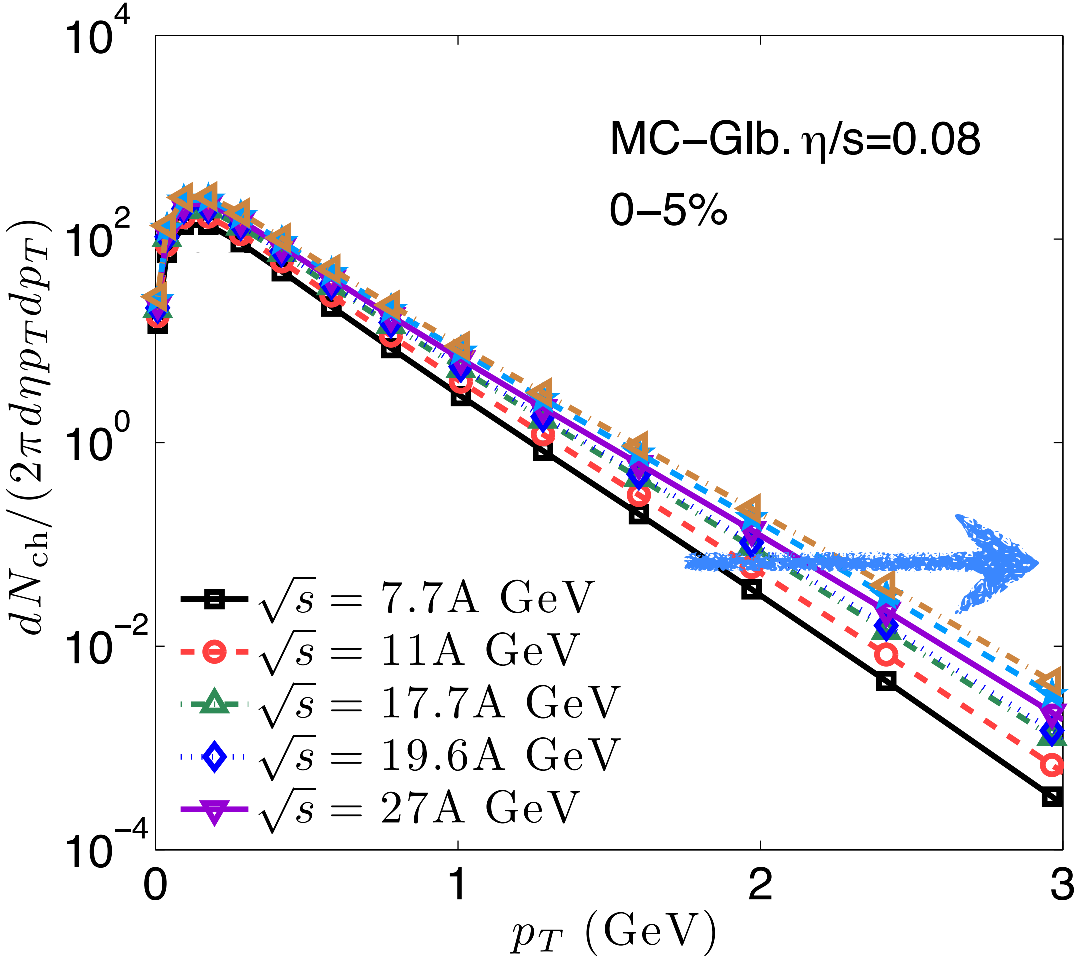

Differential $v_2(p_T)$

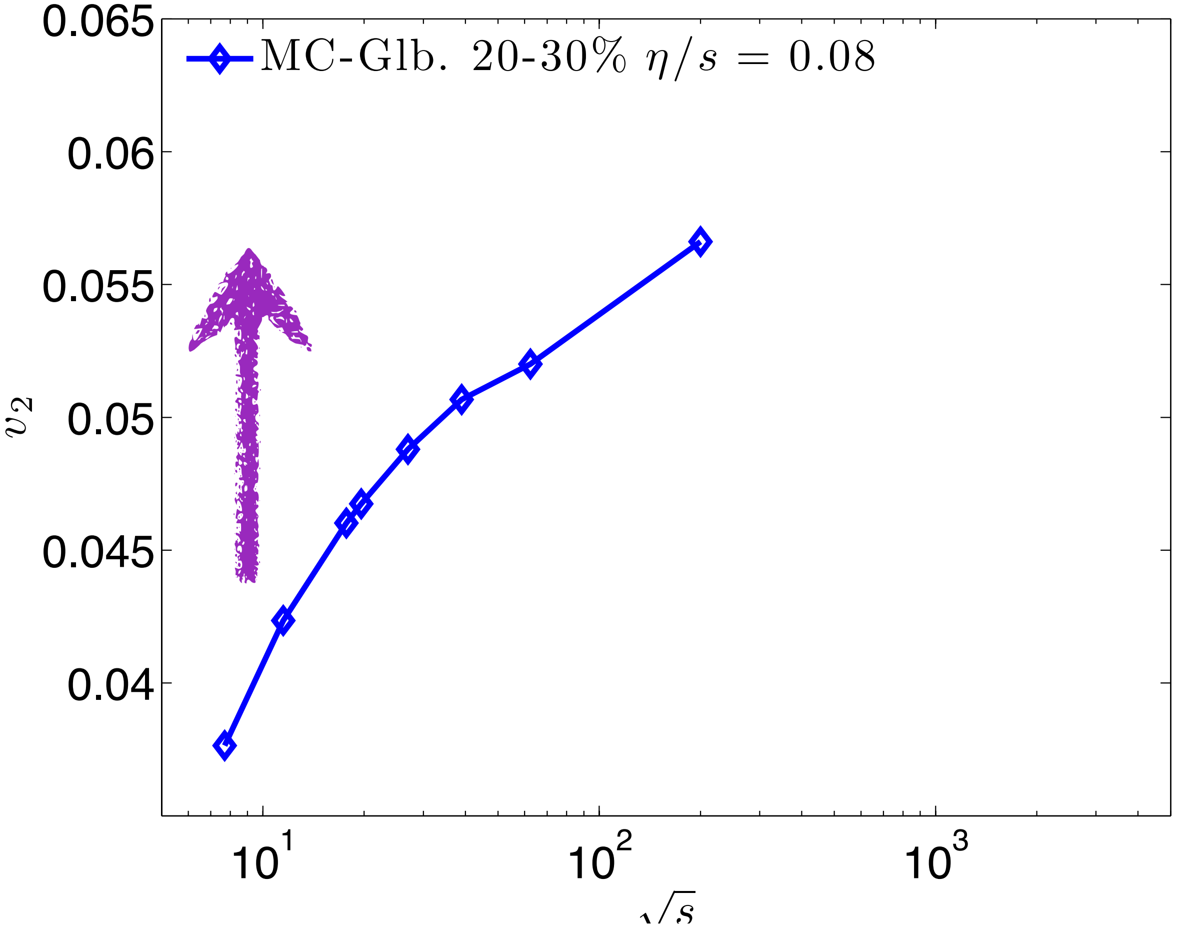

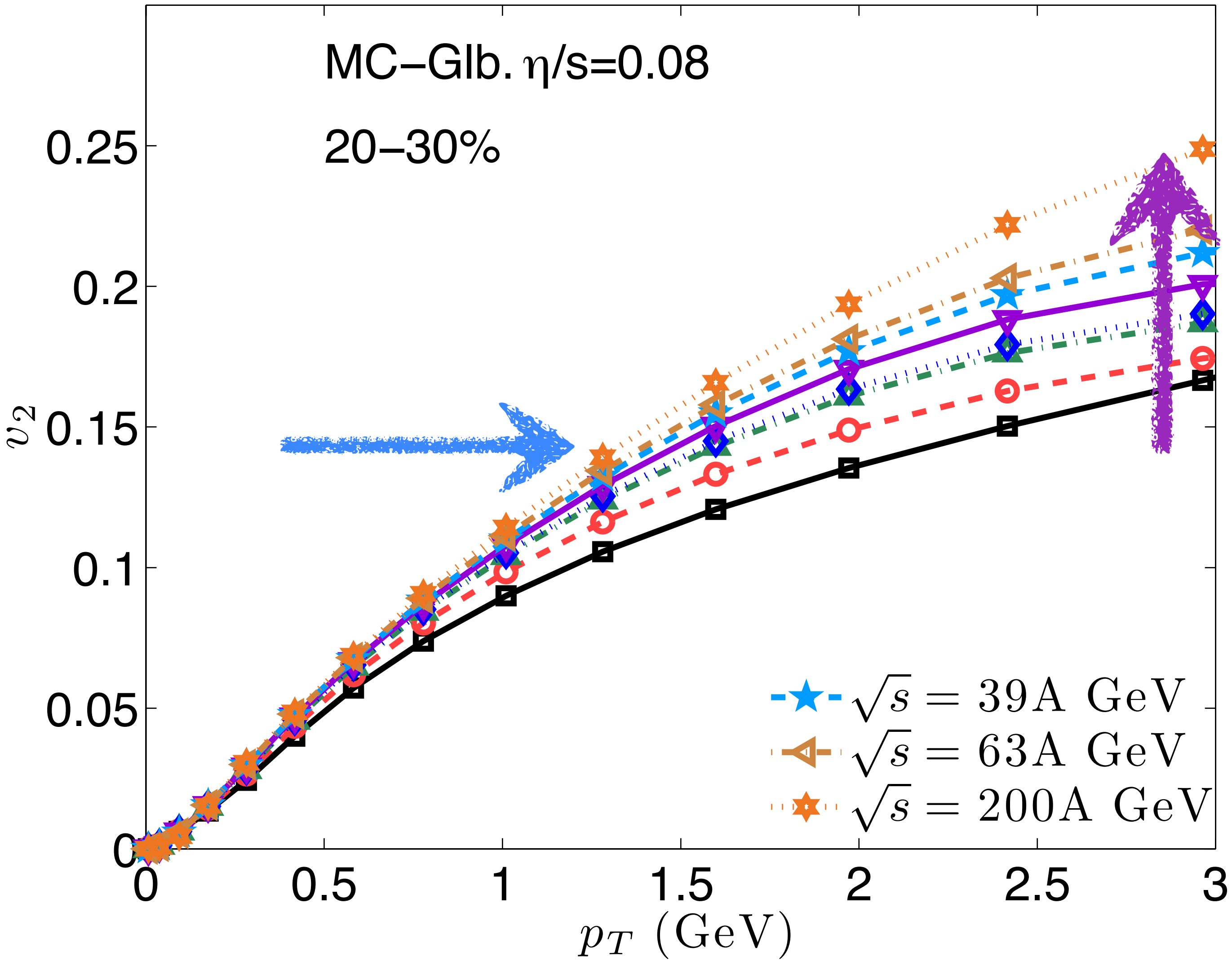

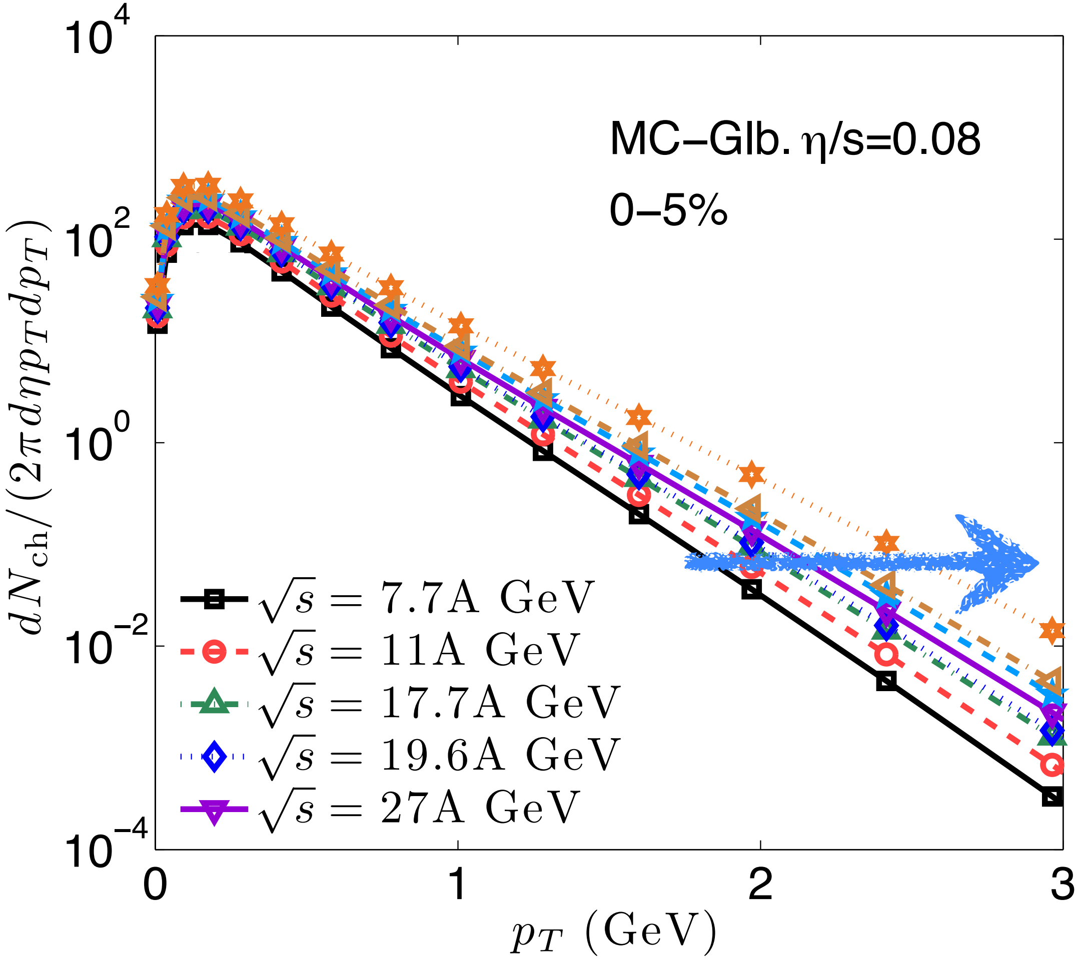

Differential $v_2(p_T)$

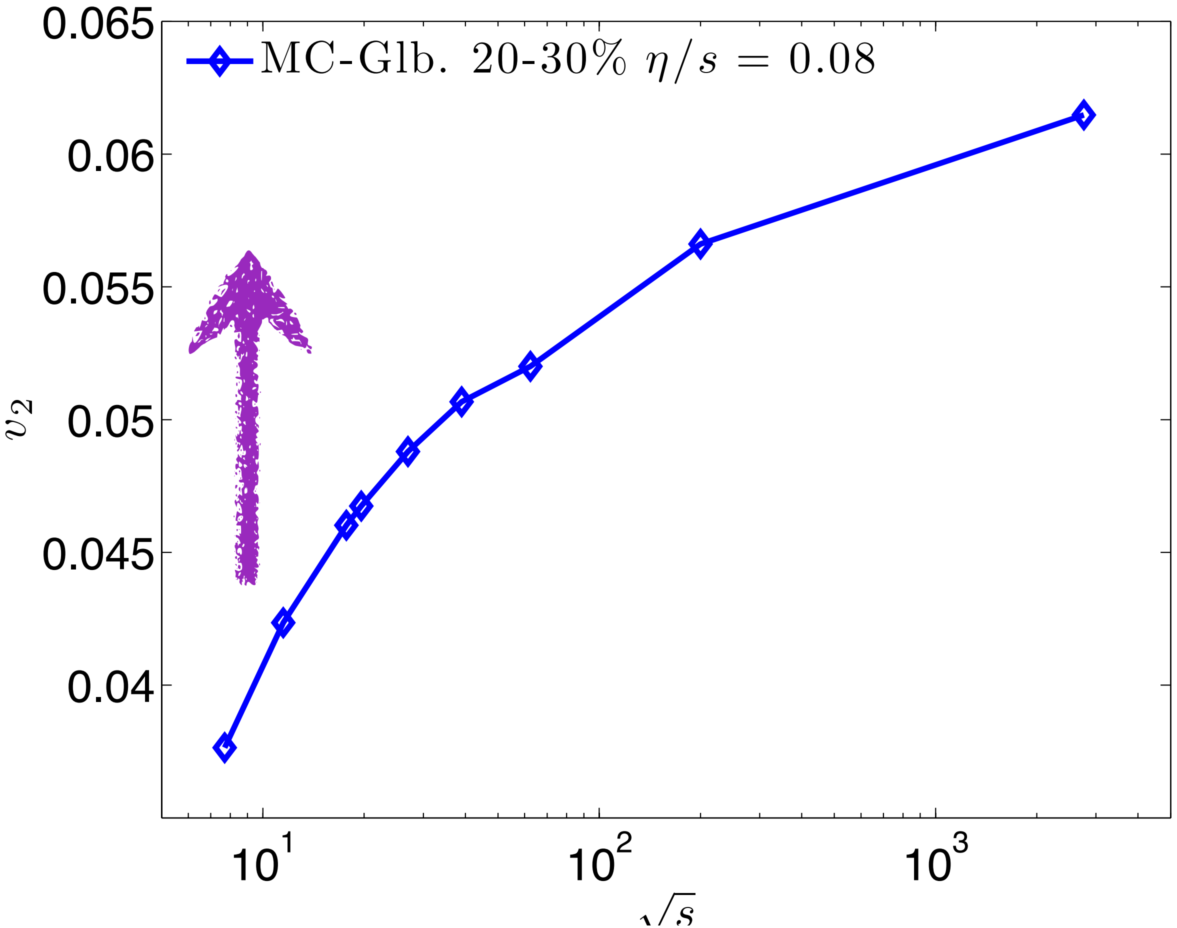

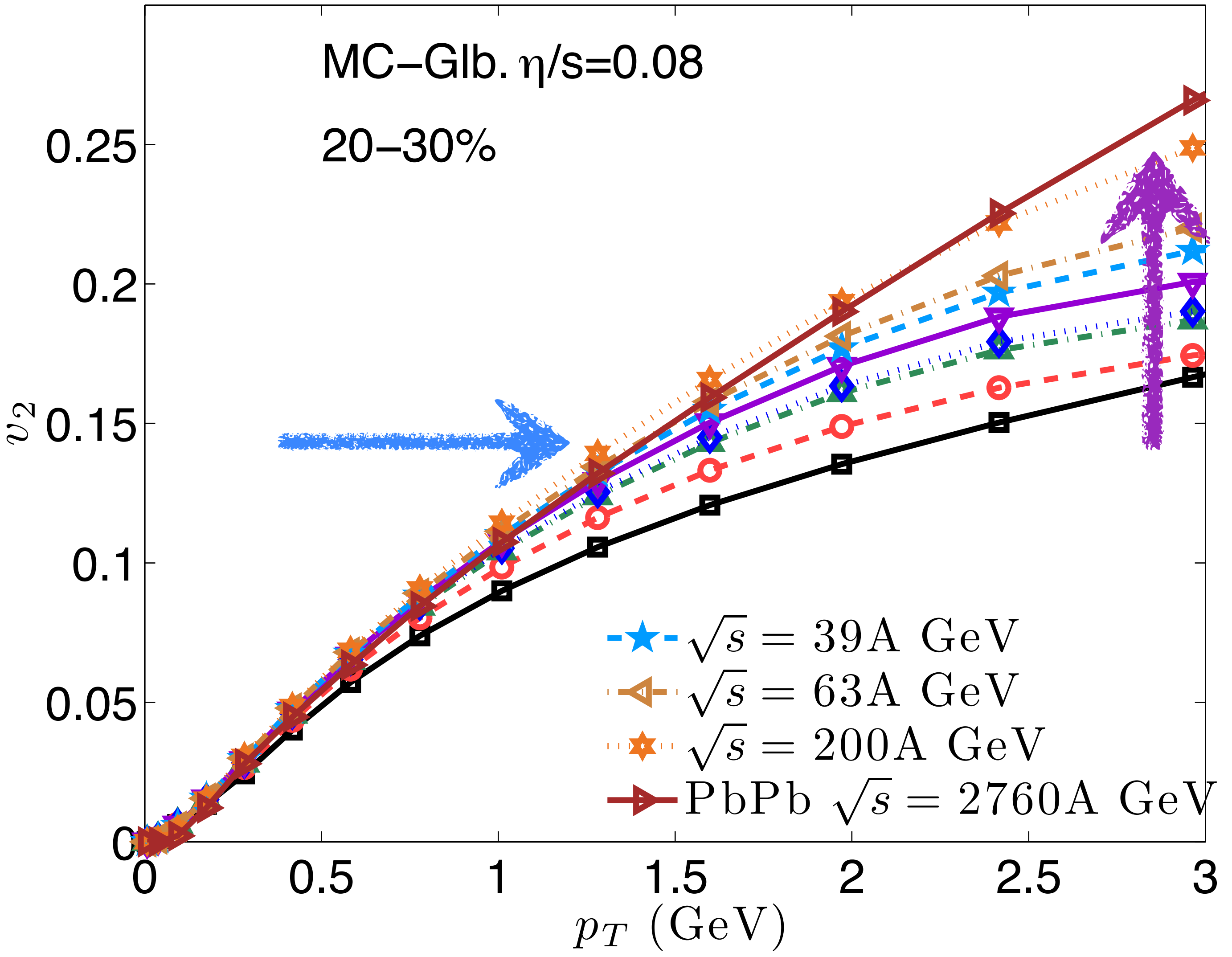

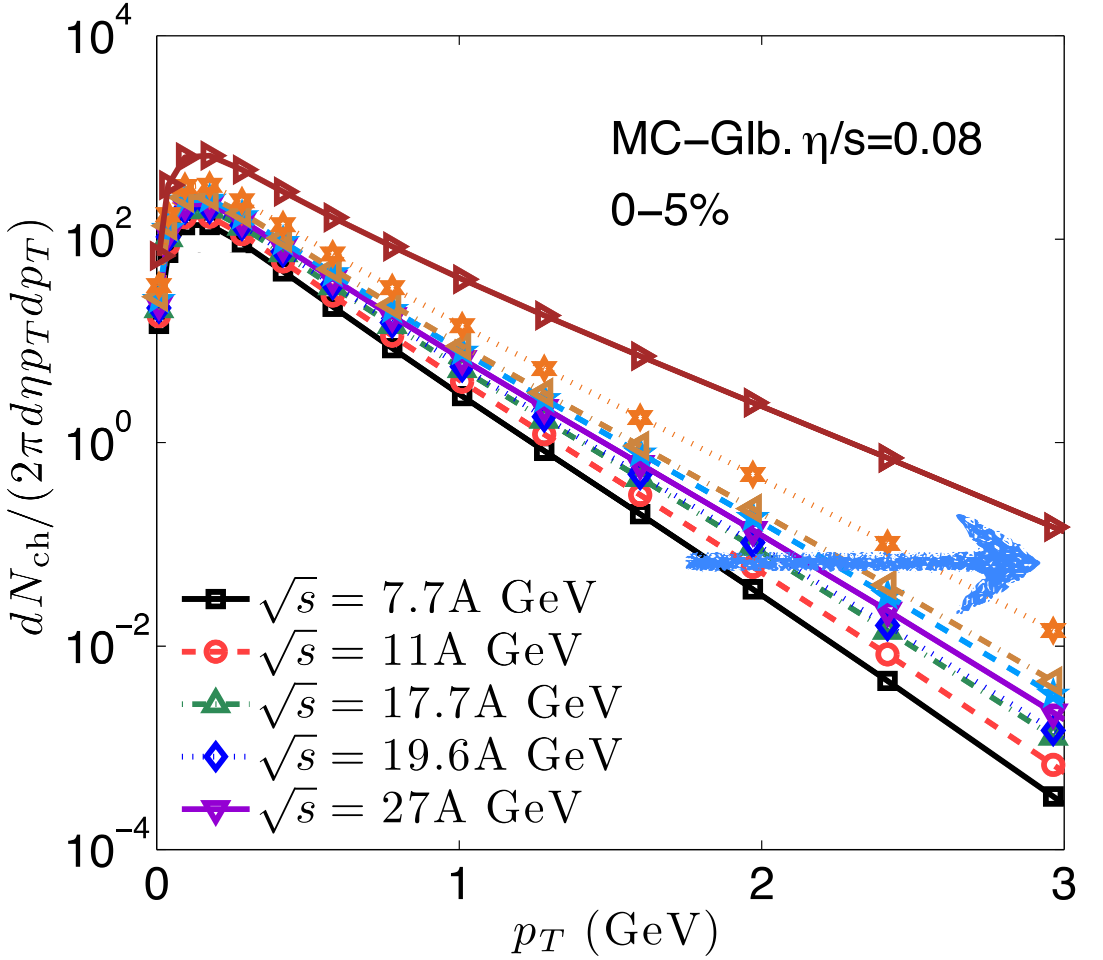

Differential $v_2(p_T)$

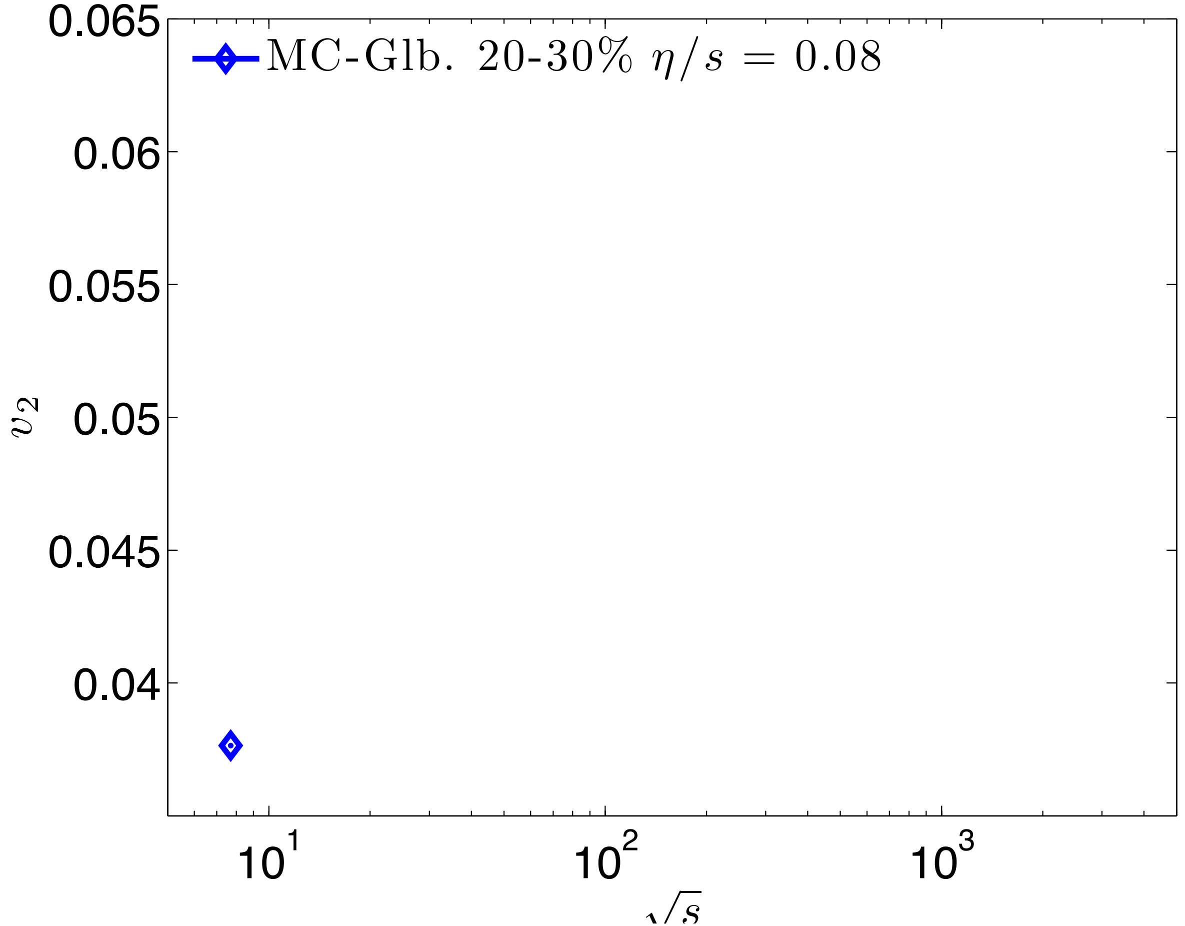

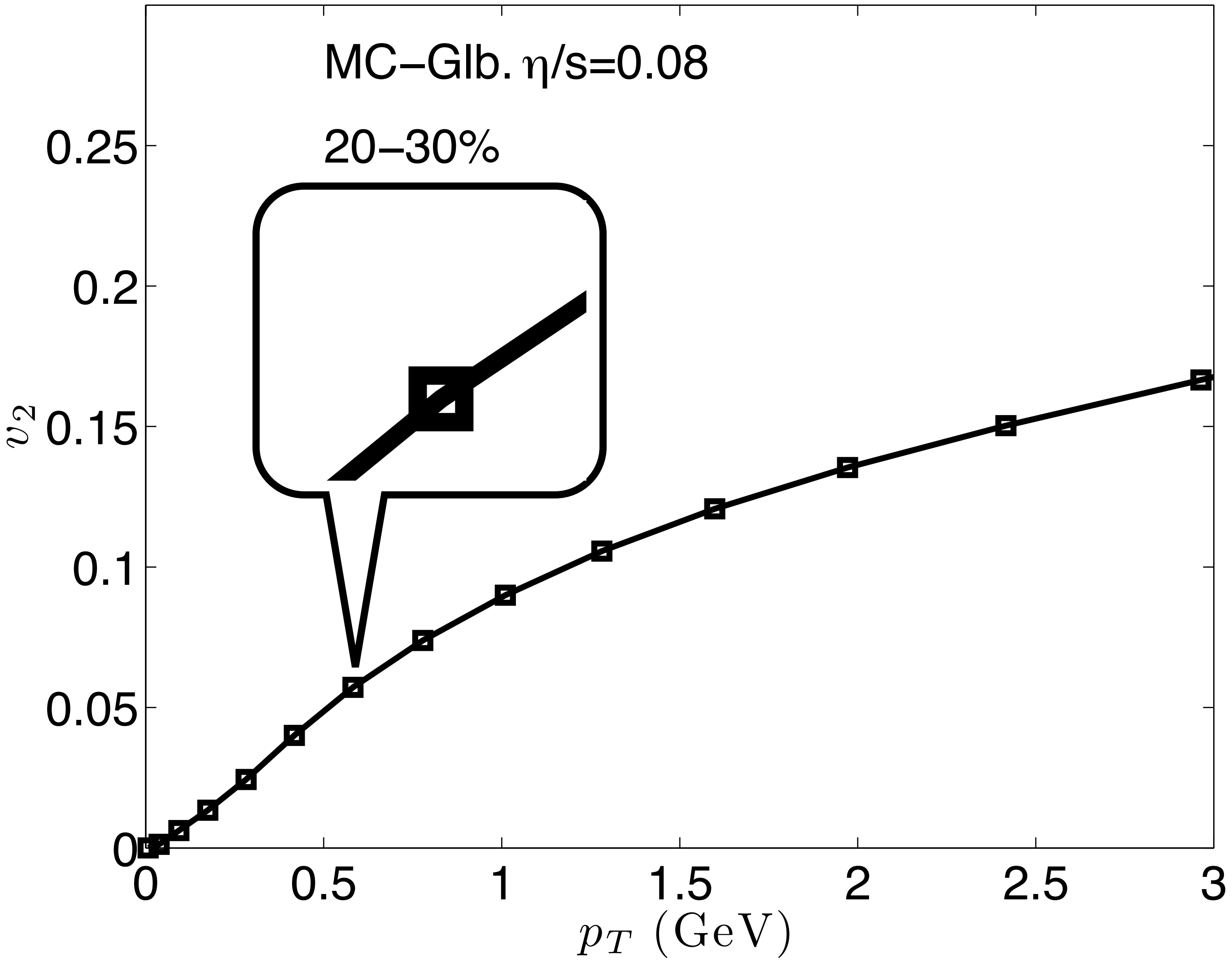

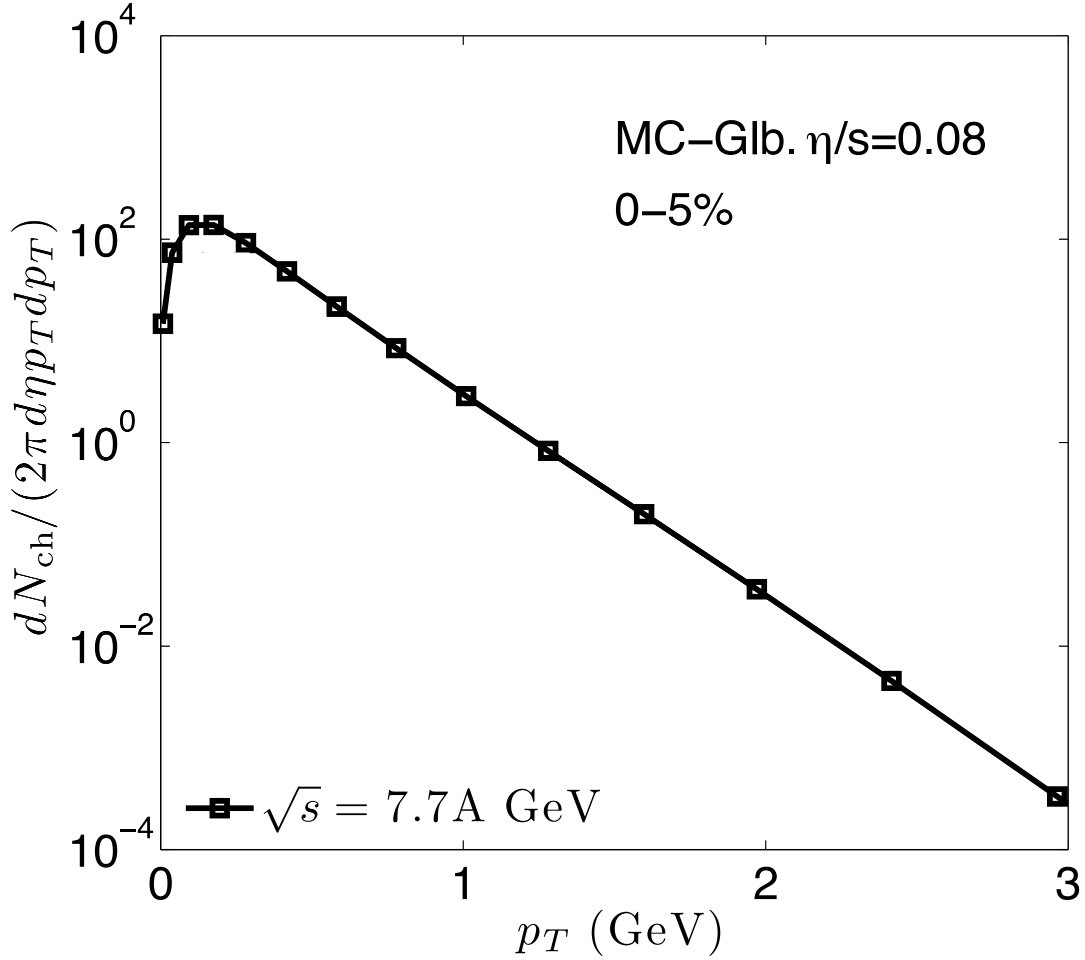

Differential $v_2(p_T)$

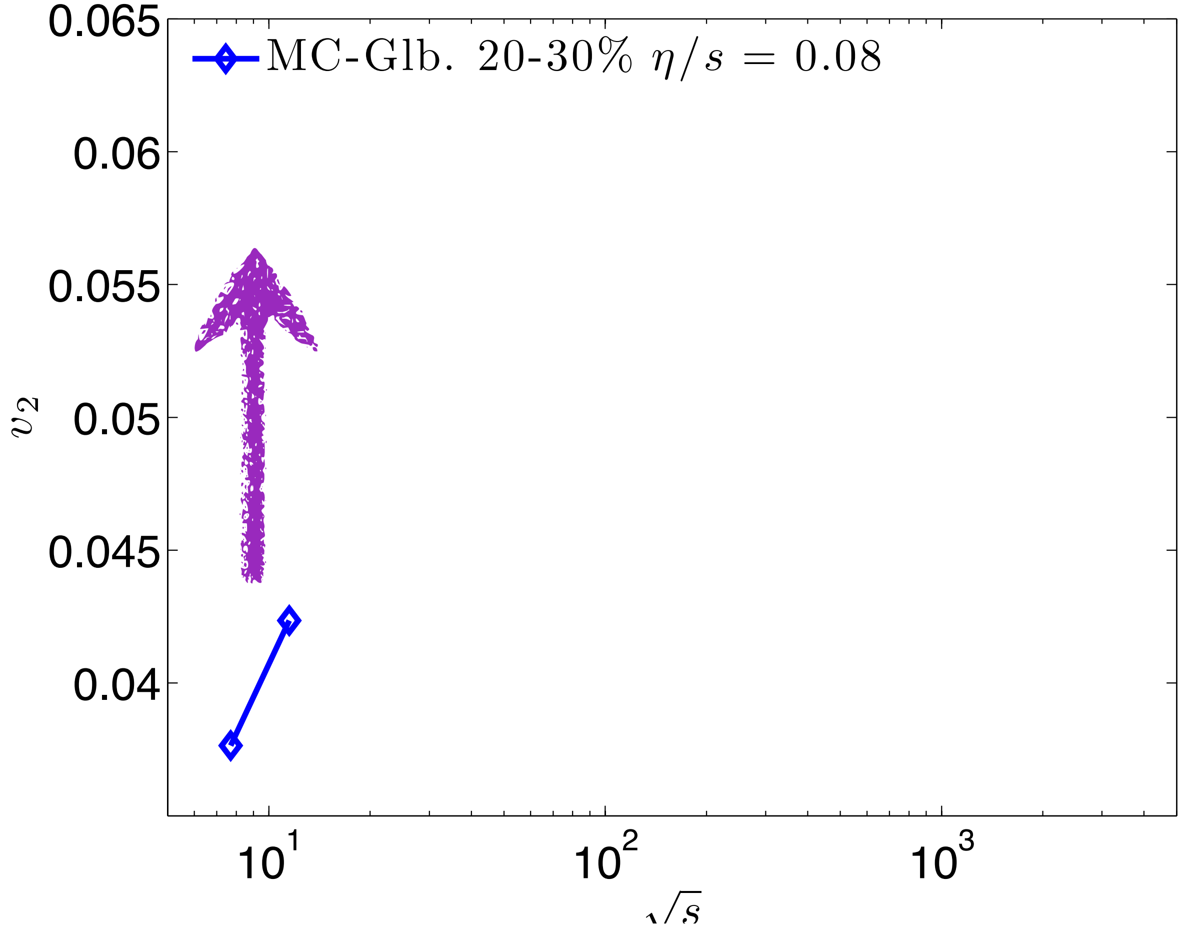

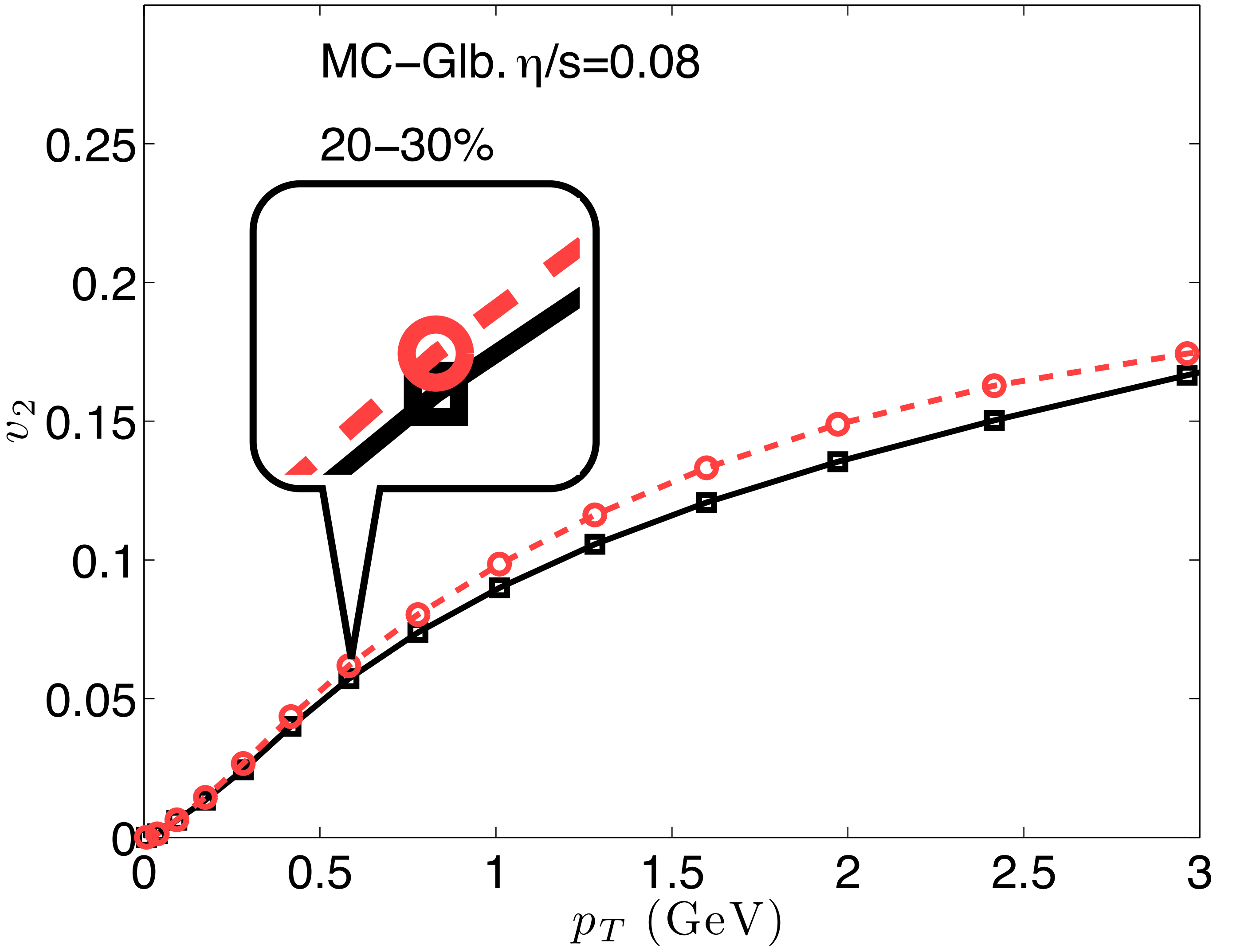

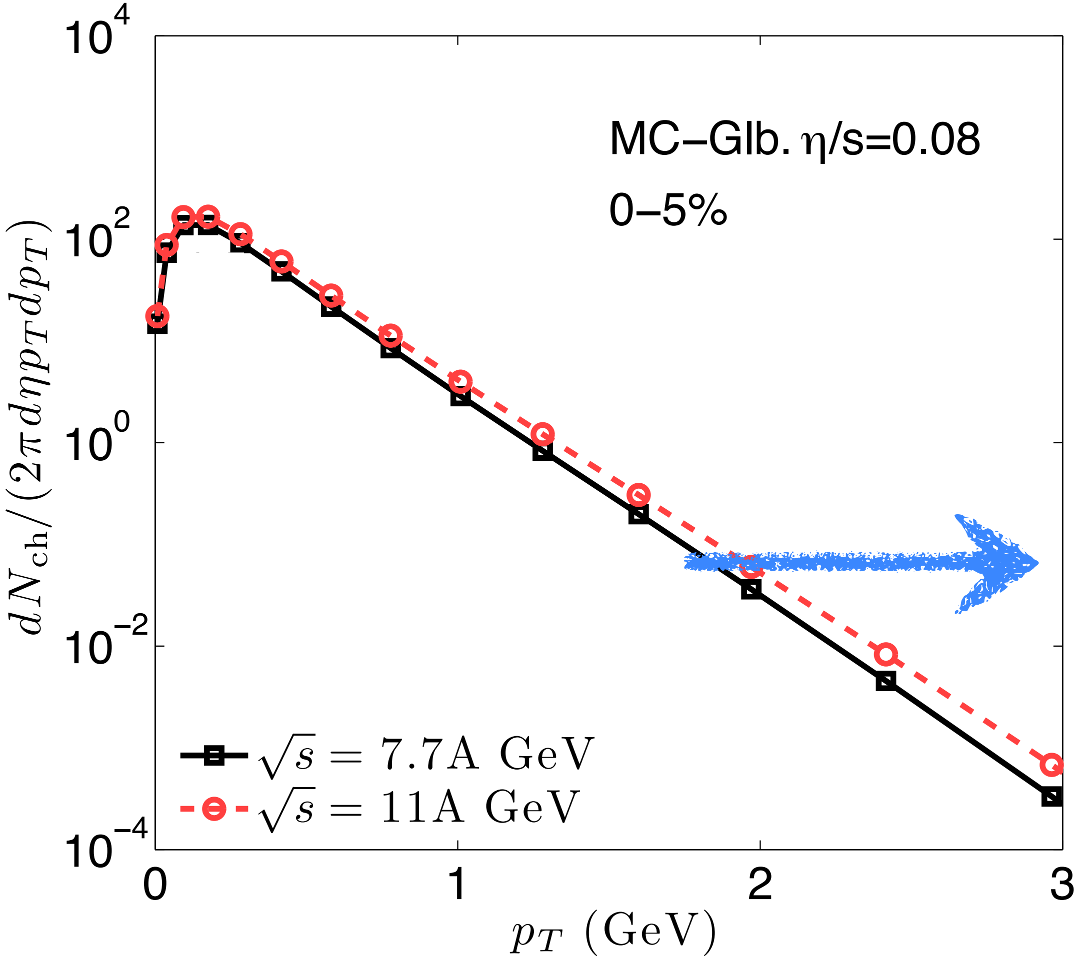

Differential $v_2(p_T)$

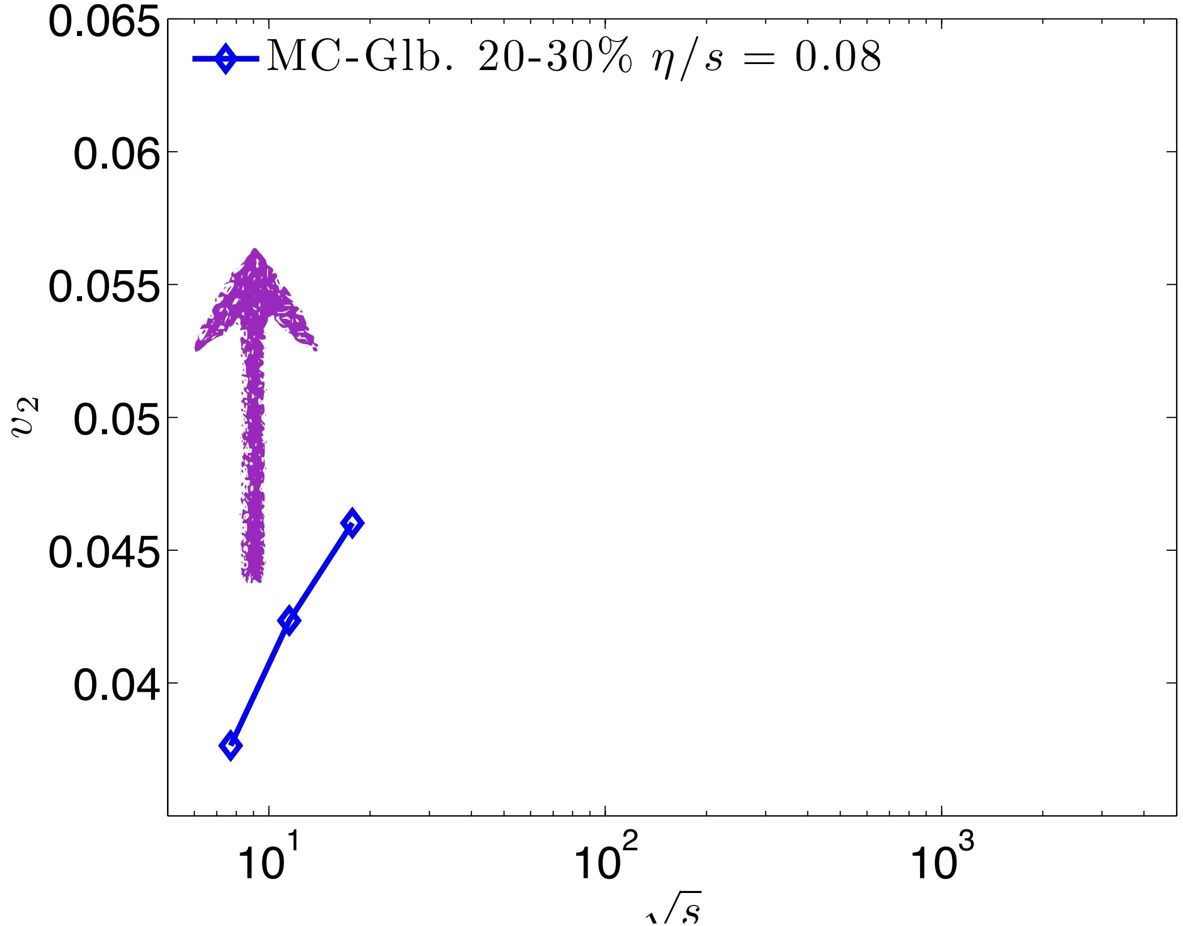

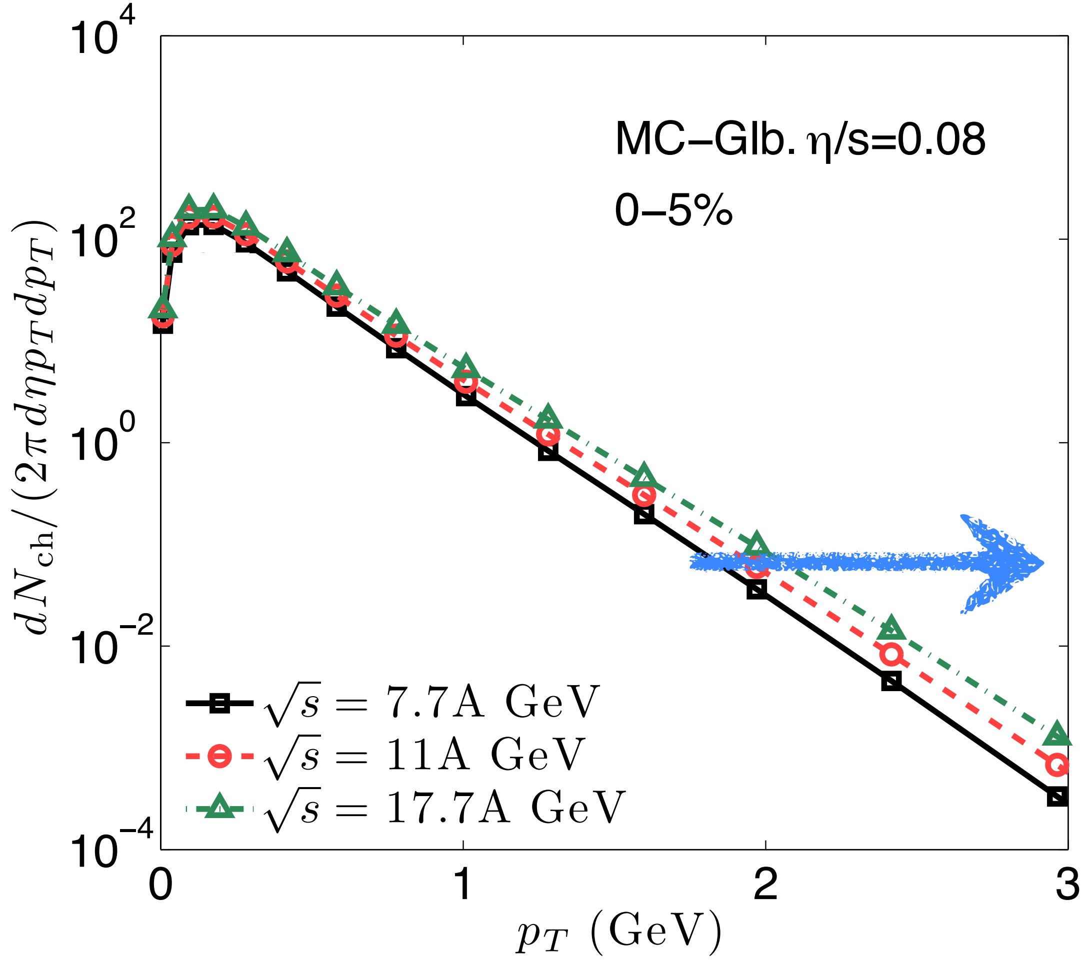

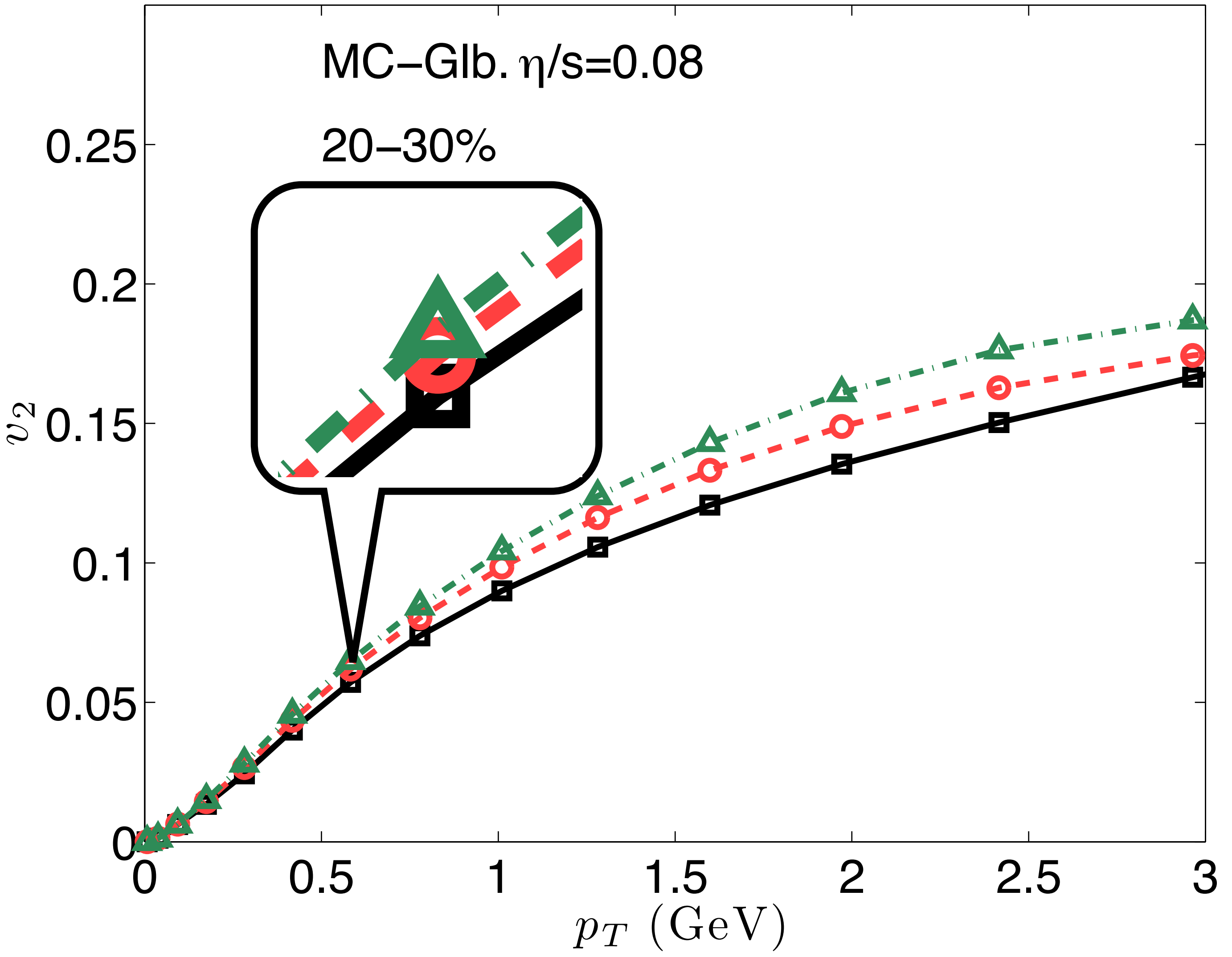

Differential $v_2(p_T)$

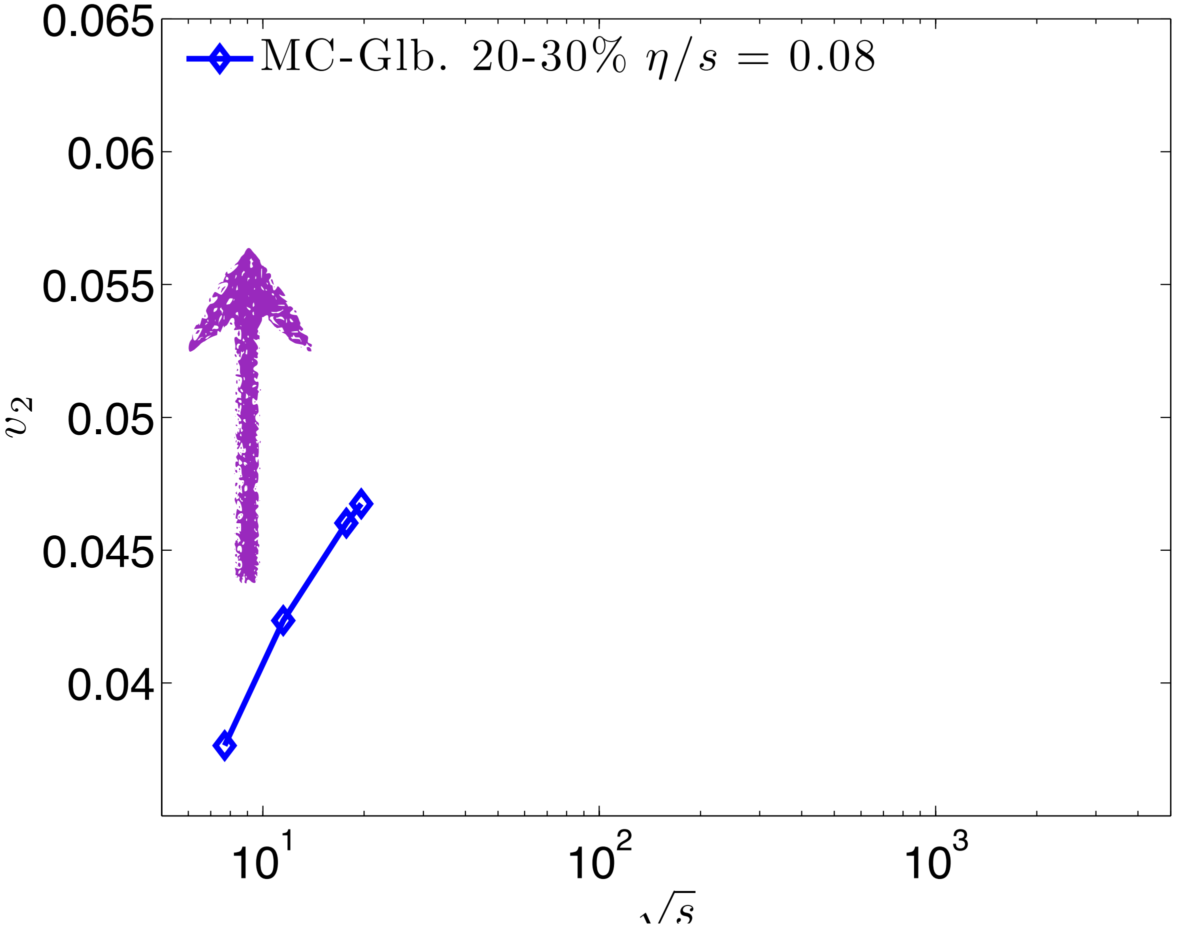

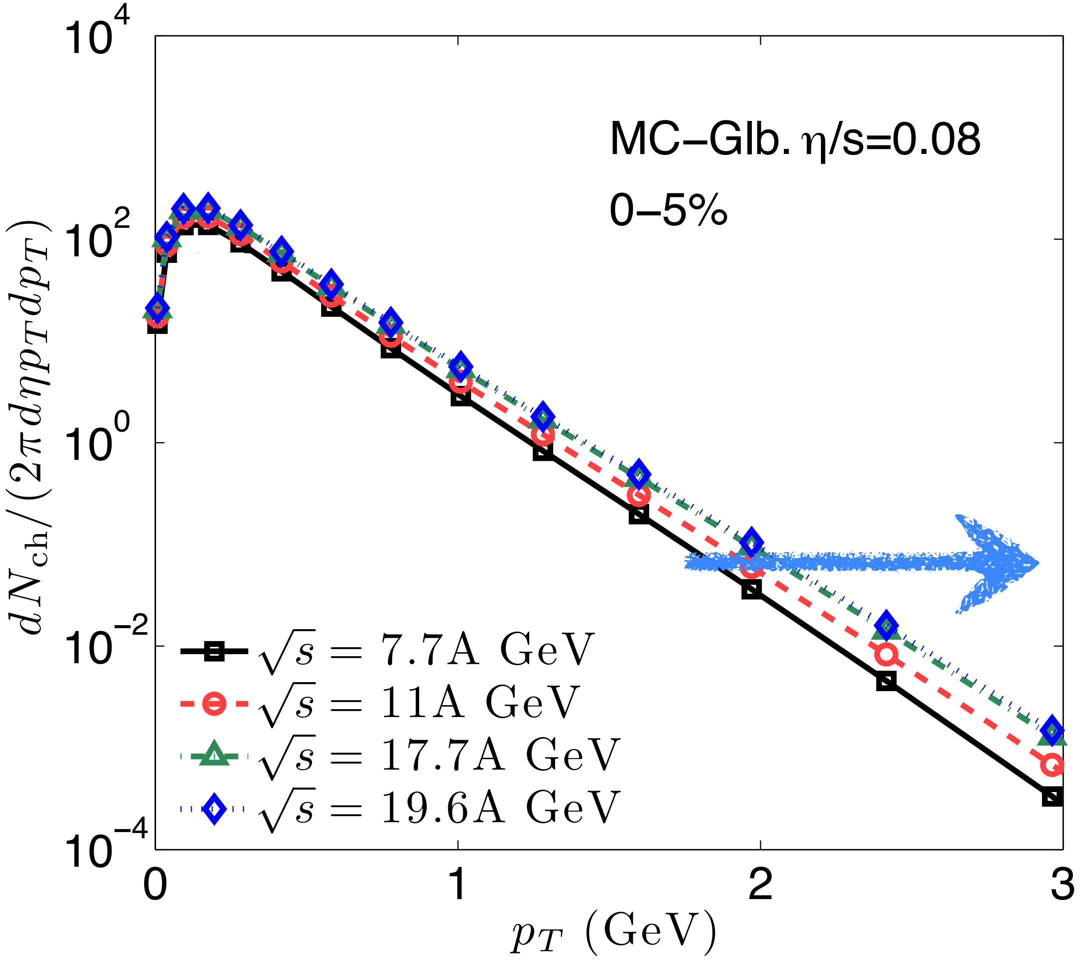

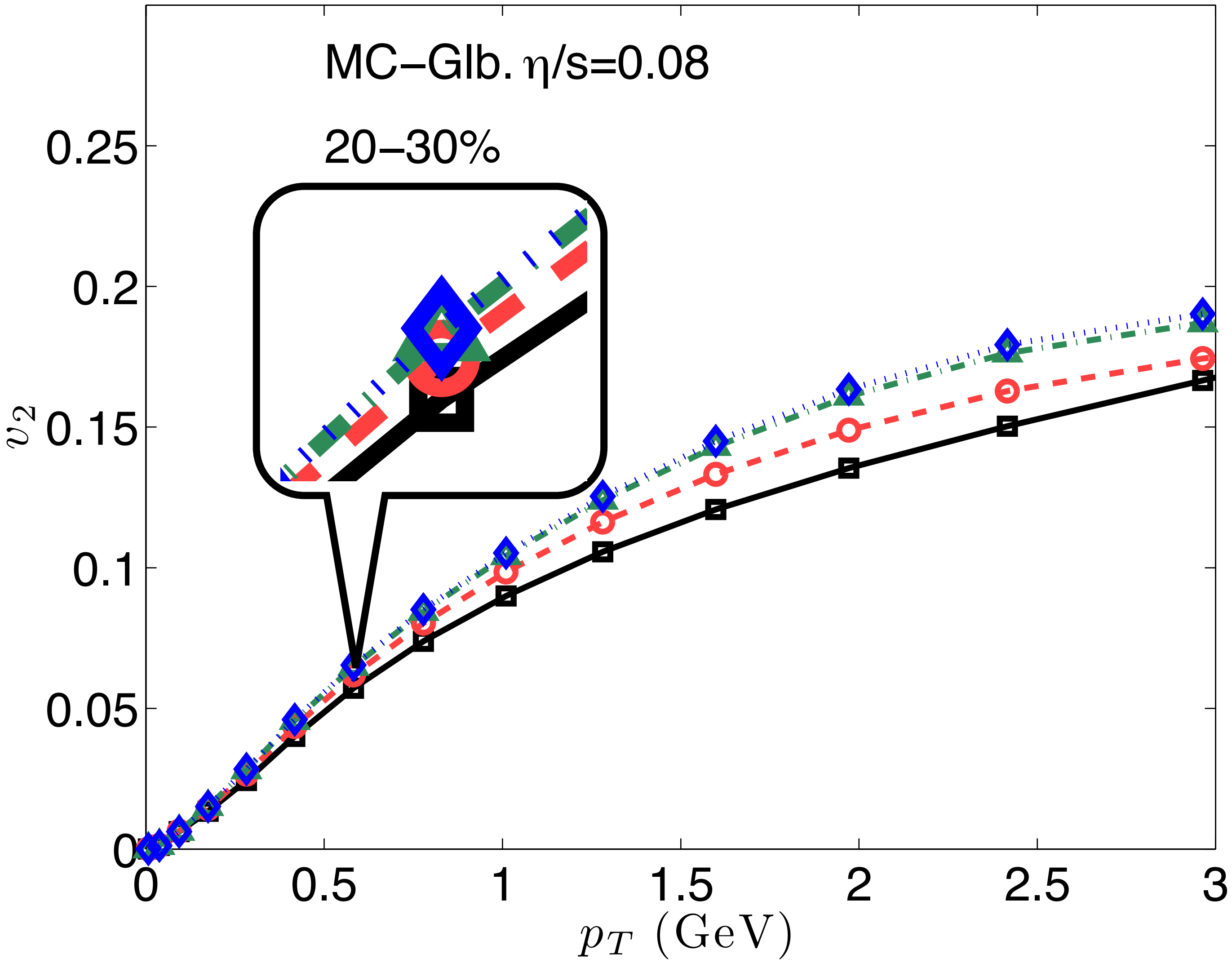

Differential $v_2(p_T)$

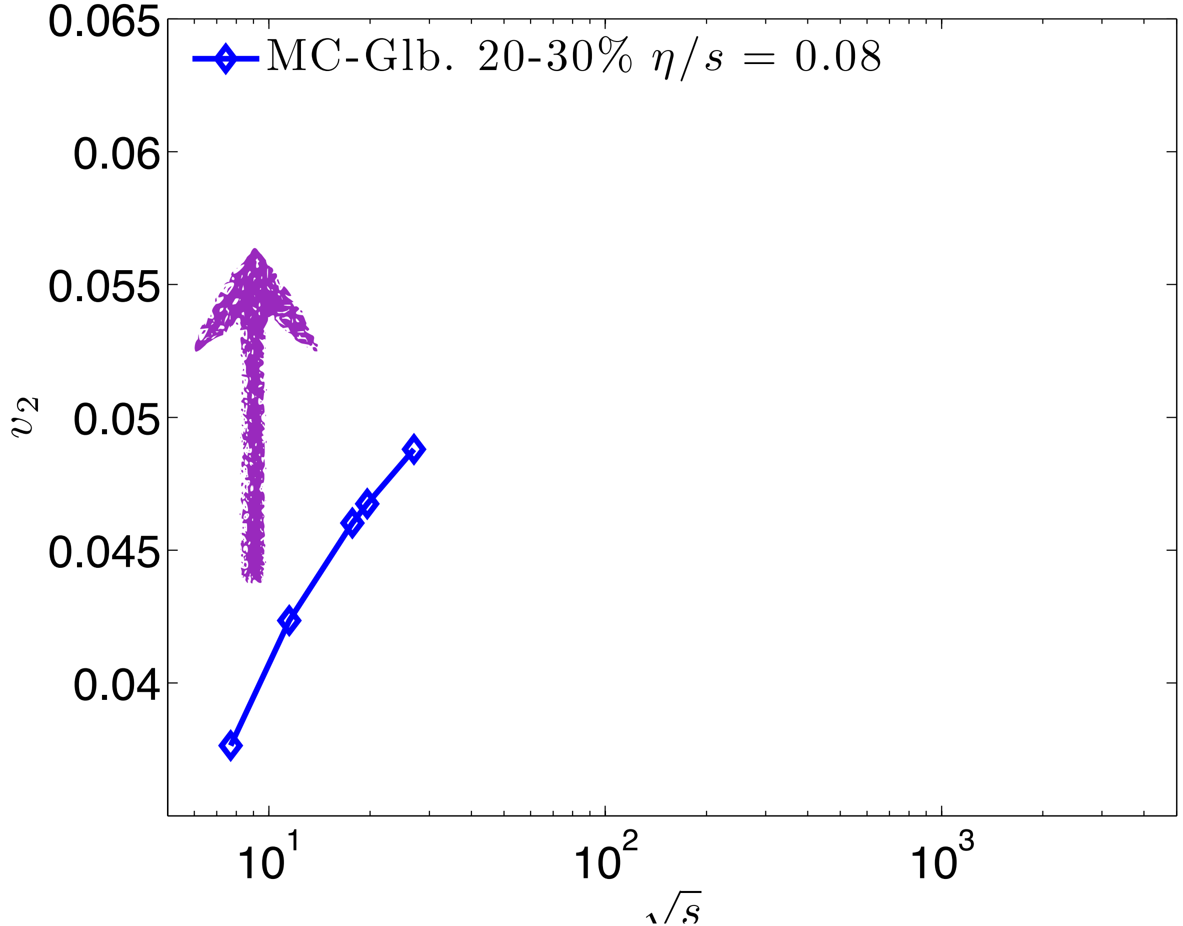

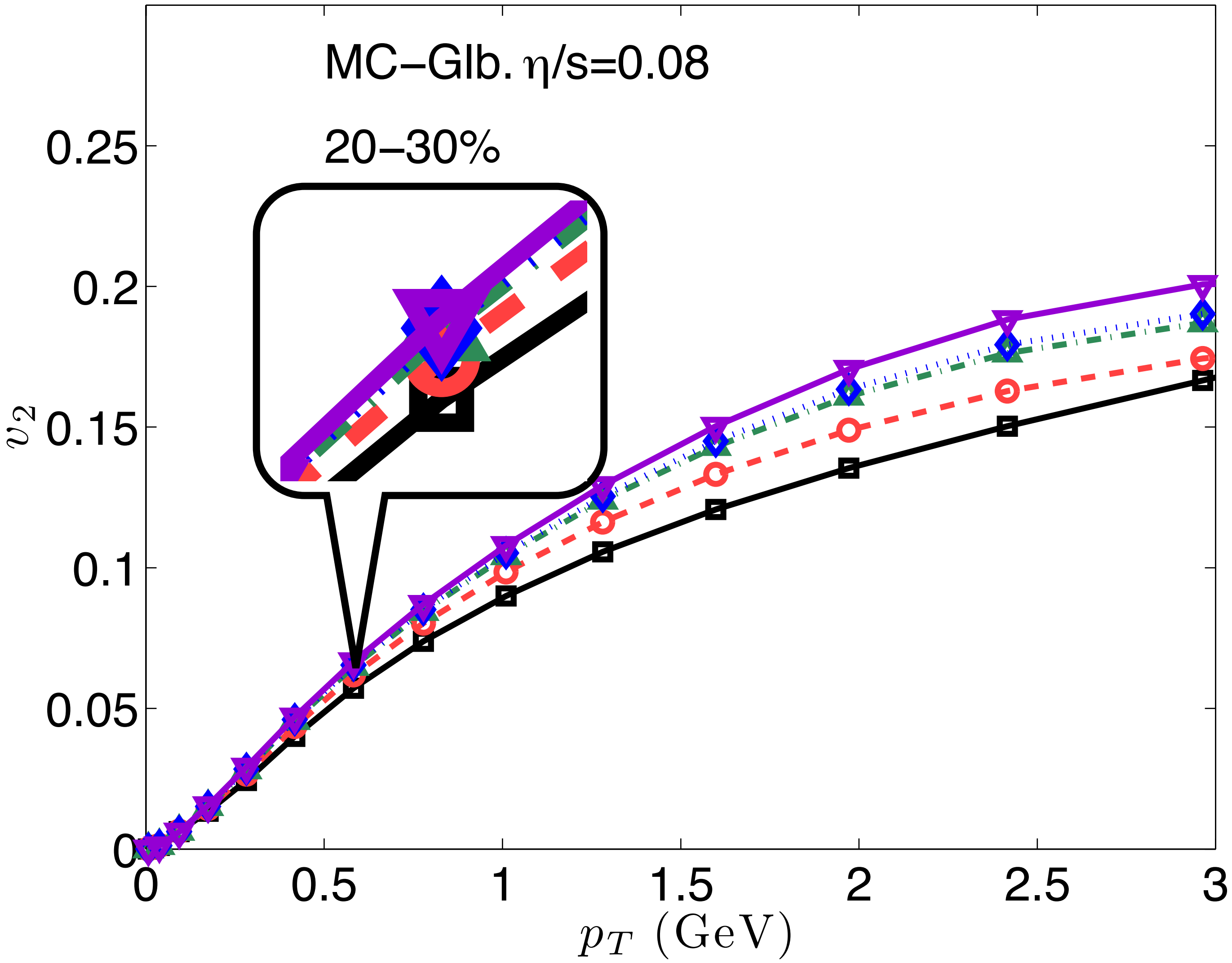

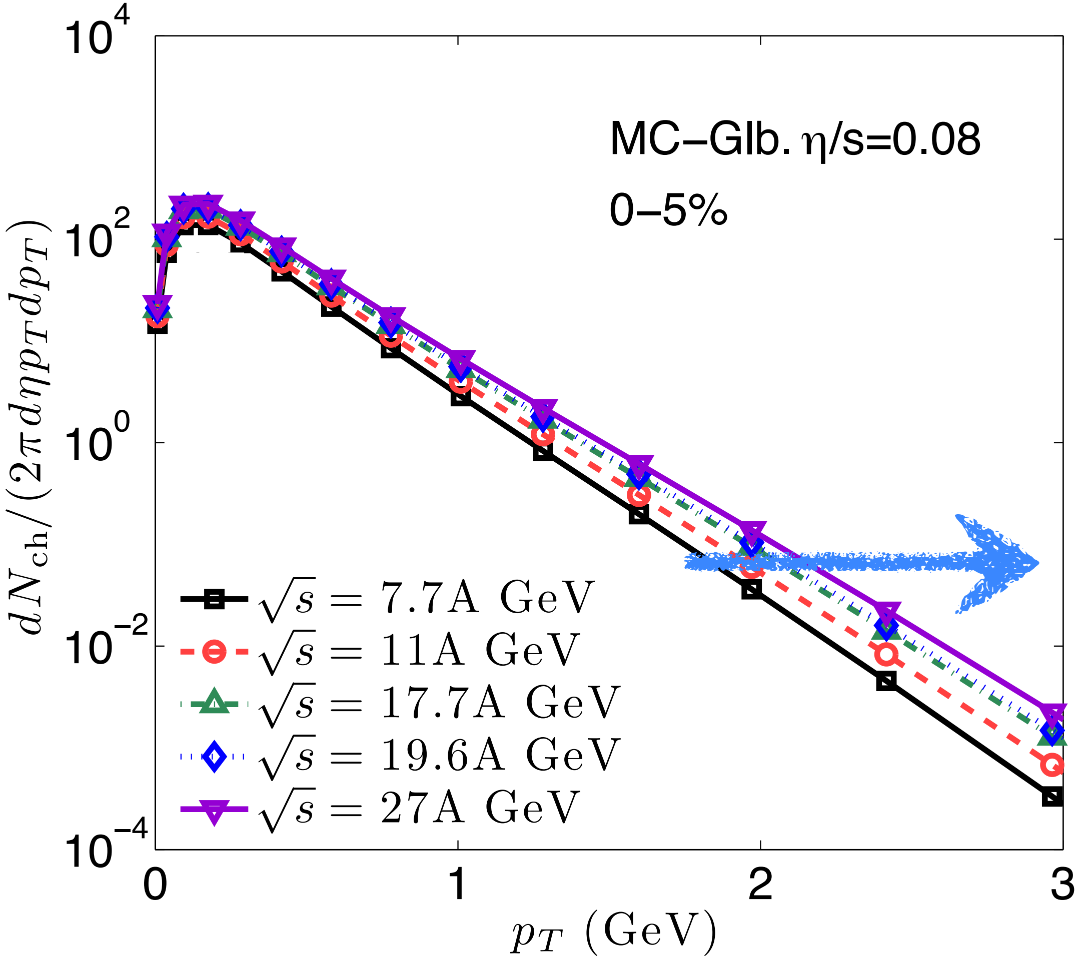

Differential $v_2(p_T)$

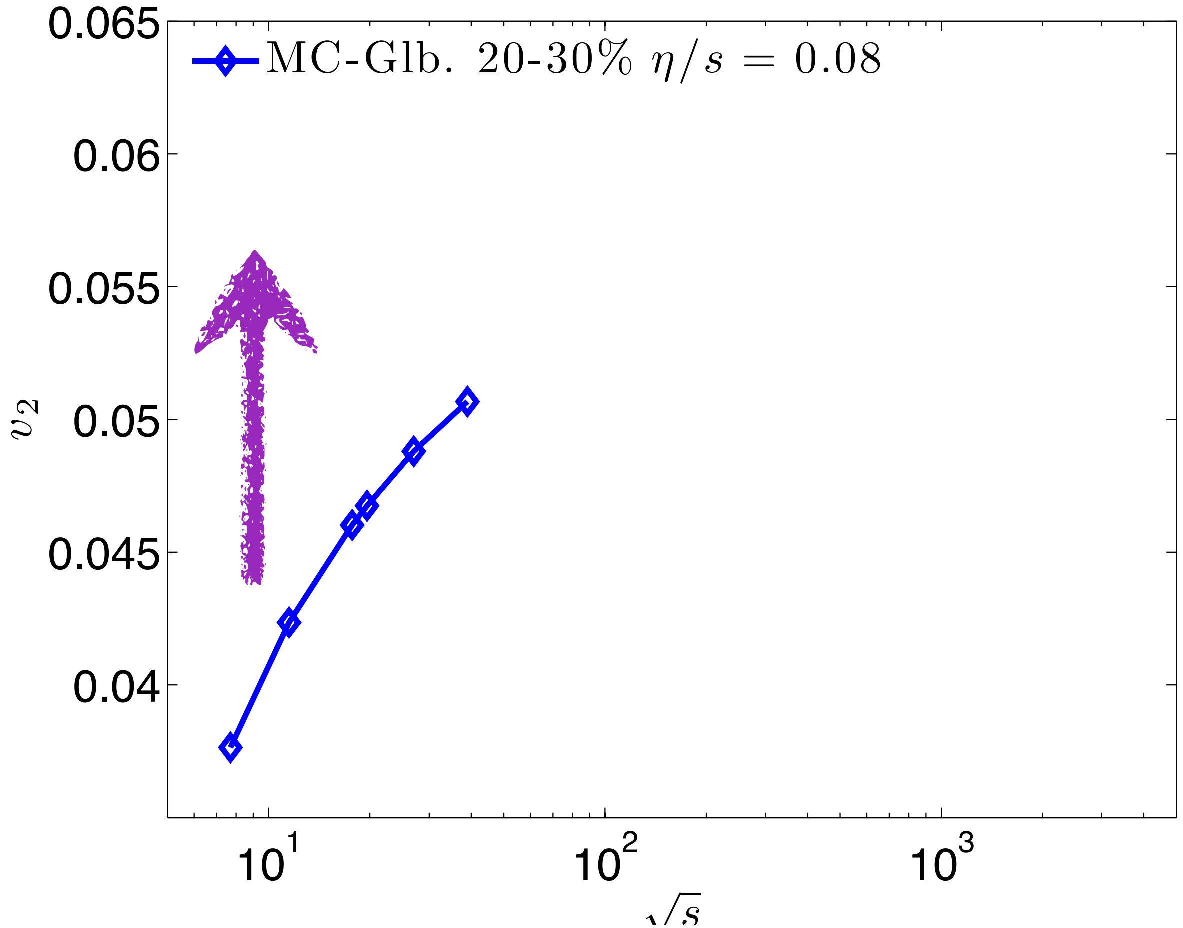

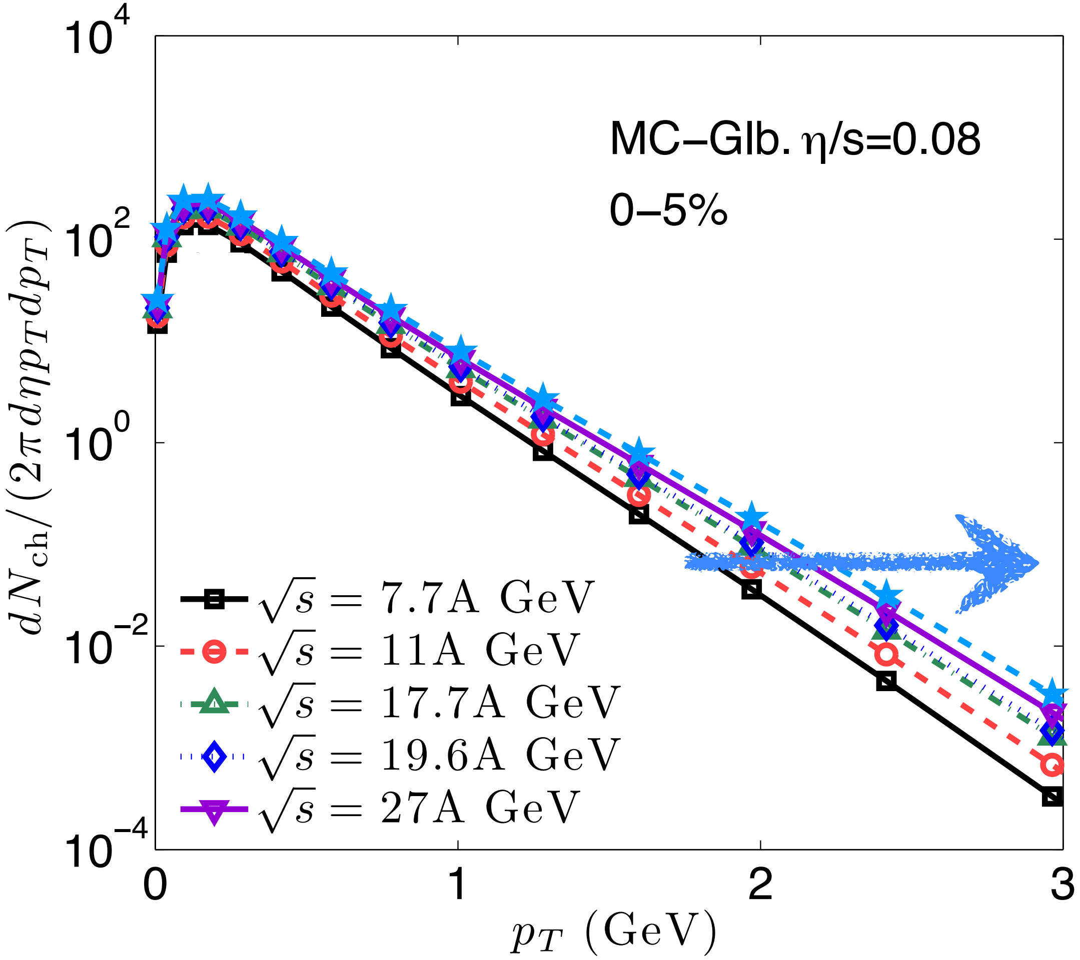

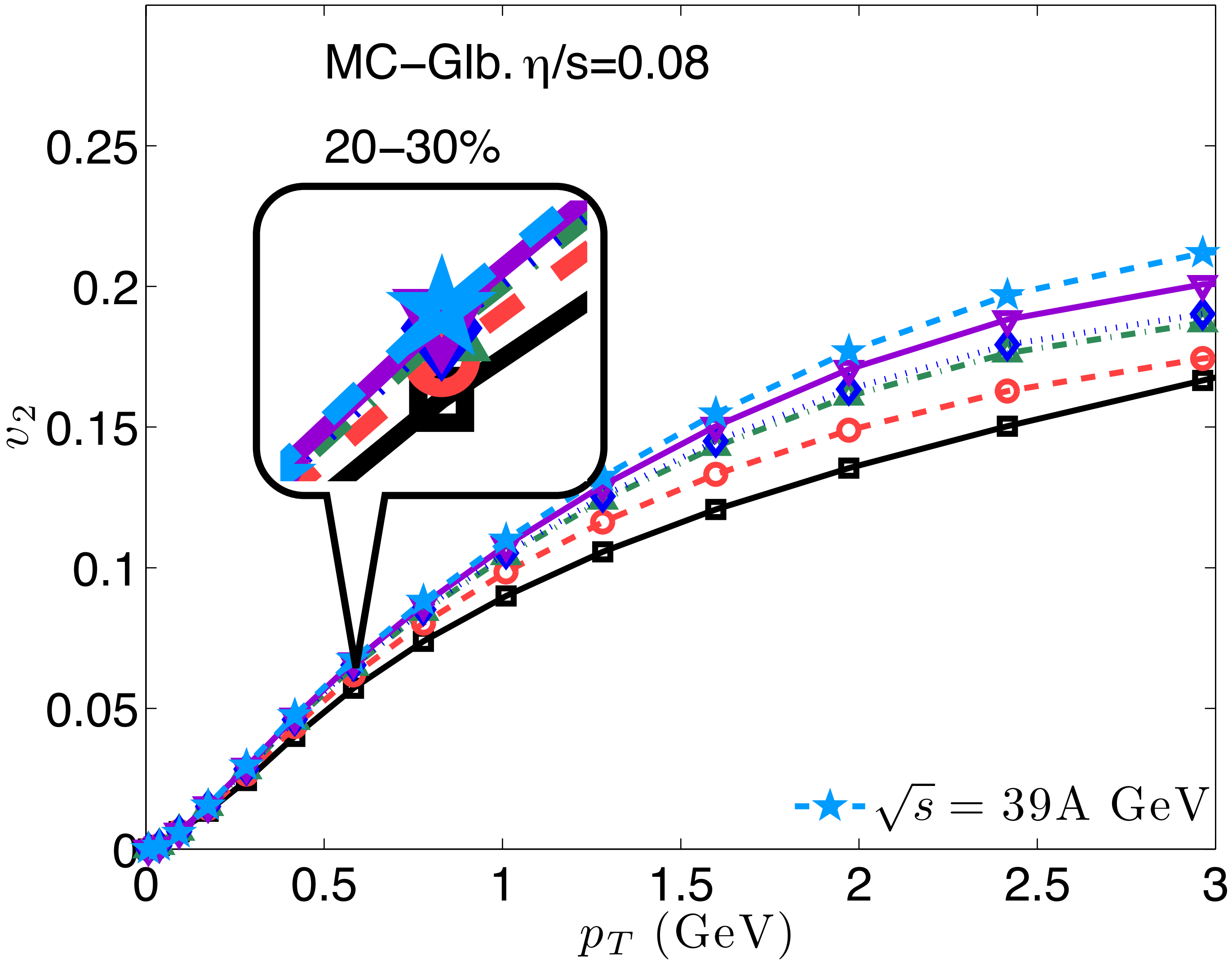

Differential $v_2(p_T)$

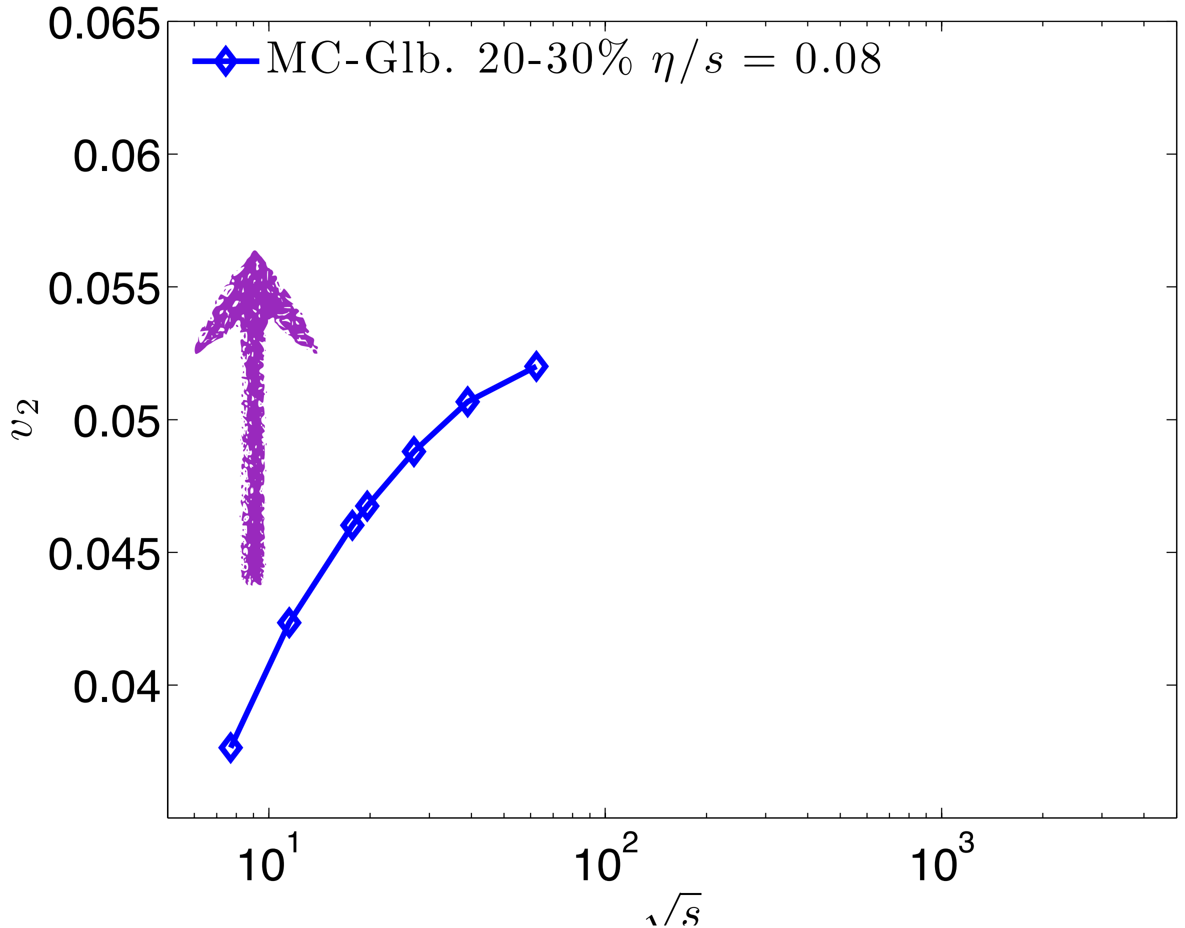

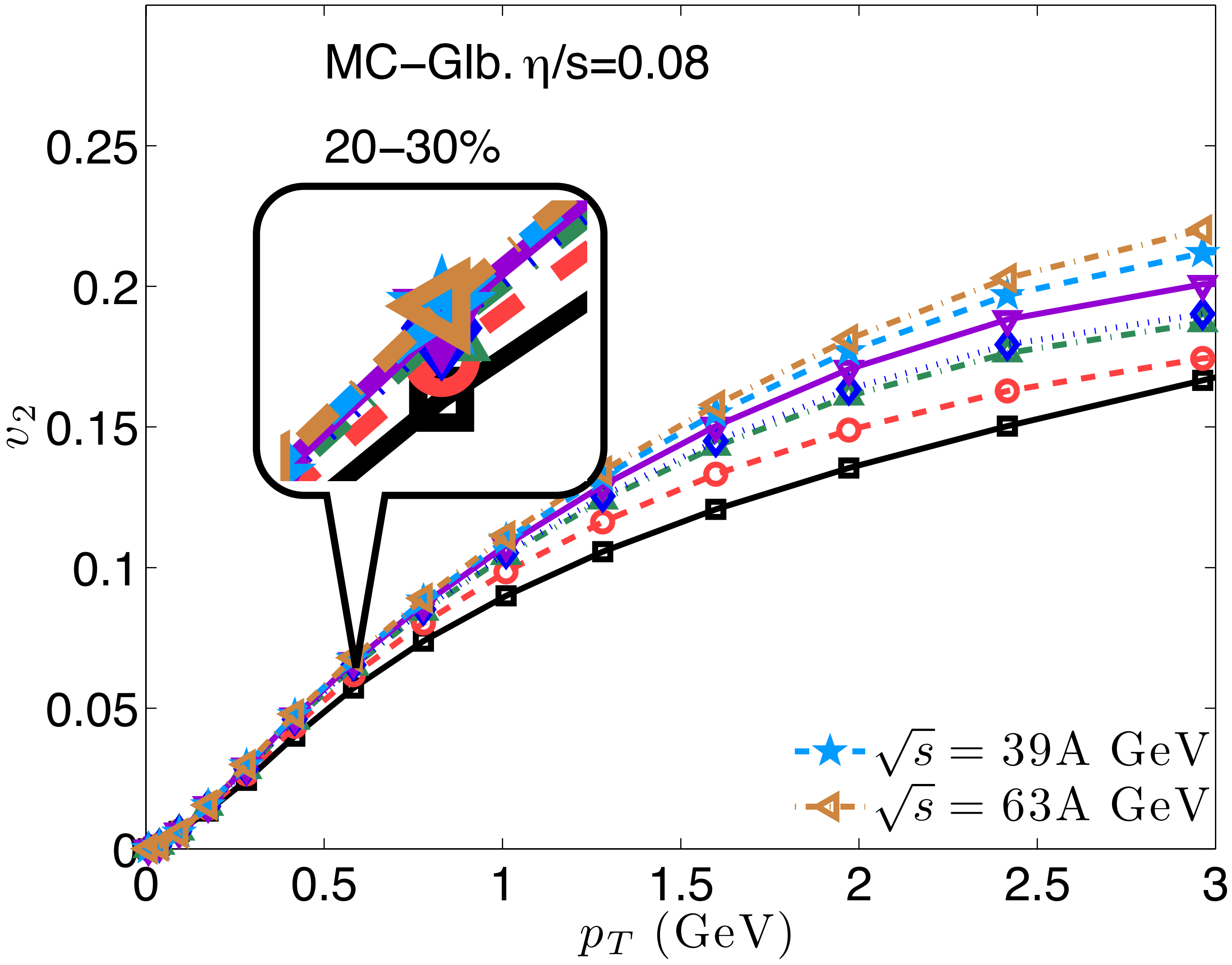

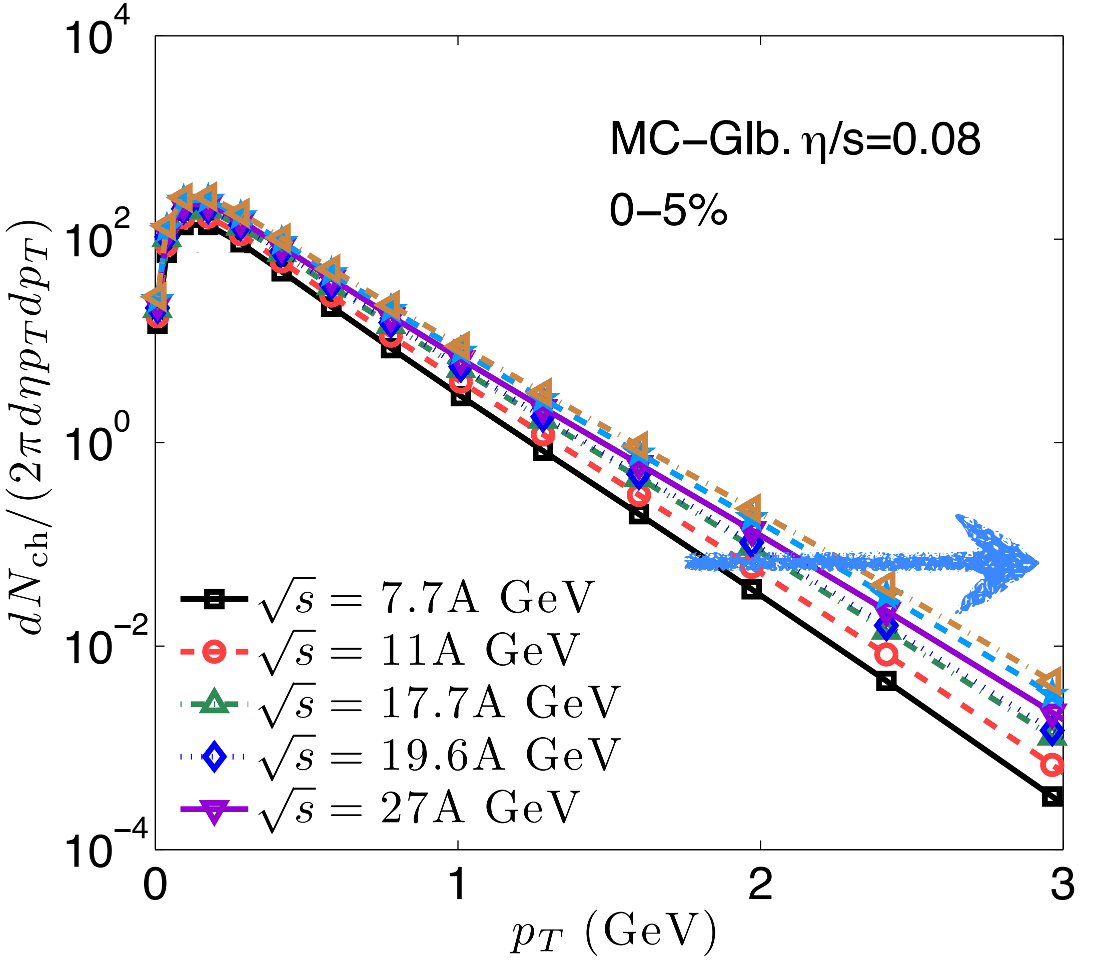

Differential $v_2(p_T)$

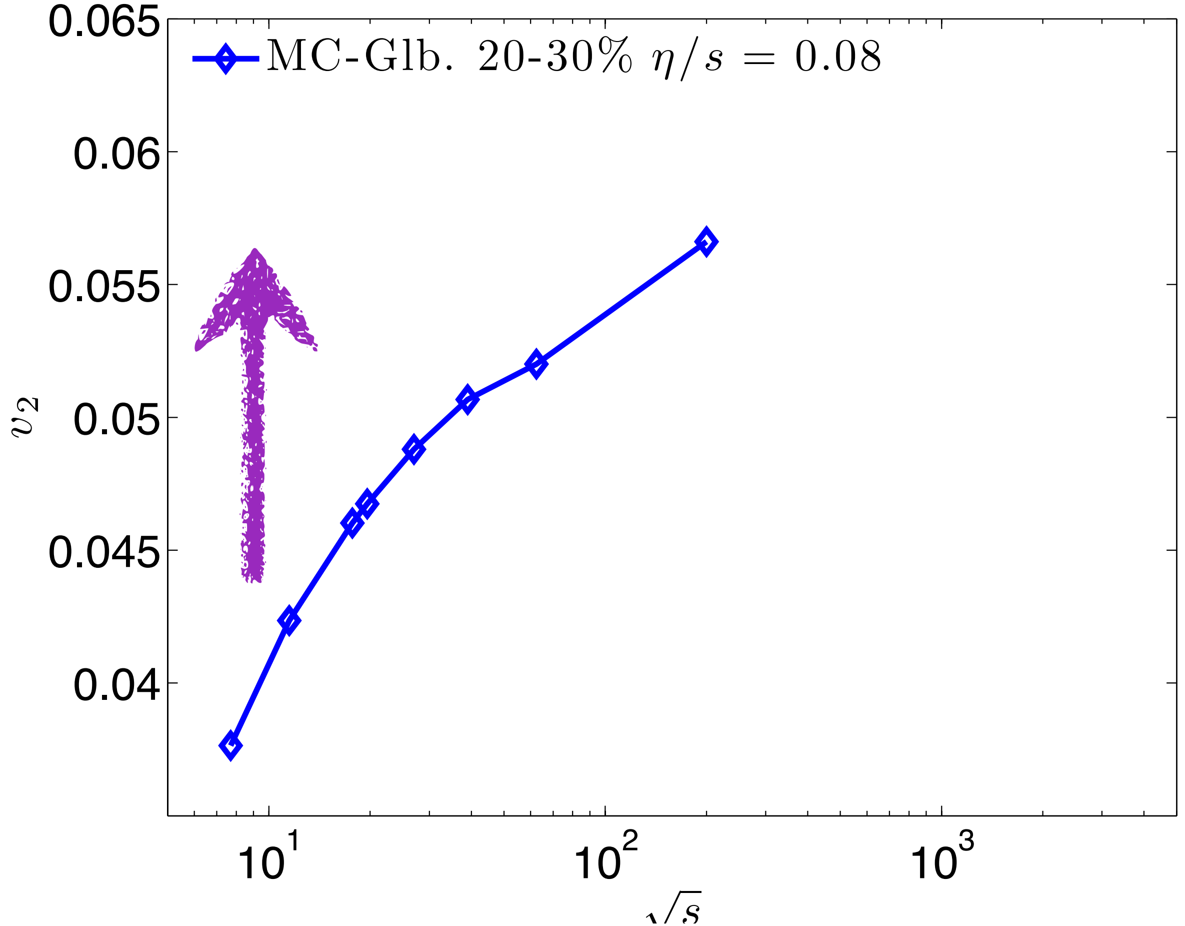

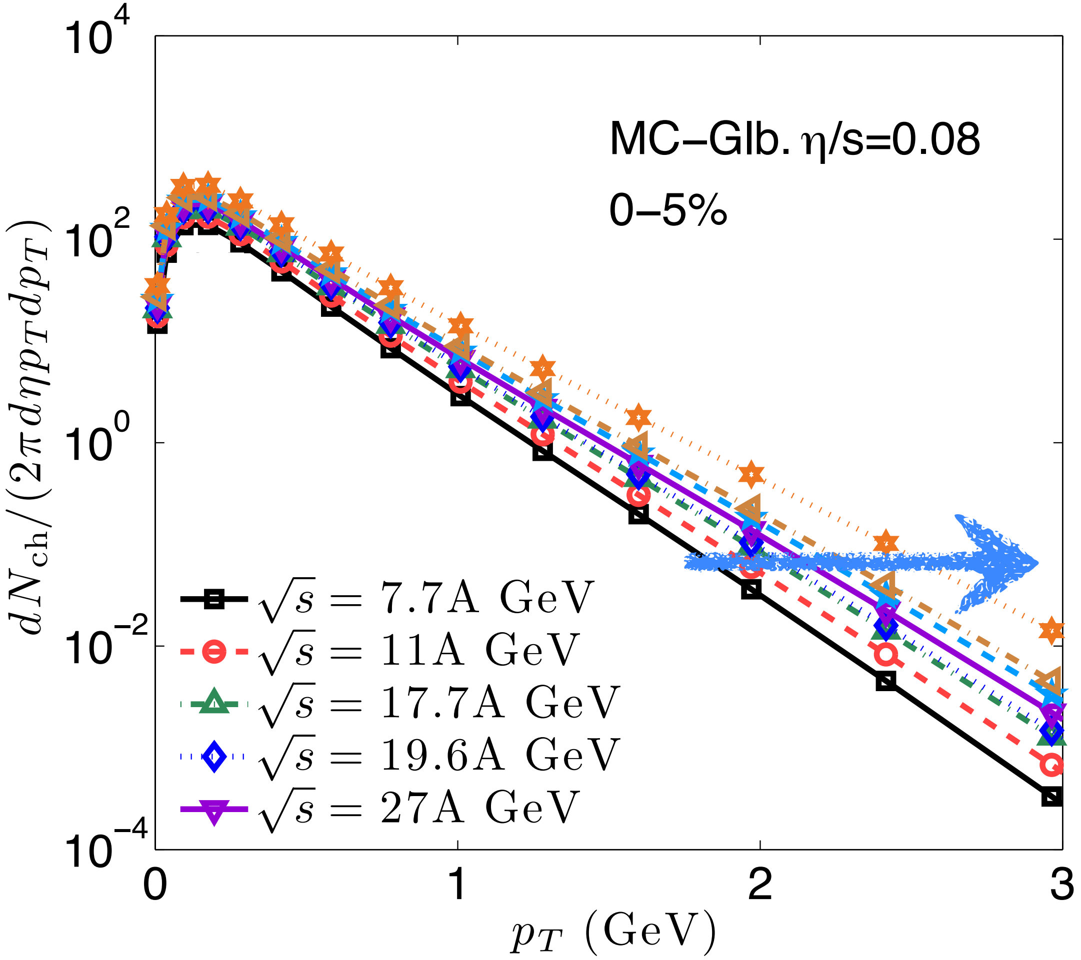

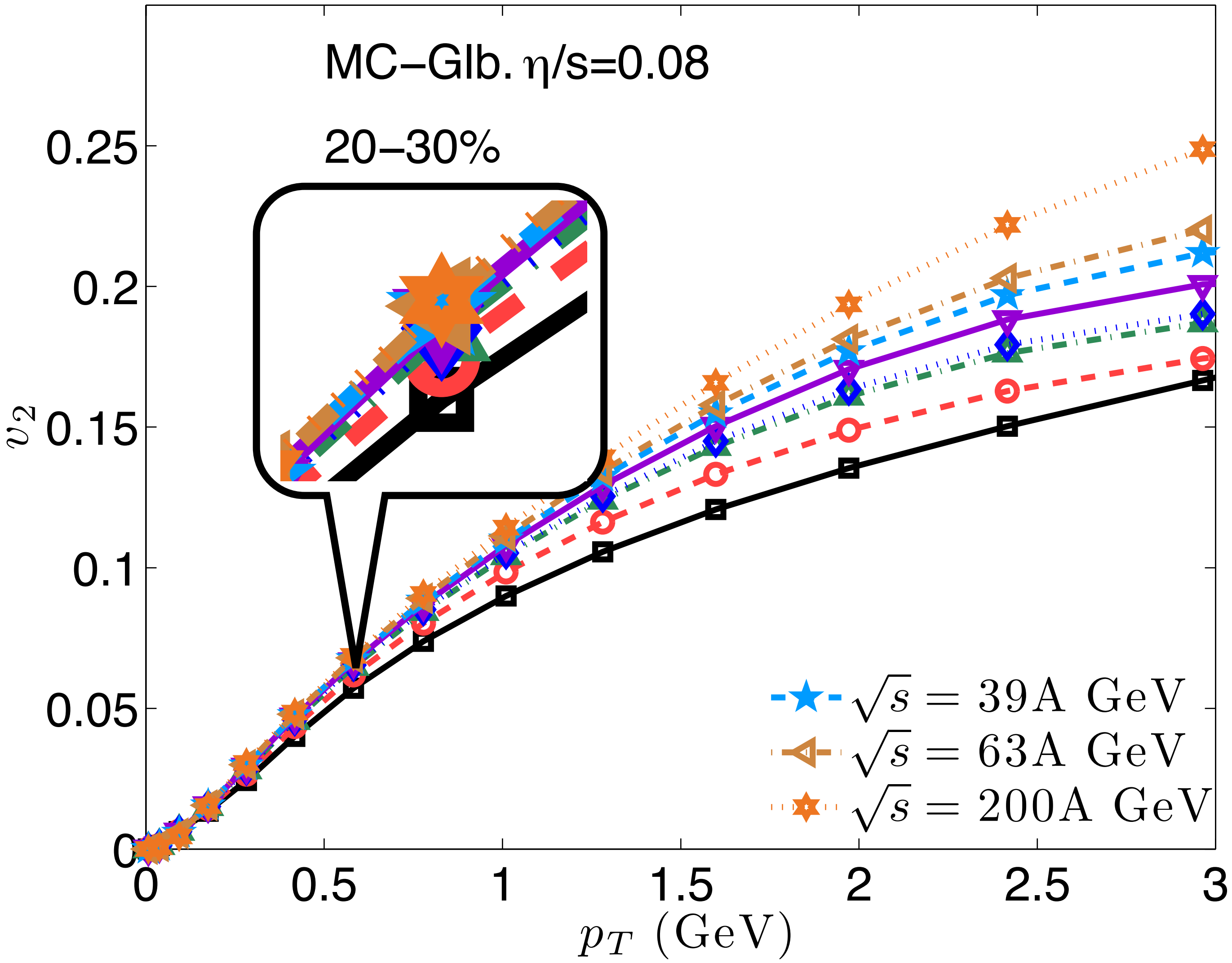

Differential $v_2(p_T)$

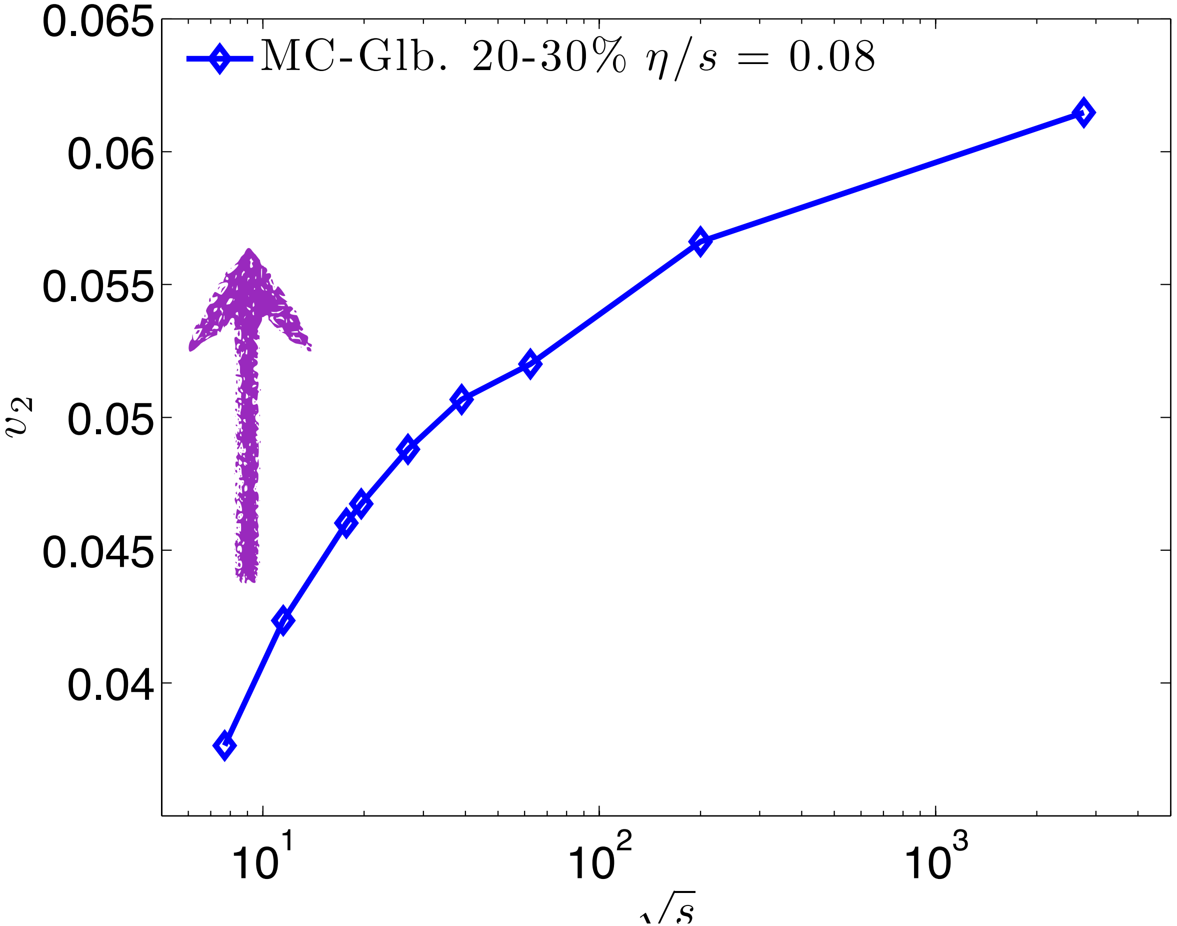

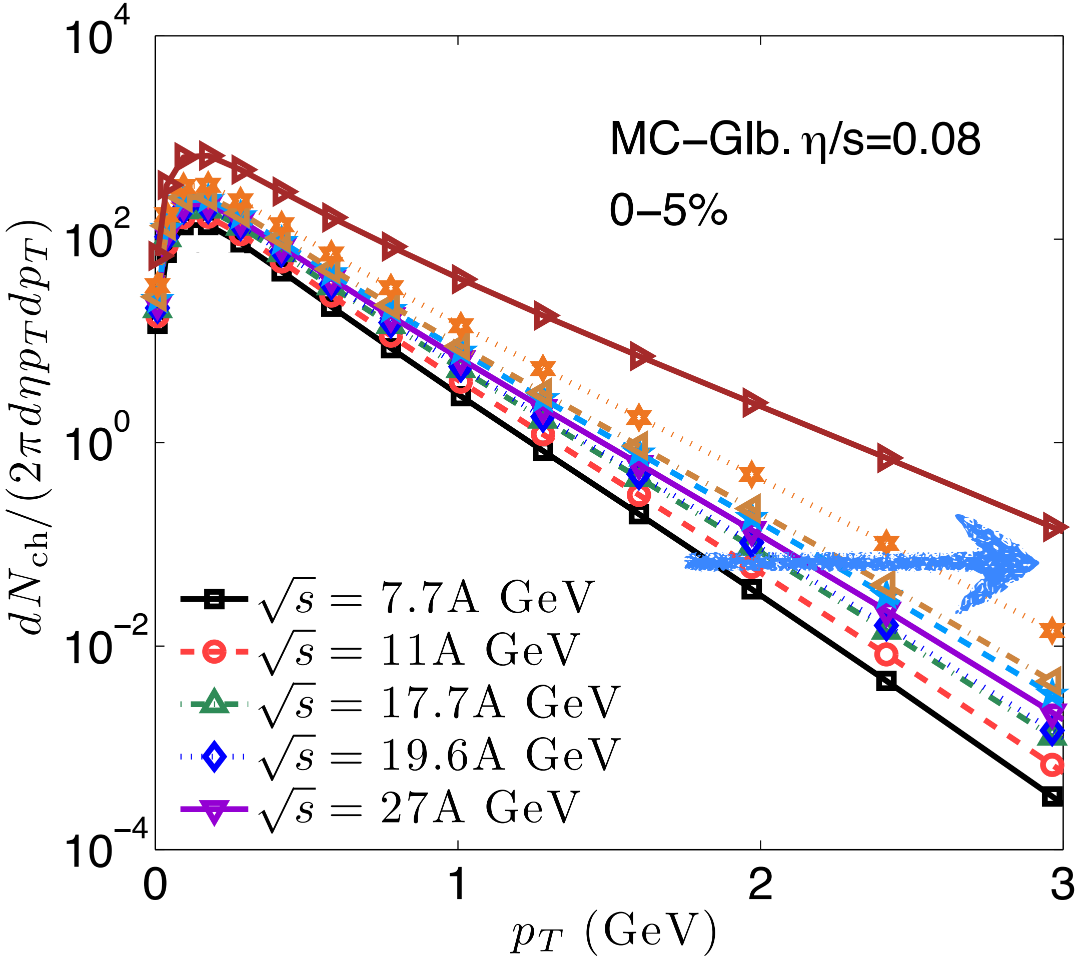

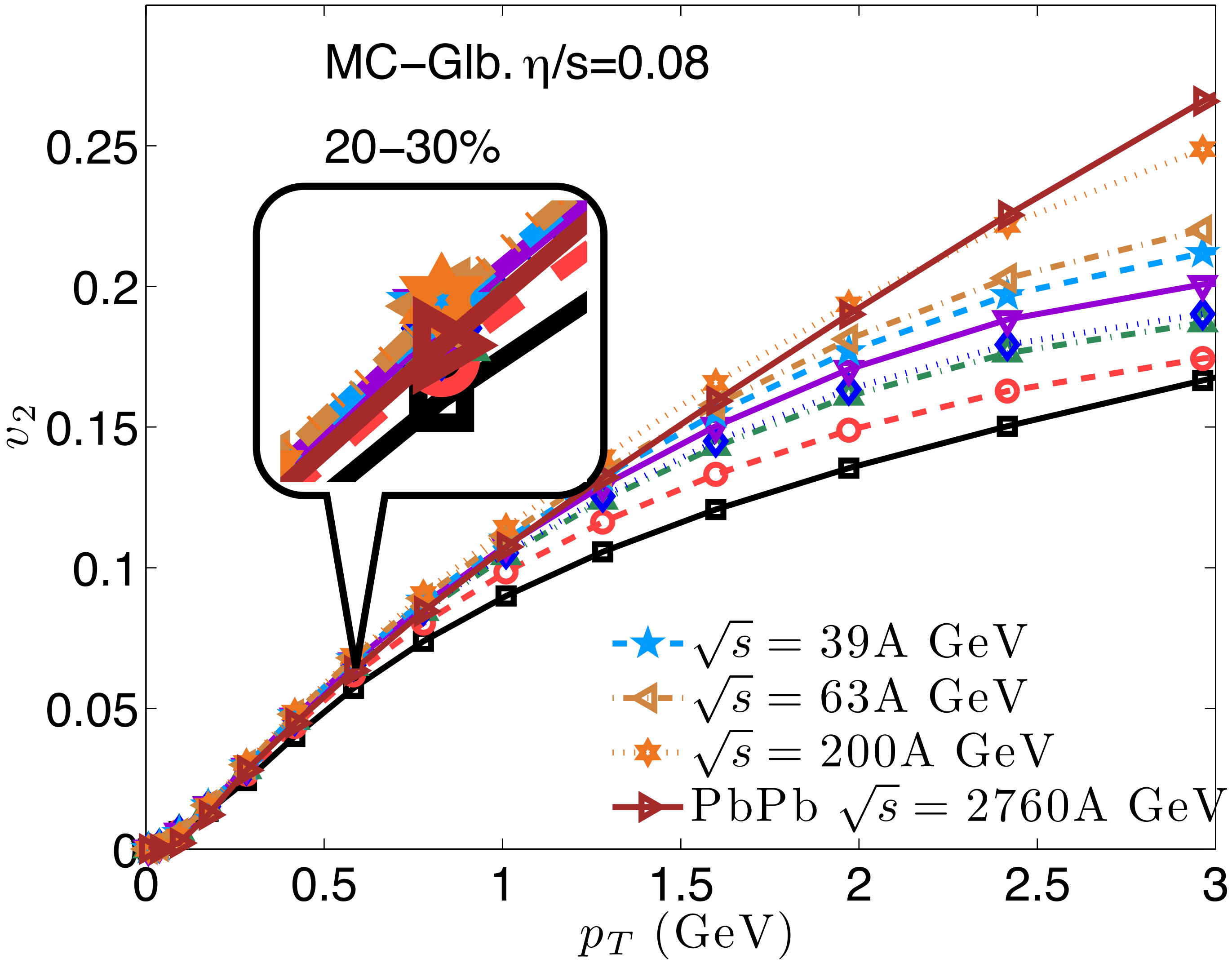

Differential $v_2(p_T)$

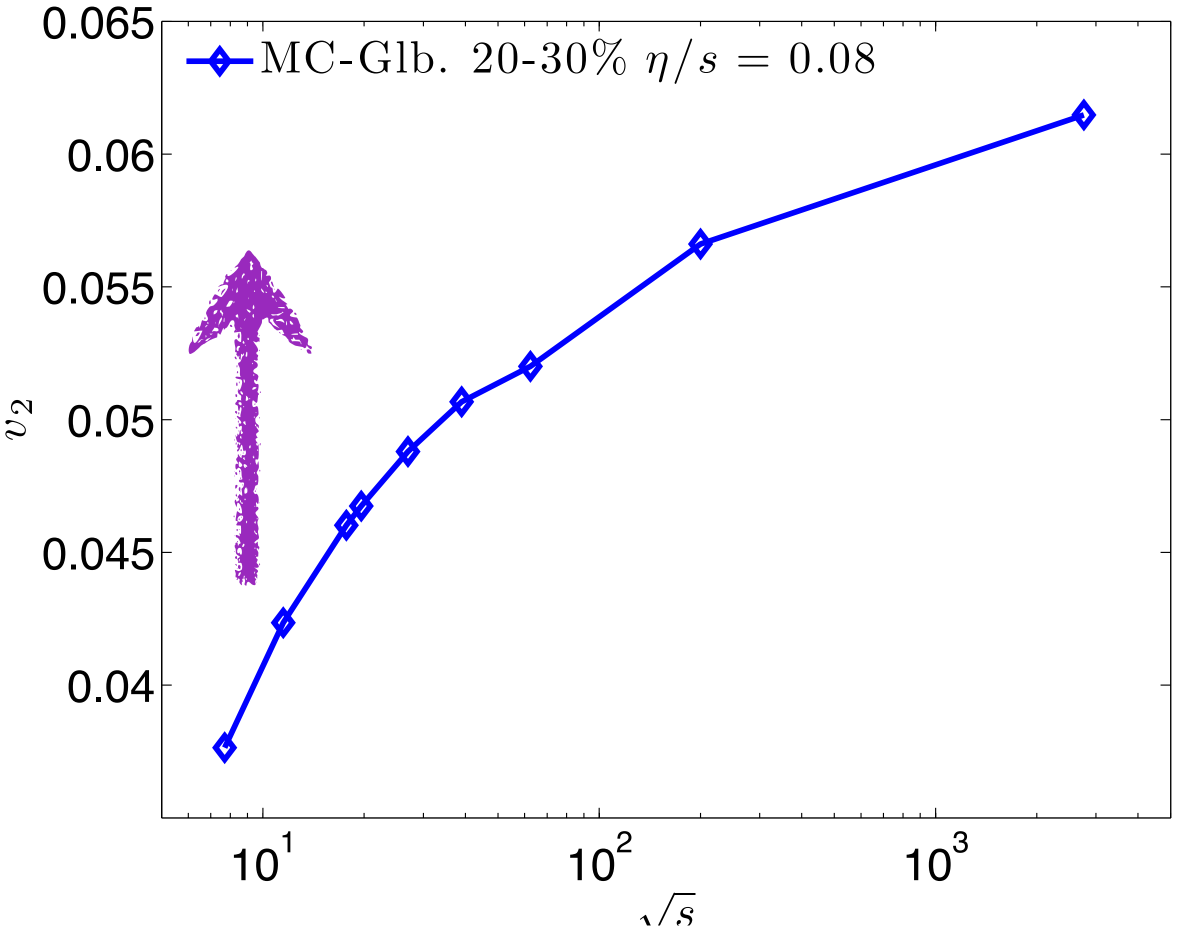

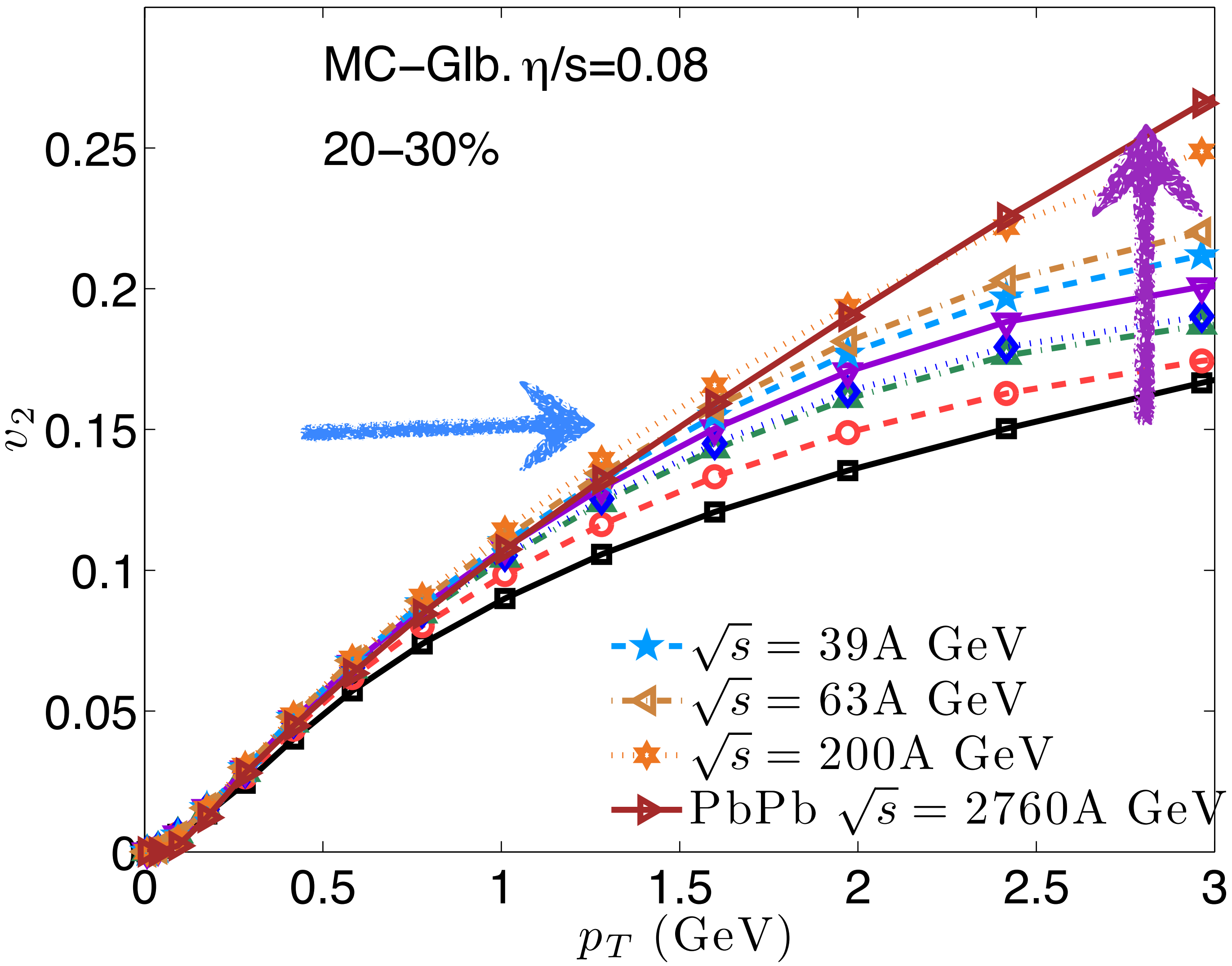

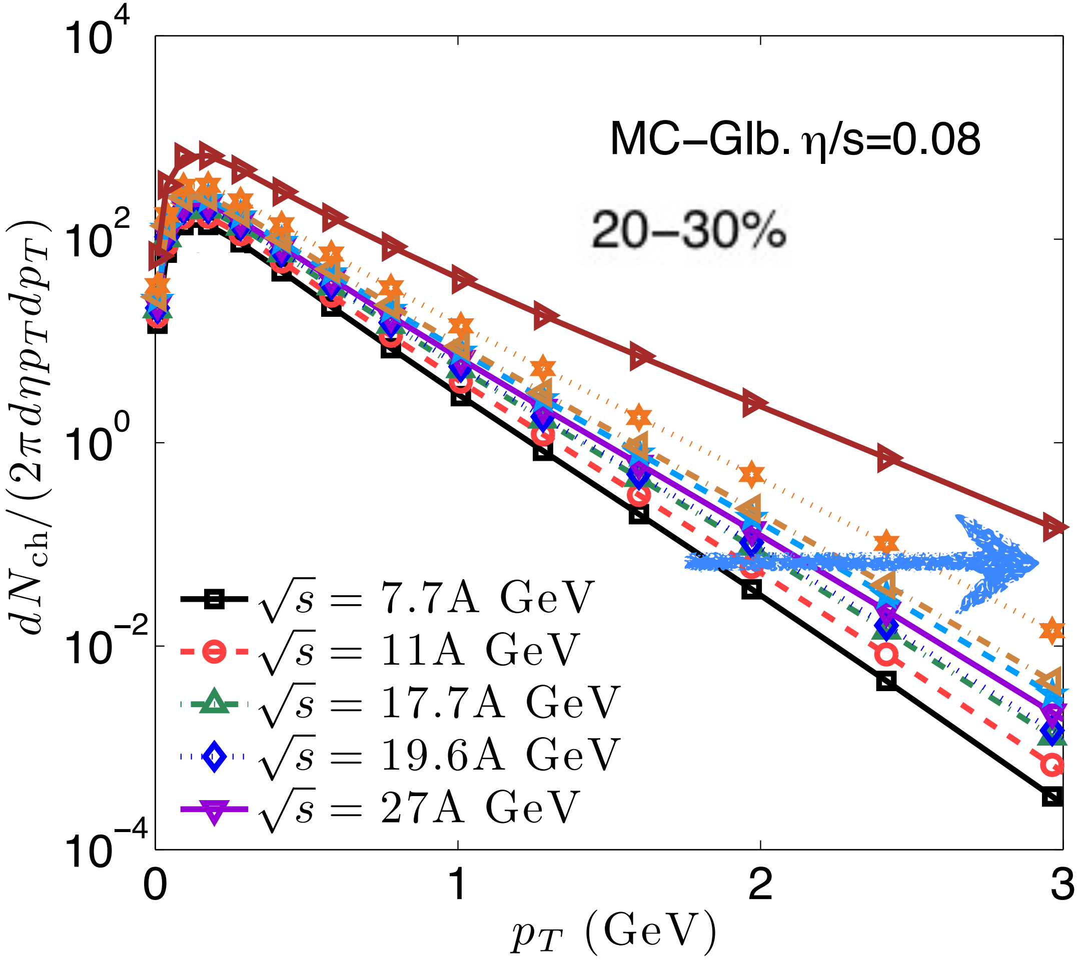

As $\sqrt{s}$ ↗,

the increase of elliptic flow interplays with the stronger radial flow, resulting in a broad maximum for $v_2(p_T, \sqrt{s})$ at fixed p_T as a function of $\sqrt{s}$

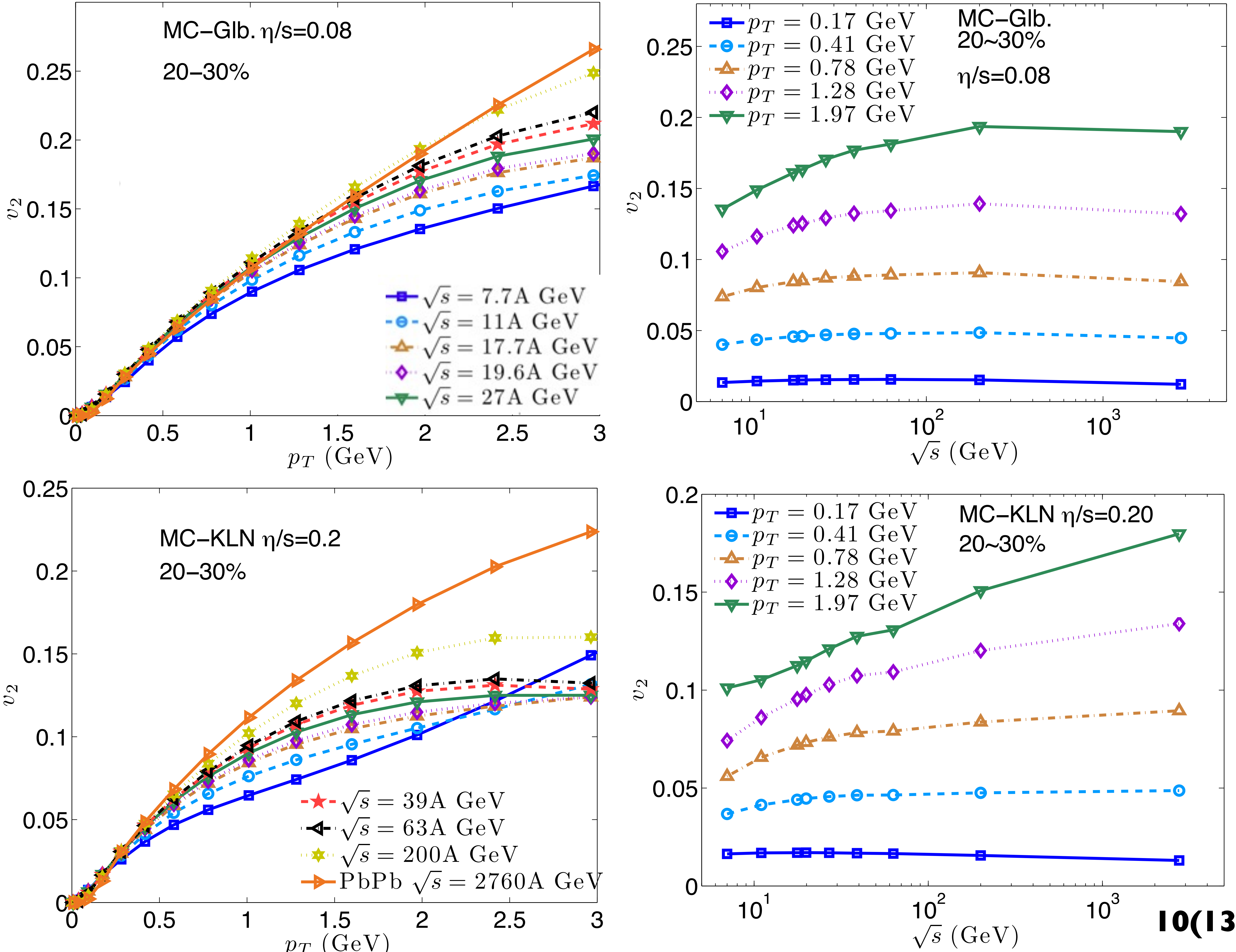
MC−Glb. η/s=0.08
20−30%
v_2
p_T (GeV)
0
0.05
0.1
0.15
0.2
0.25
0
0.5
1
1.5
2
2.5
3
$\sqrt{s} = 7.7$A GeV
$\sqrt{s} = 11$A GeV
$\sqrt{s} = 17.7$A GeV
$\sqrt{s} = 19.6$A GeV
$\sqrt{s} = 27$A GeV
$p_T = 0.17$ GeV
$p_T = 0.41$ GeV
$p_T = 0.78$ GeV
$p_T = 1.28$ GeV
$p_T = 1.97$ GeV
MC−Glb.
20~30%
η/s=0.08
v_2
$\sqrt{s}$ (GeV)
10^1
10^2
10^3
MC−KLN η/s=0.2
20−30%
$\sqrt{s} = 39$A GeV
$\sqrt{s} = 63$A GeV
$\sqrt{s} = 200$A GeV
PbPb $\sqrt{s} = 2760$A GeV
MC−KLN η/s=0.20
20~30%

Differential $v_2(p_T)$

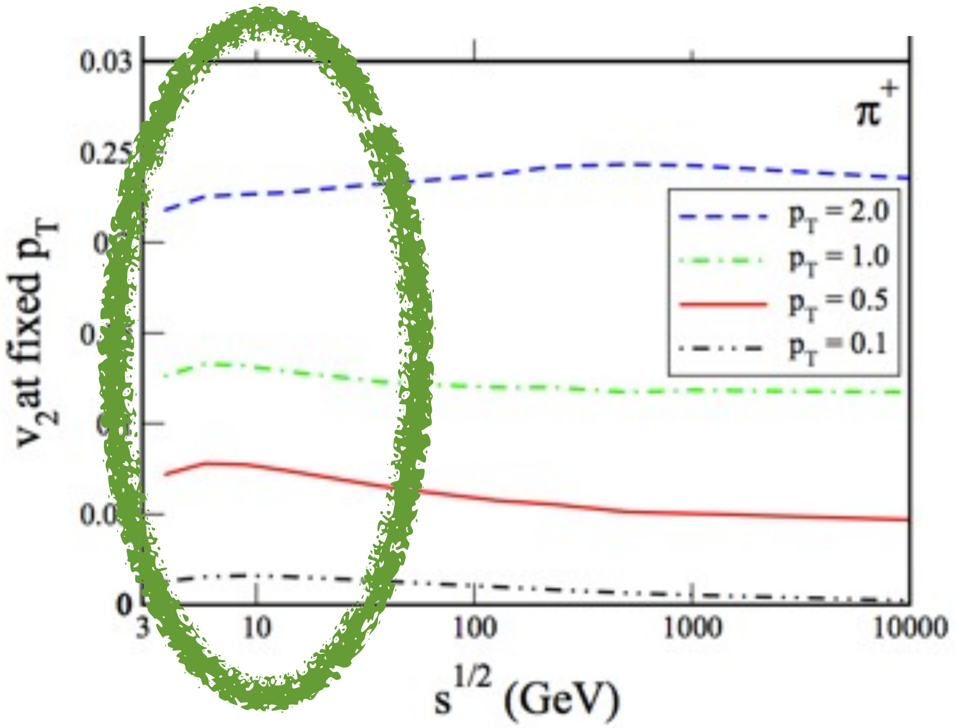

G. Kestin and U. Heinz, *Eur. Phys. J. C* **61**, 545(2009)

$$\eta/s = 0$$

- Ideal hydro: $v_2(p_T)$ peaks at around $\sqrt{s} \sim 5$ GeV

Differential $v_2(p_T)$

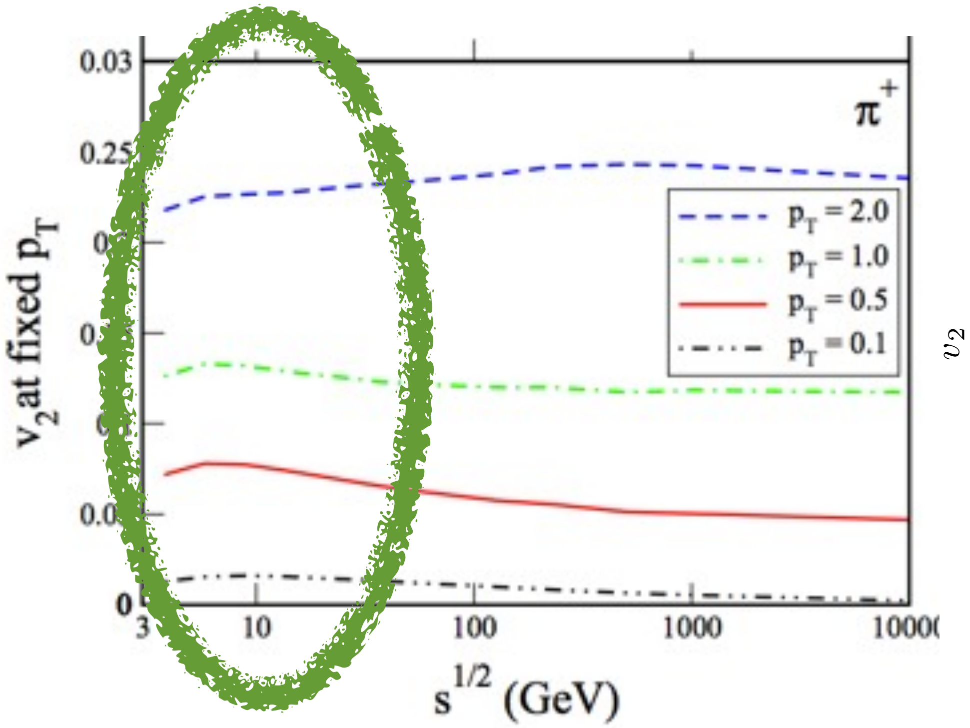

G. Kestin and U. Heinz, *Eur. Phys. J. C* **61**, 545(2009)

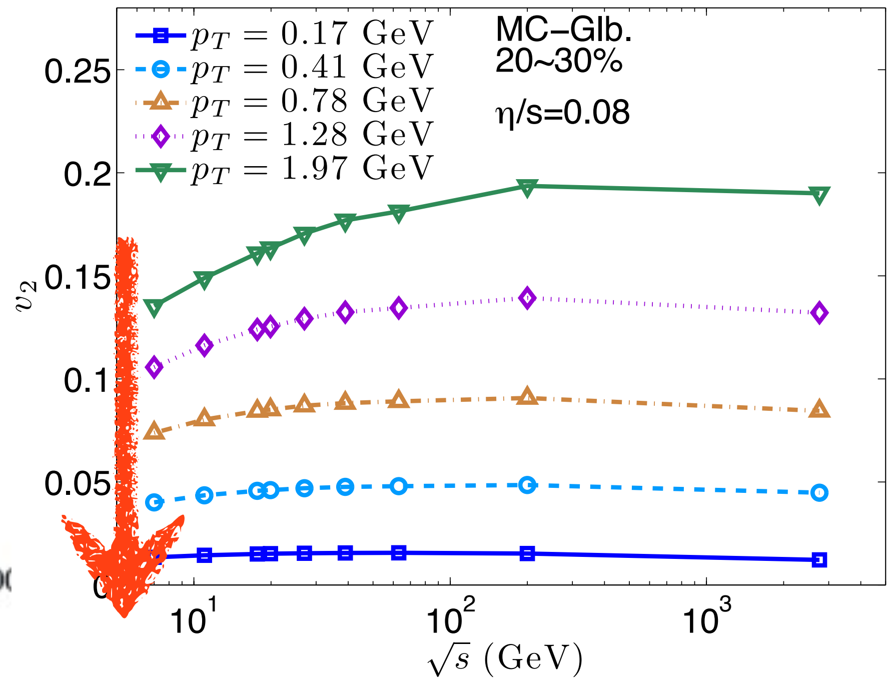

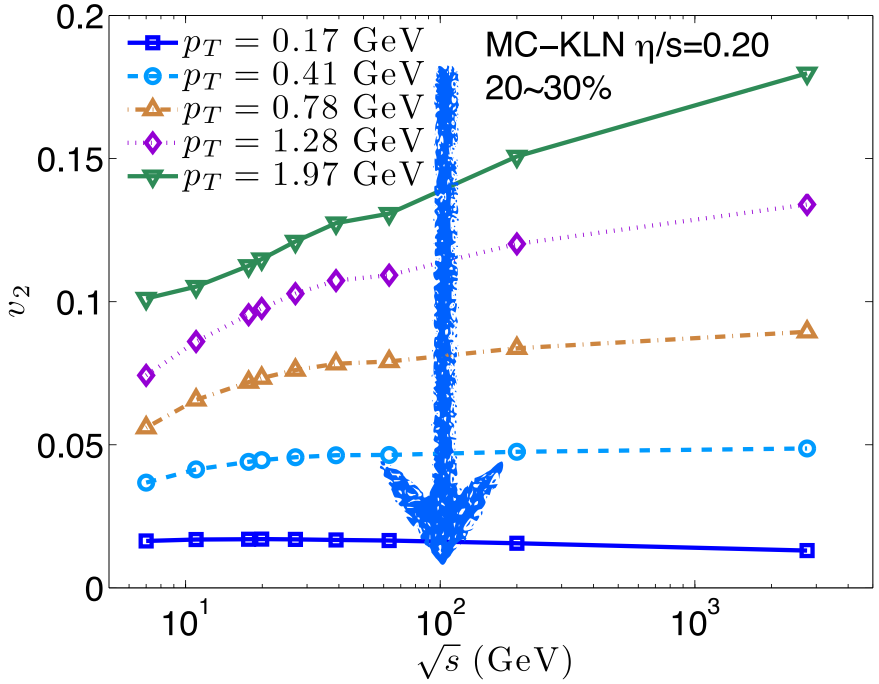

$\eta/s = 0$ $\eta/s = 0.08$ $\eta/s = 0.20$

- Ideal hydro: $v_2(p_T)$ peaks at around $\sqrt{s} \sim 5$ GeV

Differential $v_2(p_T)$

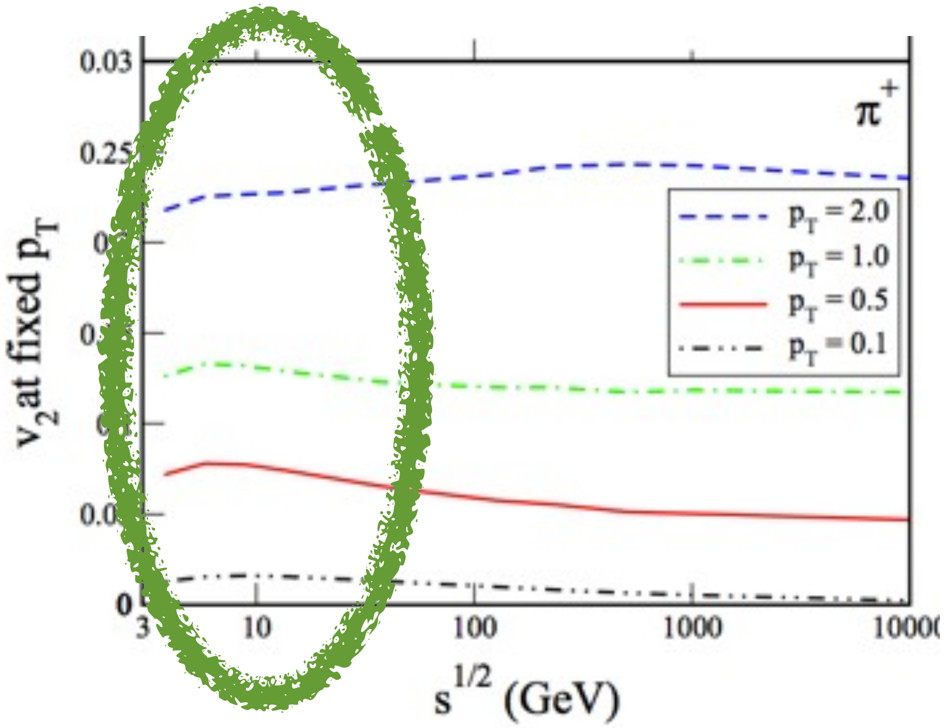

G. Kestin and U. Heinz, *Eur. Phys. J. C* **61**, 545(2009)

$\eta/s = 0$

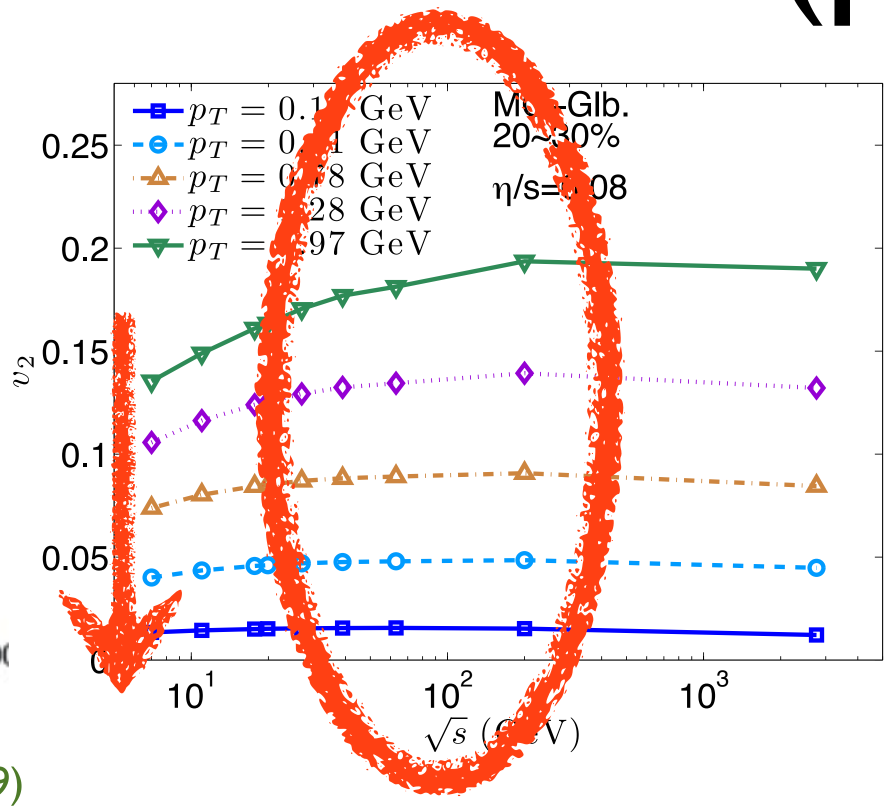

$\eta/s = 0.08$

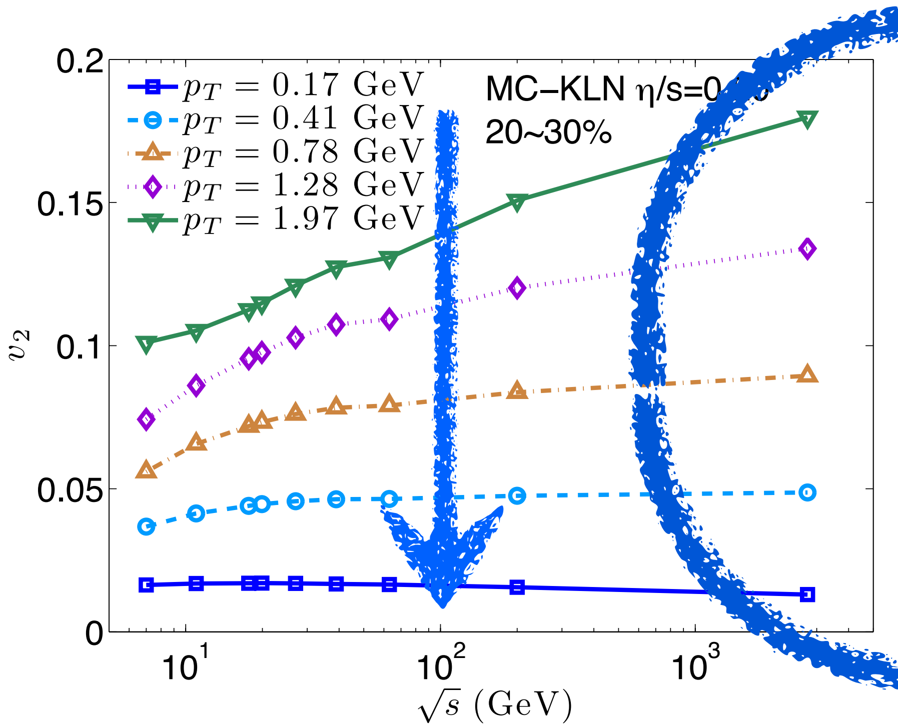

$\eta/s = 0.20$

- Ideal hydro: $v_2(p_T)$ peaks at around $\sqrt{s} \sim 5$ GeV
- MC-Glb. $\eta/s = 0.08$: $v_2(p_T)$ reaches broad maximum for $\sqrt{s} \sim 200$ GeV
- MC-KLN $\eta/s = 0.20$: $v_2(p_T)$ will peak somewhere at $\sqrt{s} > 2760$ GeV

Differential $v_2(p_T)$

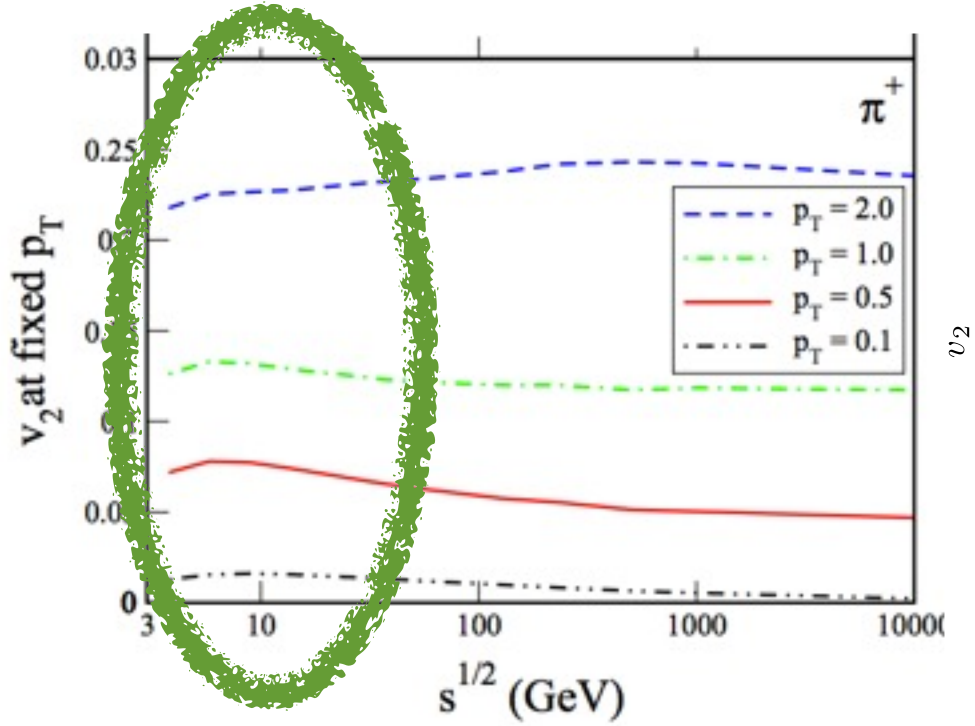

G. Kestin and U. Heinz, *Eur. Phys. J. C* **61**, 545(2009)

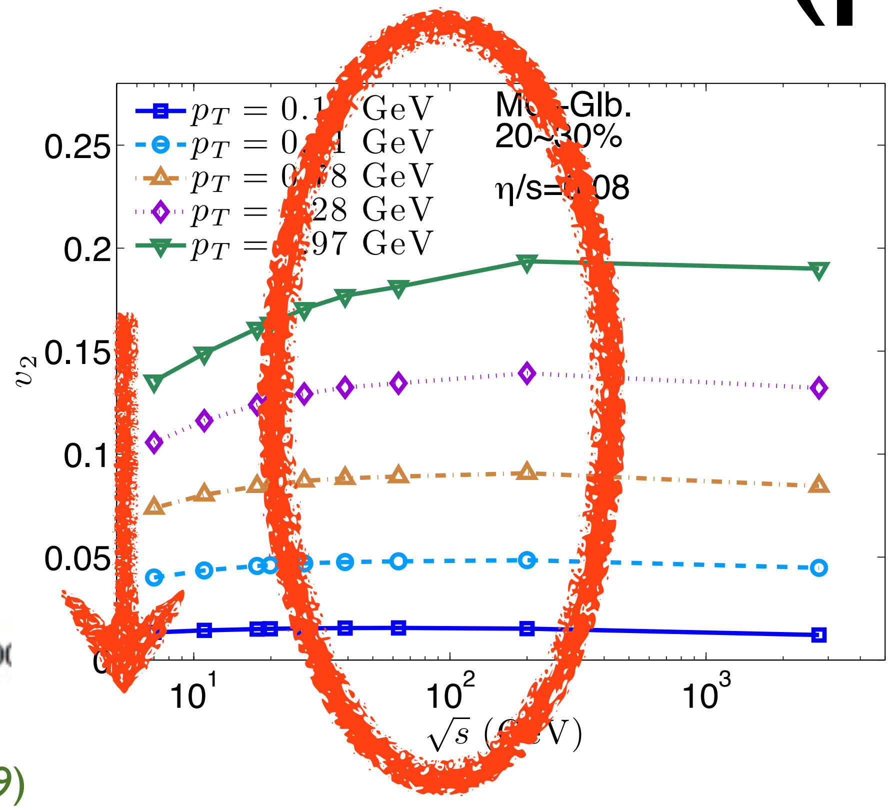

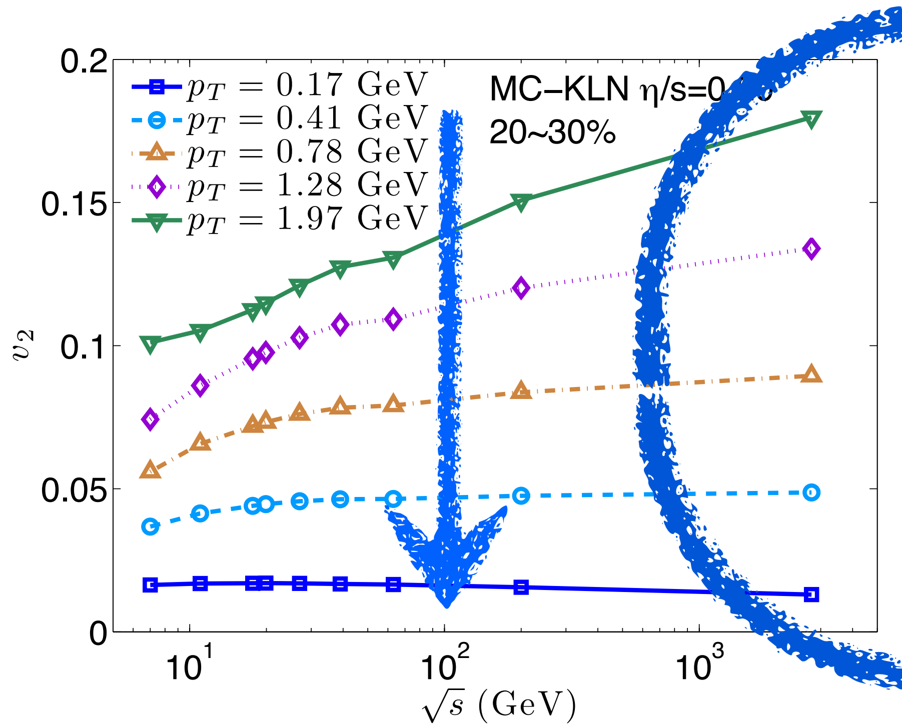

$\eta/s = 0$ $\eta/s = 0.08$ $\eta/s = 0.20$

- Ideal hydro: $v_2(p_T)$ peaks at around $\sqrt{s} \sim 5$ GeV
- MC-Glb. : $v_2(p_T)$ reaches broad maximum for $\sqrt{s} \sim 200$ GeV
  $\eta/s = 0.08$
- MC-KLN : $v_2(p_T)$ will peak somewhere at $\sqrt{s} > 2760$ GeV
  $\eta/s = 0.20$

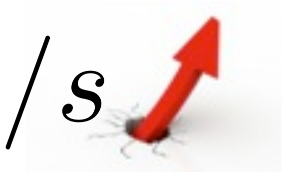

η/s ⇒ peak in $v_2(p_T, \sqrt{s})$ moves to larger $\sqrt{s}$

Freeze-out shape analysis

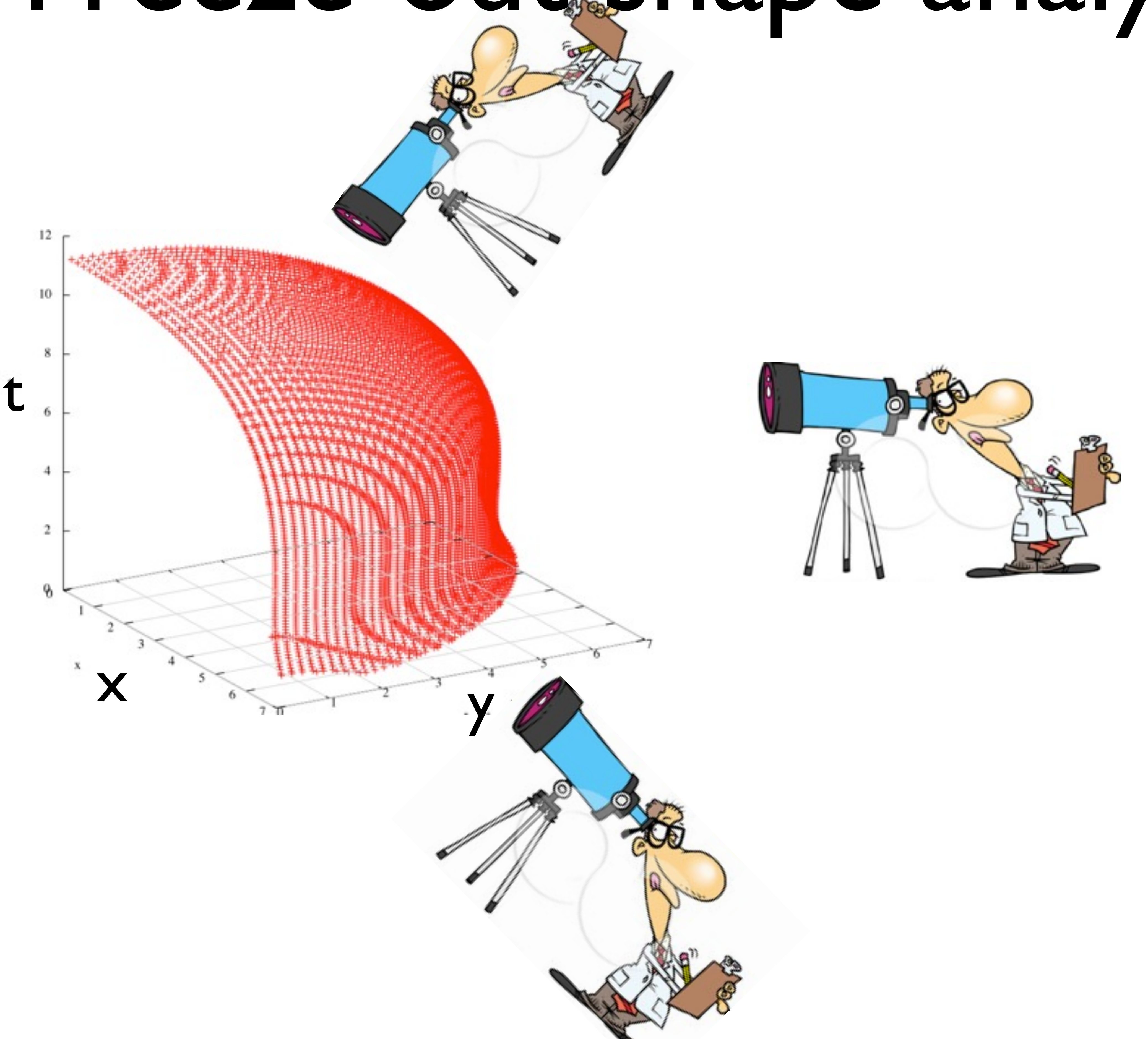

Freeze-out shape analysis

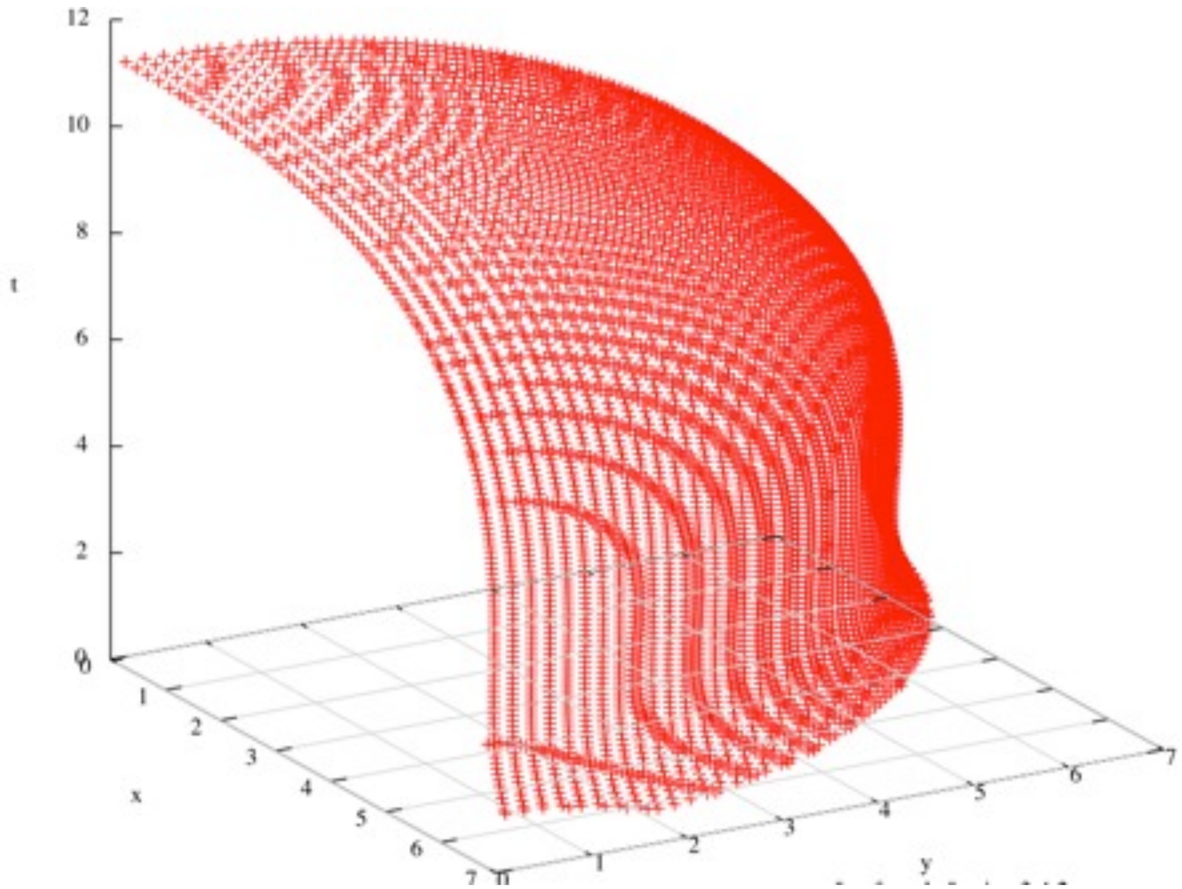

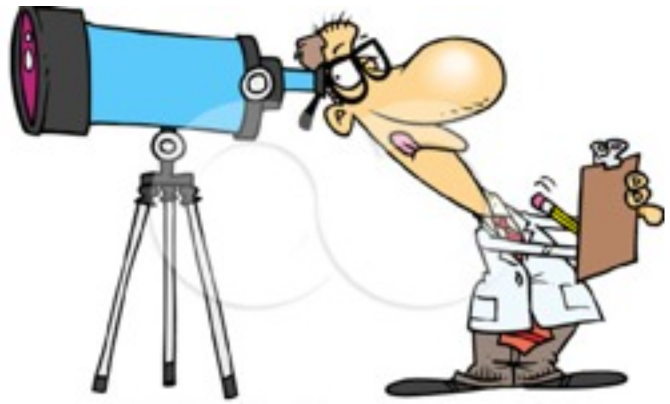

PbPb 20-30% LHC

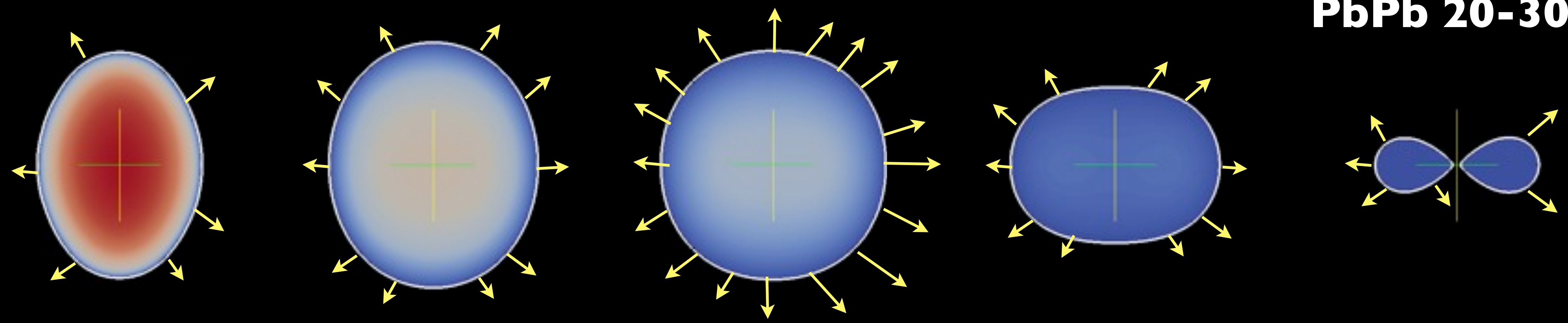

Freeze-out shape analysis

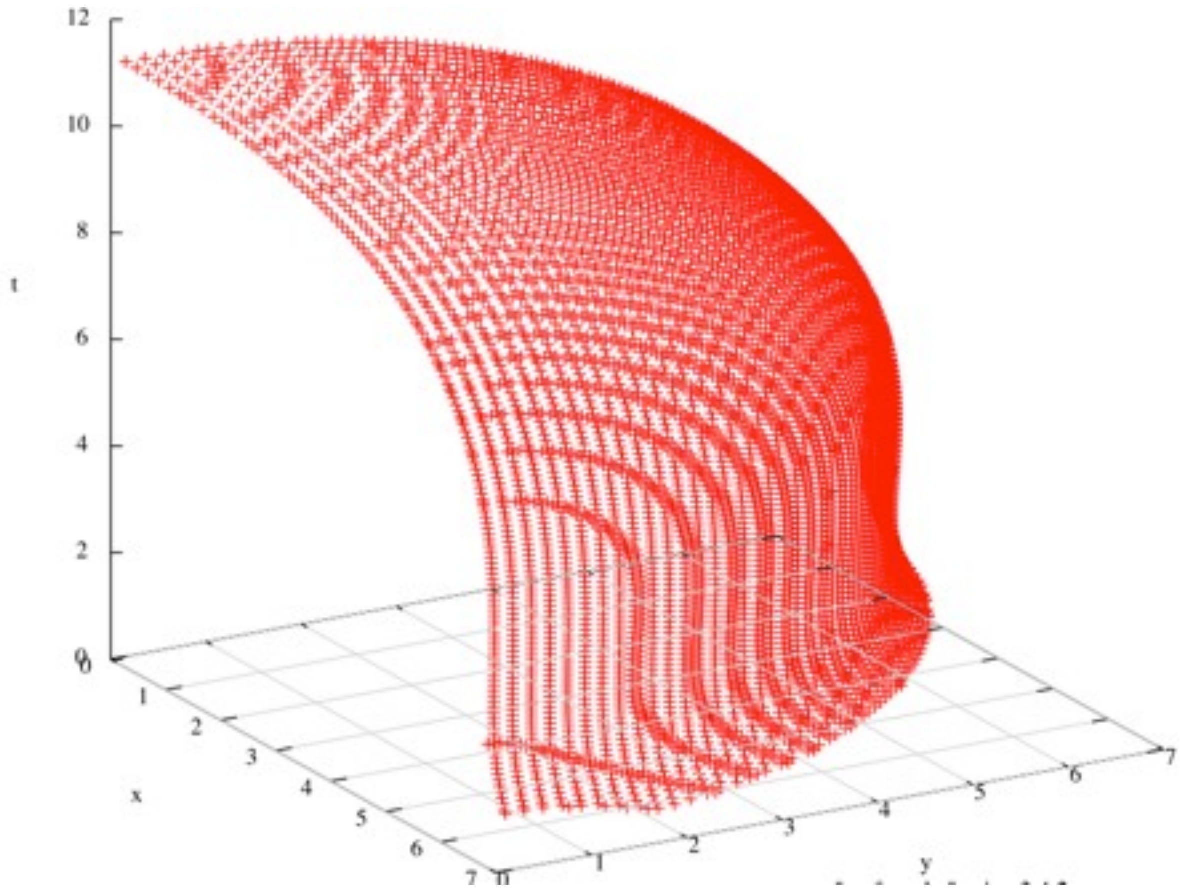

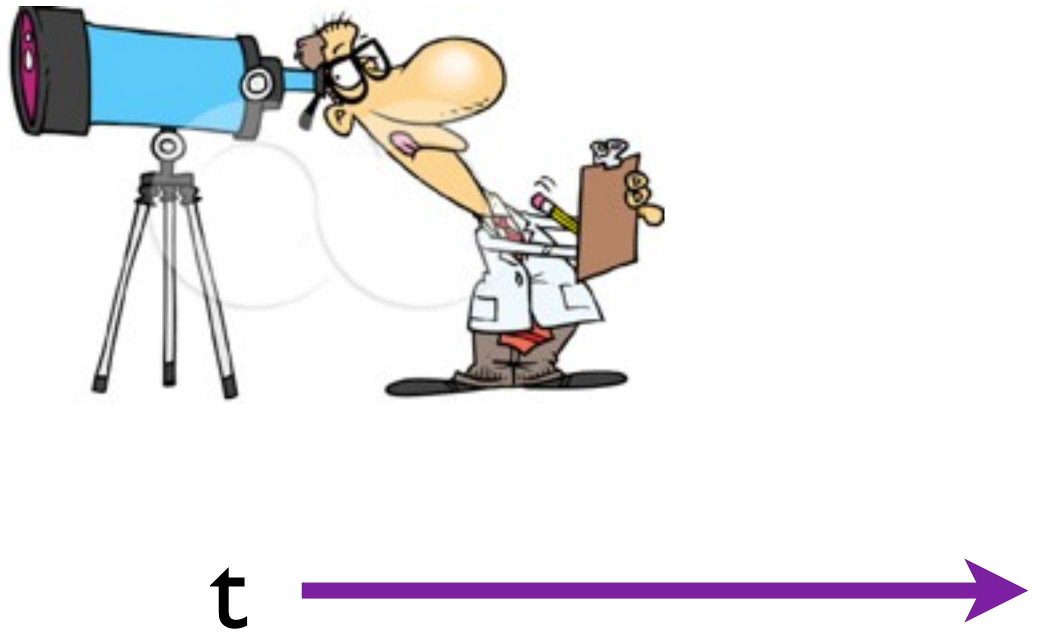

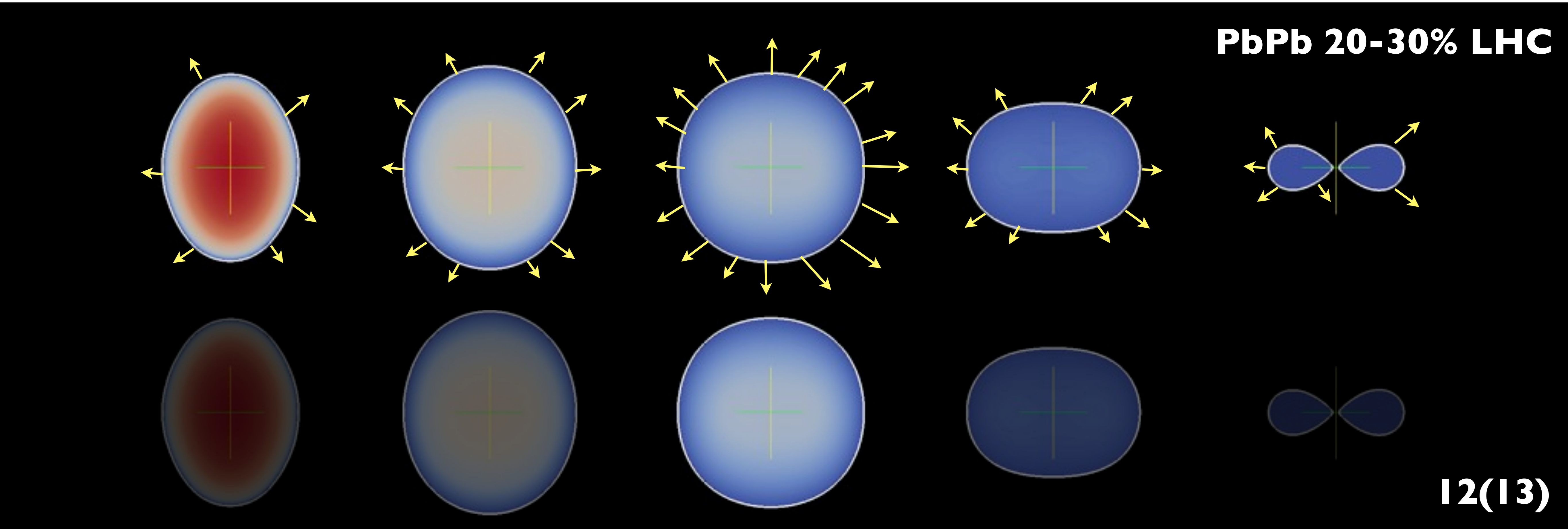

PbPb 20-30% LHC

Freeze-out shape analysis

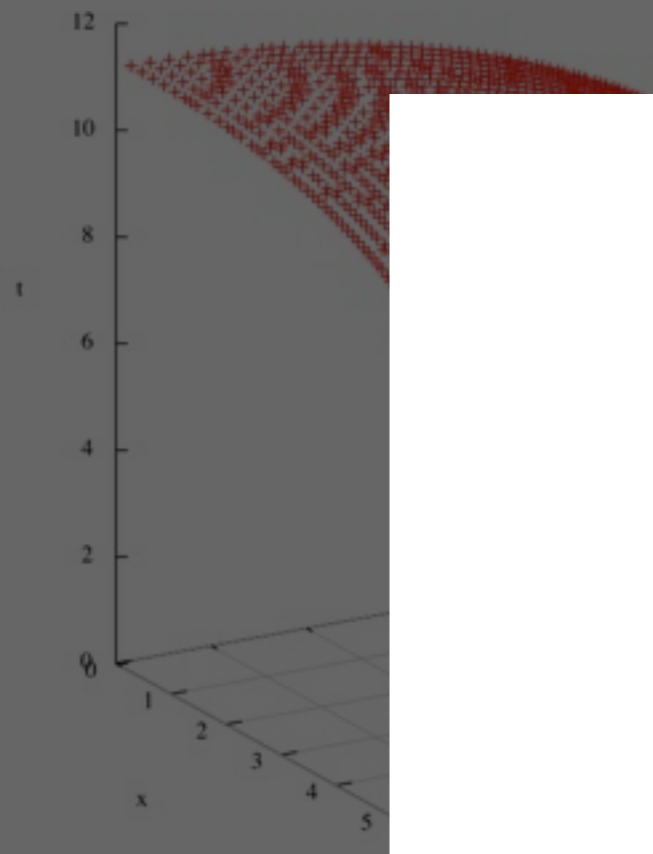

$$\epsilon_x(\Sigma) = \frac{\int_\Sigma u^\mu d^3\sigma_\mu \,(y^2 - x^2)}{\int_\Sigma u^\mu d^3\sigma_\mu \,(y^2 + x^2)},$$


20-30% LHC

Freeze-out shape analysis

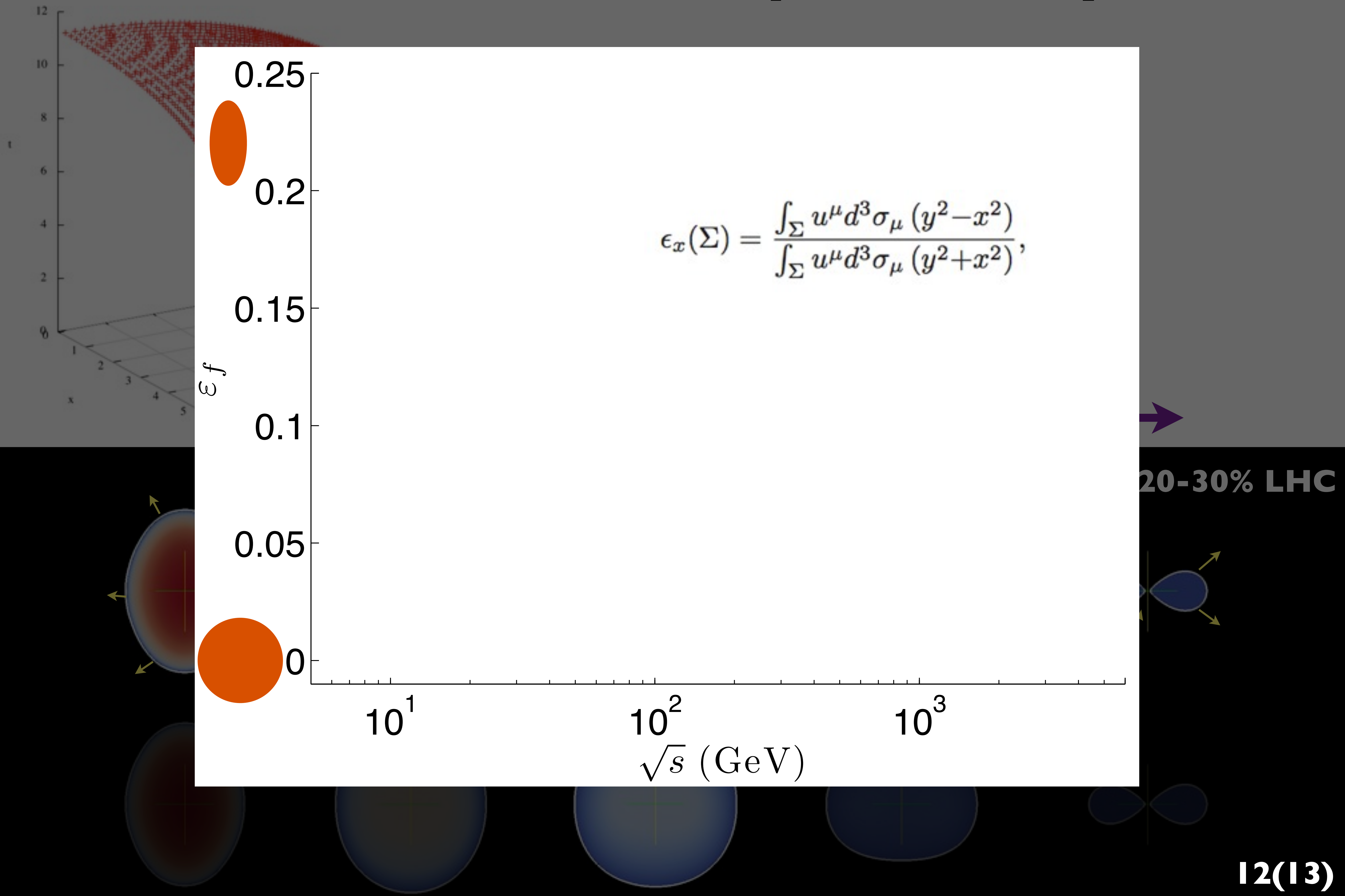

$$\epsilon_x(\Sigma) = \frac{\int_\Sigma u^\mu d^3\sigma_\mu \,(y^2-x^2)}{\int_\Sigma u^\mu d^3\sigma_\mu \,(y^2+x^2)},$$

Freeze-out shape analysis

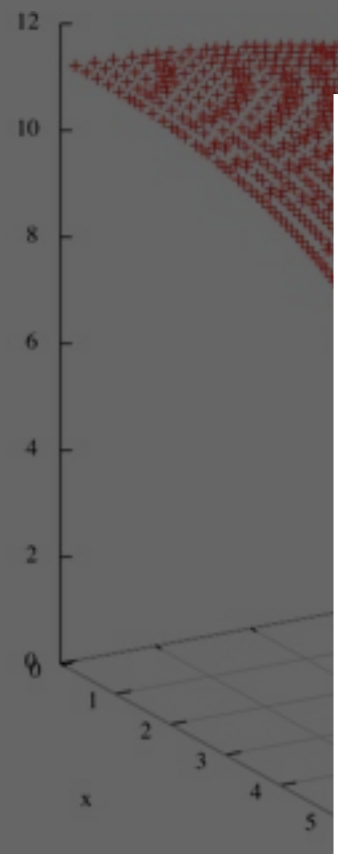

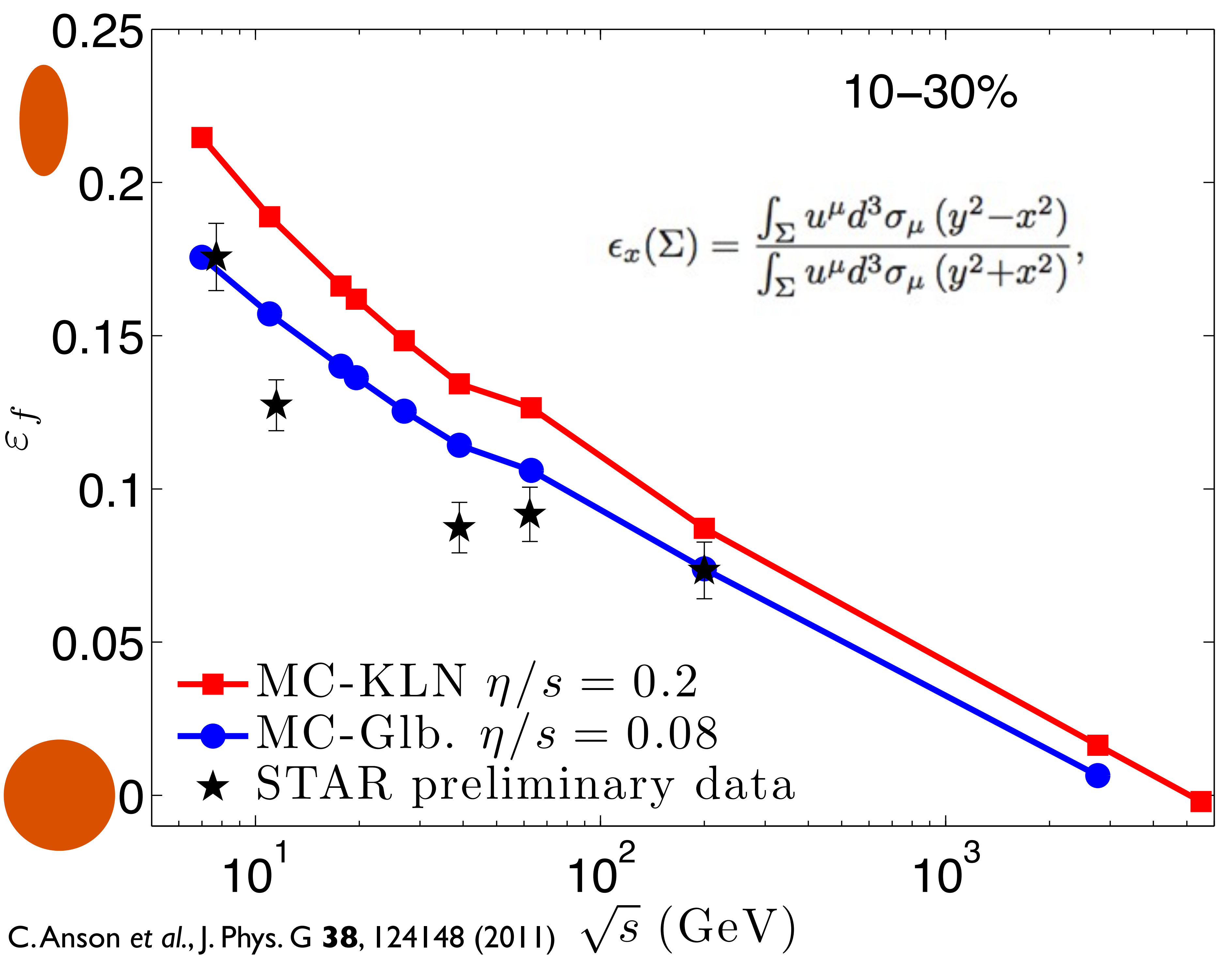

$$\epsilon_x(\Sigma) = \frac{\int_\Sigma u^\mu d^3\sigma_\mu \, (y^2 - x^2)}{\int_\Sigma u^\mu d^3\sigma_\mu \, (y^2 + x^2)},$$

C. Anson *et al.*, J. Phys. G **38**, 124148 (2011)

20-30% LHC

Freeze-out shape analysis

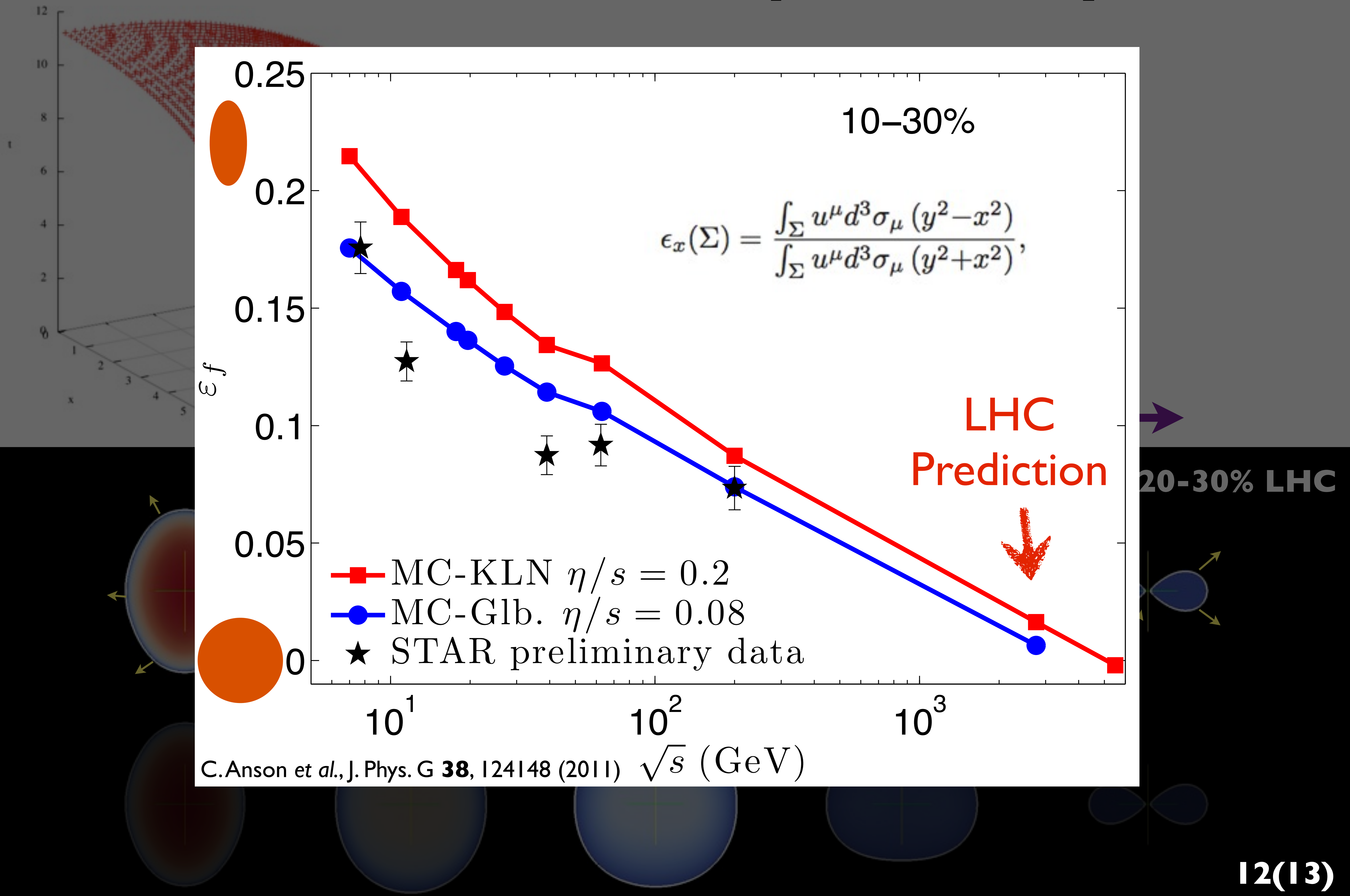

$$\epsilon_x(\Sigma) = \frac{\int_\Sigma u^\mu d^3\sigma_\mu \, (y^2 - x^2)}{\int_\Sigma u^\mu d^3\sigma_\mu \, (y^2 + x^2)},$$

C. Anson *et al.*, J. Phys. G **38**, 124148 (2011)

Summary

Collision energy dependence of soft hadron observables will help us constrain initial conditions as well as evolution dynamics

- MC-Glb. with $\eta/s = 0.08$ shows good $\sqrt{s}$-scaling behavior

  $$\frac{dN/d\eta}{N_{\rm part}/2} \text{ vs } N_{\rm part} \qquad v_2/\epsilon_2 \text{ vs } \frac{1}{S}\frac{dN}{d\eta}$$

  MC-KLN model with $\eta/s = 0.20$ does **not**

- Increasing shear viscosity changes the balance between radial and elliptic flow, shifting the peak of $v_2(\sqrt{s}, p_T)$ to larger $\sqrt{s}$

- Novel final shape analysis predicts the spatial eccentricity at freeze-out approaches zero at LHC energy

Back up

Centrality Dependence of the Initial Entropy Densities

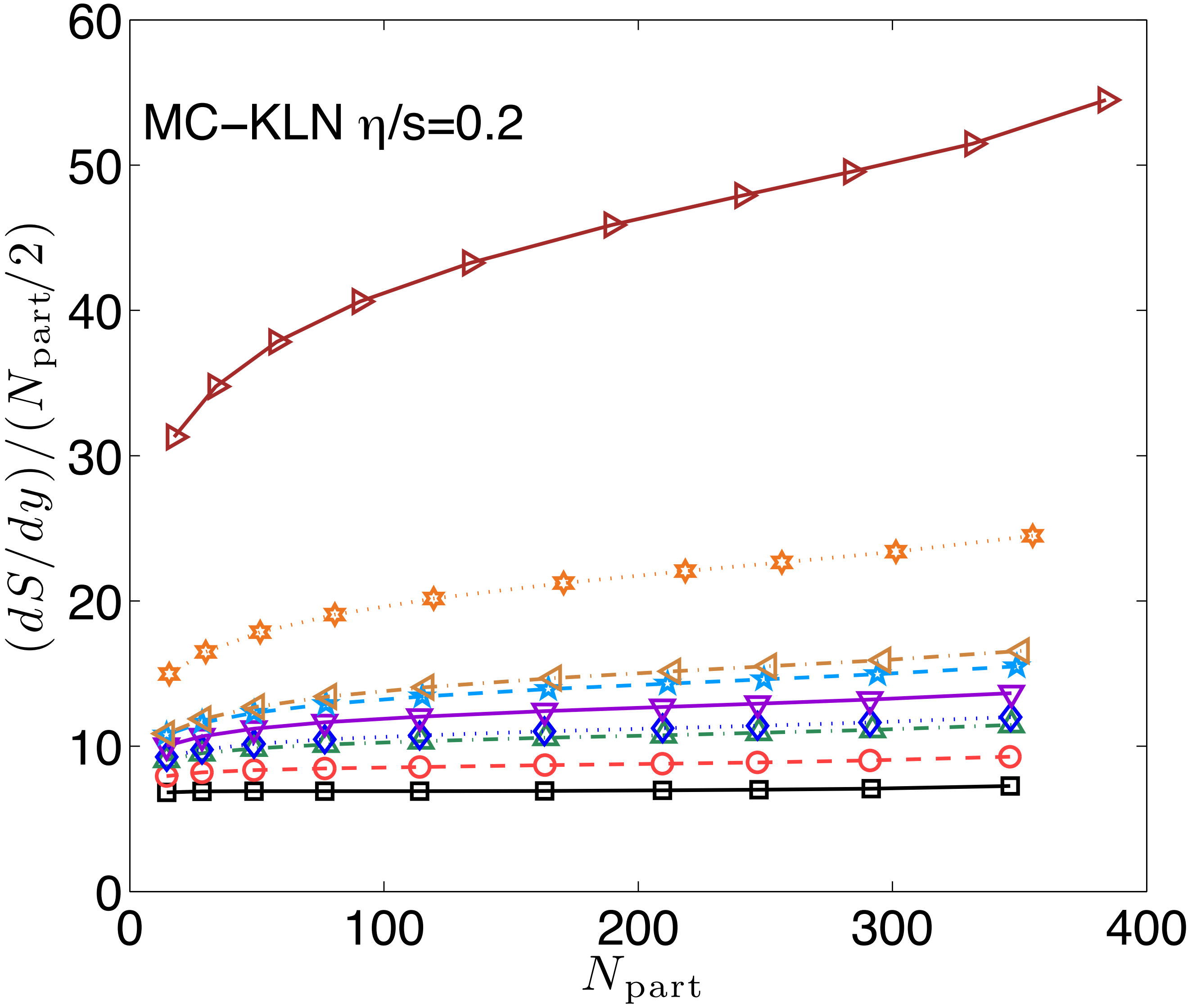

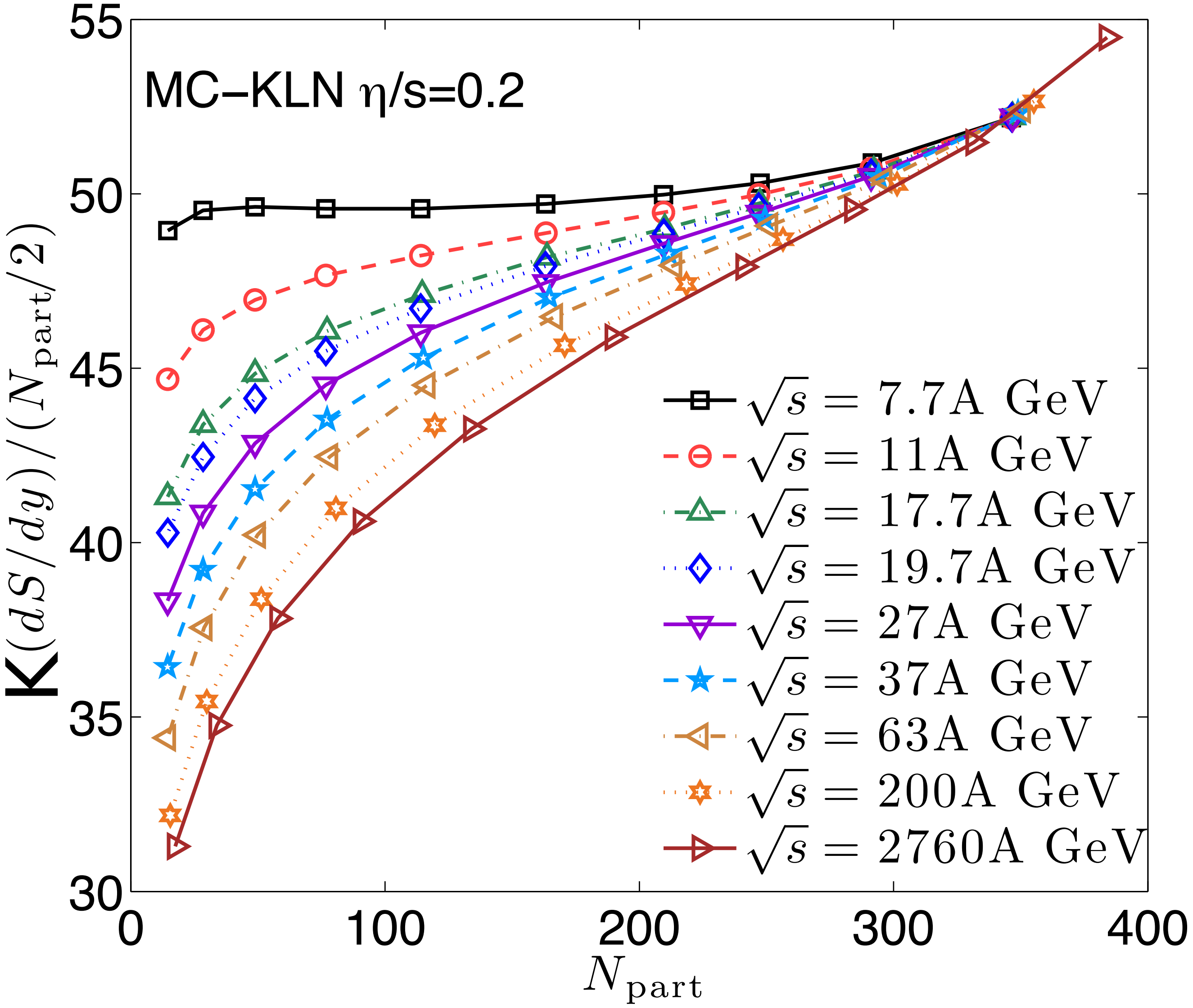

radial flow and particle p_T-spectra

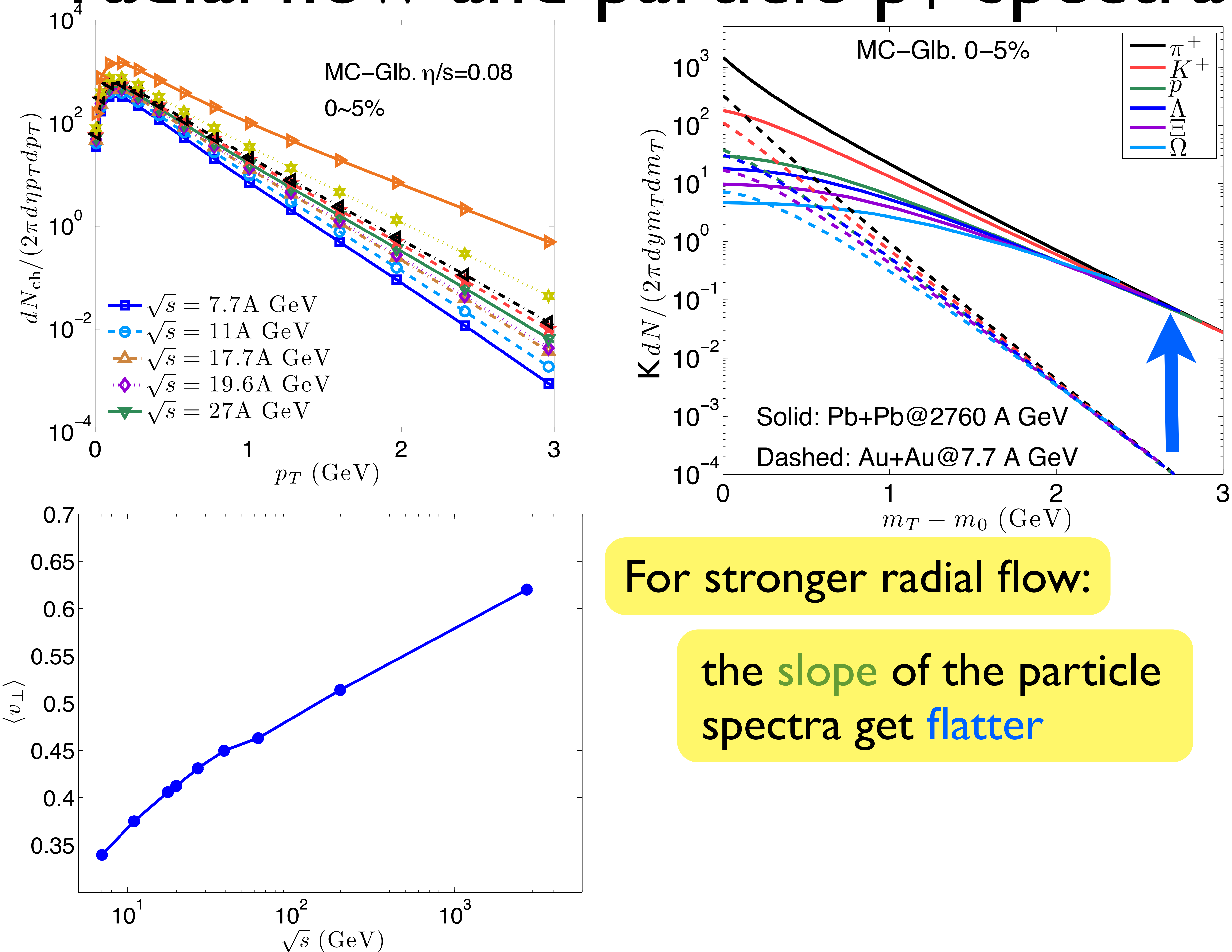

For stronger radial flow:

the slope of the particle spectra get flatter

radial flow and particle p_T-spectra

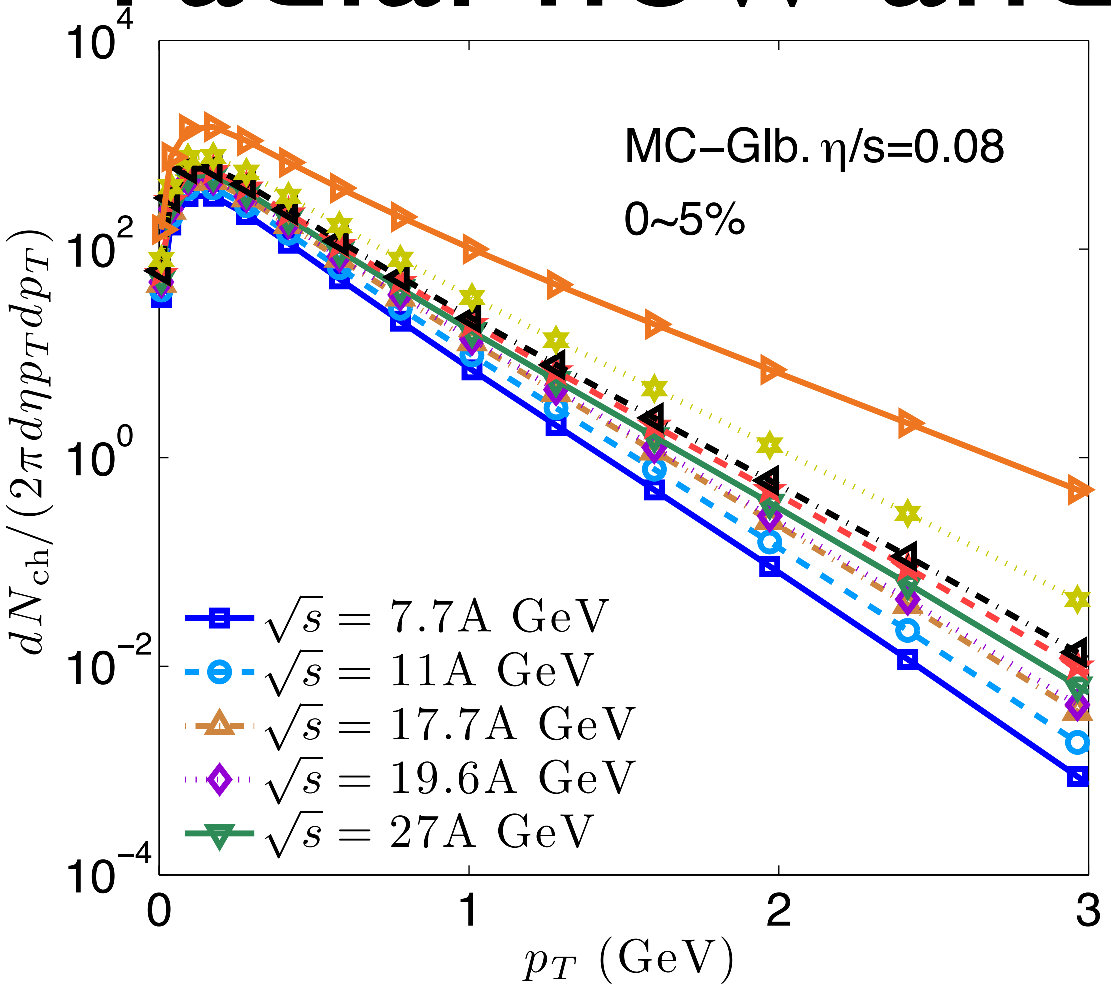

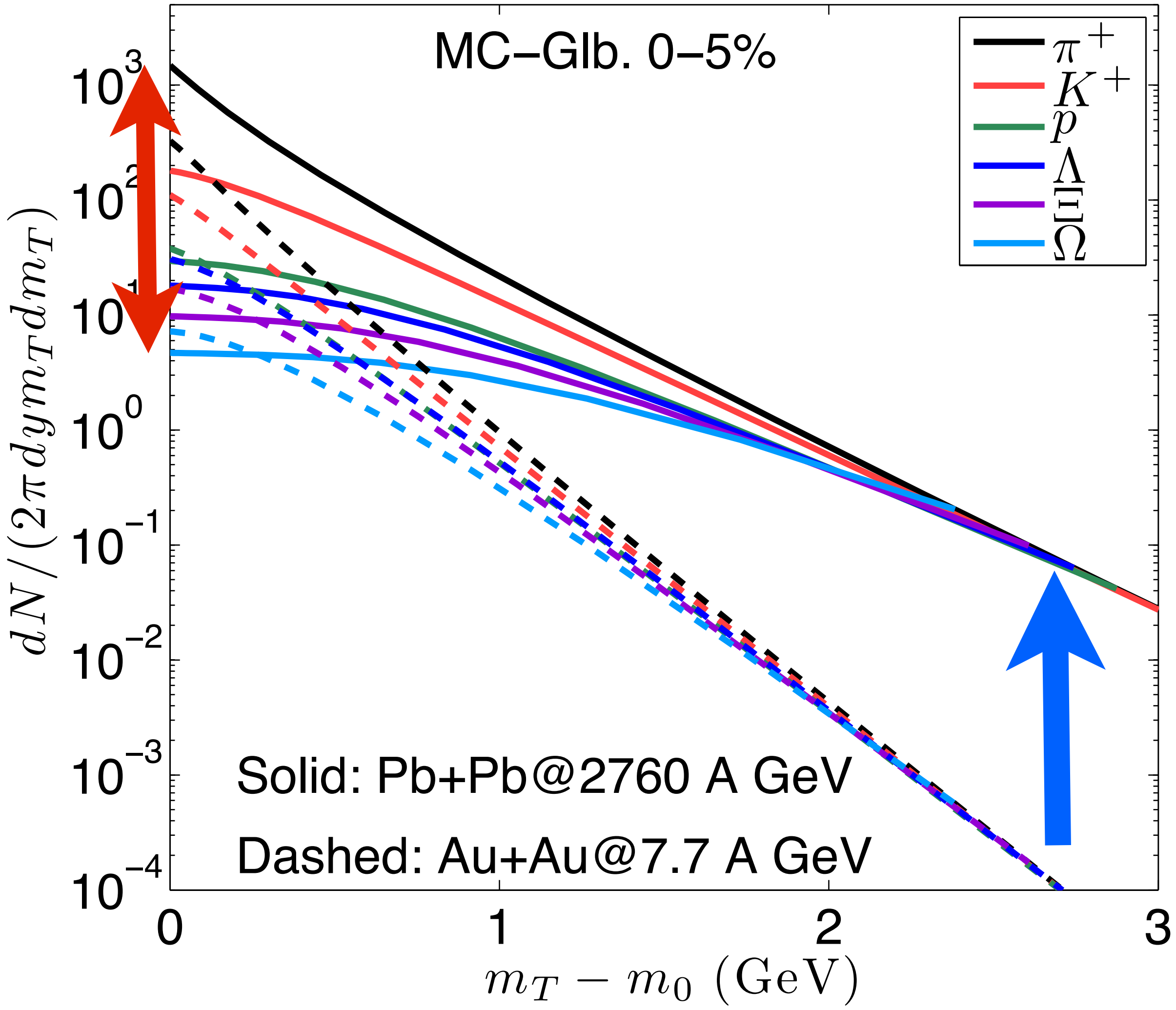

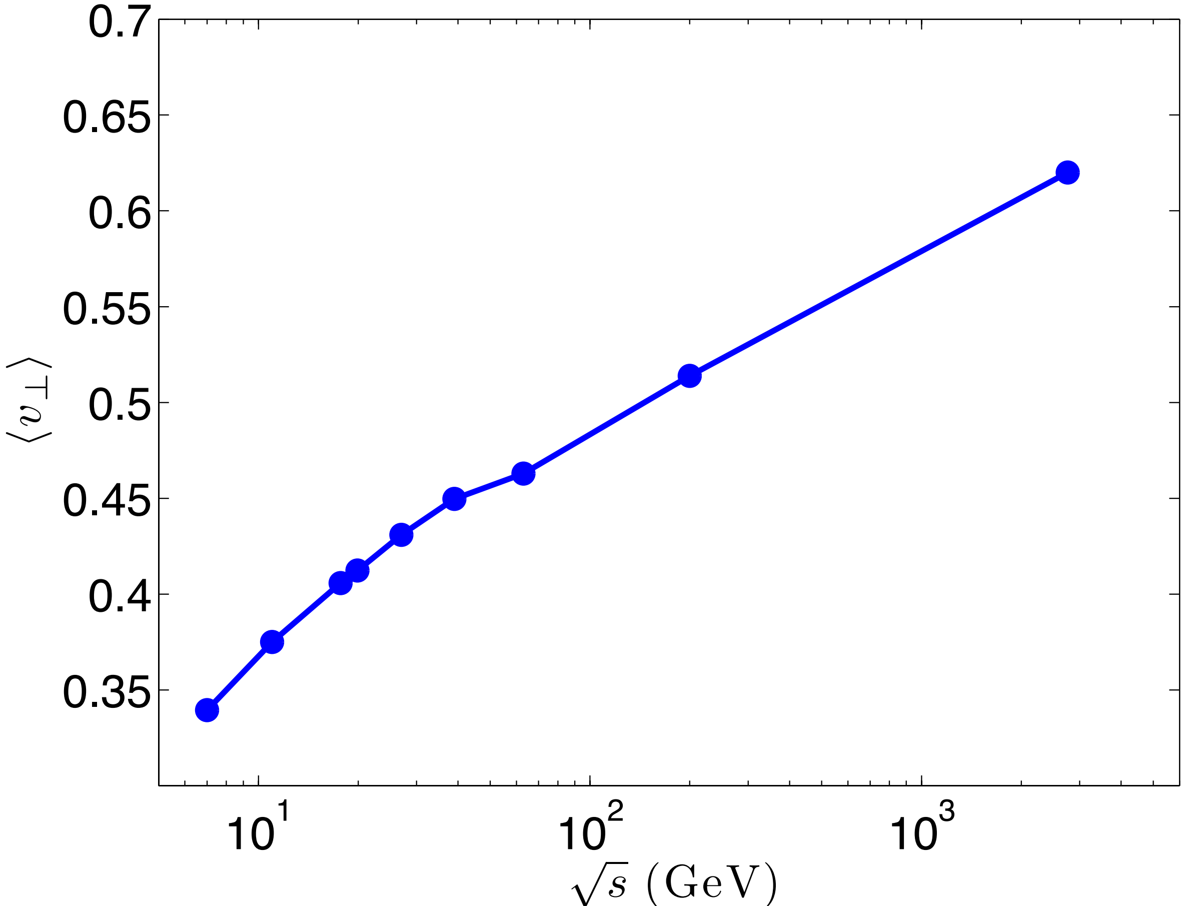

For stronger radial flow:

the slope of the particle spectra get flatter

the splitting between different species of particles get larger

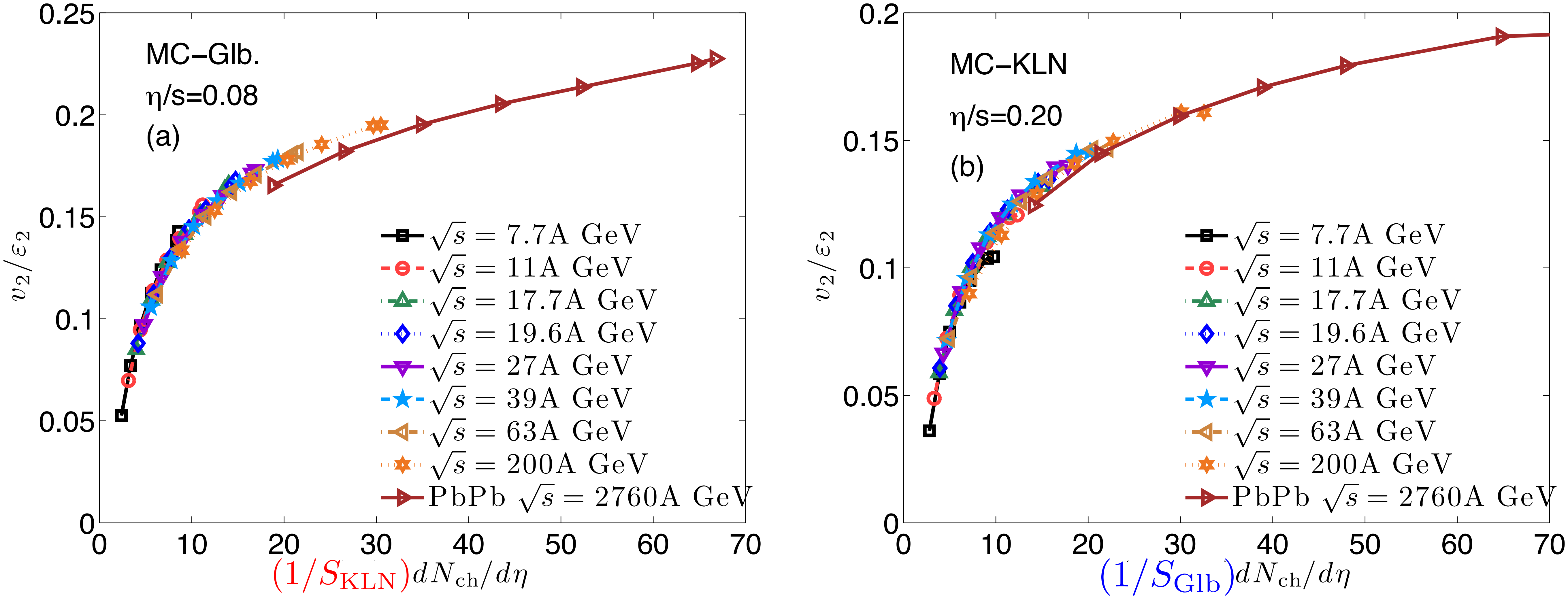
MC−Glb.
η/s=0.08
(a)
v_2/ε_2
0.25
0.2
0.15
0.1
0.05
0
0
10
20
30
40
50
60
70
$(1/S_{\mathrm{KLN}})dN_{\mathrm{ch}}/d\eta$
$\sqrt{s} = 7.7\mathrm{A\ GeV}$
$\sqrt{s} = 11\mathrm{A\ GeV}$
$\sqrt{s} = 17.7\mathrm{A\ GeV}$
$\sqrt{s} = 19.6\mathrm{A\ GeV}$
$\sqrt{s} = 27\mathrm{A\ GeV}$
$\sqrt{s} = 39\mathrm{A\ GeV}$
$\sqrt{s} = 63\mathrm{A\ GeV}$
$\sqrt{s} = 200\mathrm{A\ GeV}$
PbPb $\sqrt{s} = 2760\mathrm{A\ GeV}$
MC−KLN
η/s=0.20
(b)
v_2/ε_2
0.2
0.15
0.1
0.05
0
0
10
20
30
40
50
60
70
$(1/S_{\mathrm{Glb}})dN_{\mathrm{ch}}/d\eta$
$\sqrt{s} = 7.7\mathrm{A\ GeV}$
$\sqrt{s} = 11\mathrm{A\ GeV}$
$\sqrt{s} = 17.7\mathrm{A\ GeV}$
$\sqrt{s} = 19.6\mathrm{A\ GeV}$
$\sqrt{s} = 27\mathrm{A\ GeV}$
$\sqrt{s} = 39\mathrm{A\ GeV}$
$\sqrt{s} = 63\mathrm{A\ GeV}$
$\sqrt{s} = 200\mathrm{A\ GeV}$
PbPb $\sqrt{s} = 2760\mathrm{A\ GeV}$